



CERN-EP-2017-210  
LHCb-PAPER-2017-028  
August 15, 2017

# Measurement of the $\Upsilon(nS)$ polarizations in pp collisions at $\sqrt{s} = 7$ and 8 TeV

LHCb collaboration<sup>†</sup>

## Abstract

The polarization of the  $\Upsilon(1S)$ ,  $\Upsilon(2S)$  and  $\Upsilon(3S)$  mesons, produced in pp collisions at centre-of-mass energies  $\sqrt{s} = 7$  and 8 TeV, is measured using data samples collected by the LHCb experiment, corresponding to integrated luminosities of 1 and 2 fb<sup>-1</sup>, respectively. The measurements are performed in three polarization frames, using  $\Upsilon \rightarrow \mu^+\mu^-$  decays in the kinematic region of the transverse momentum  $p_T^\Upsilon < 30$  GeV/c and rapidity  $2.2 < y^\Upsilon < 4.5$ . No large polarization is observed.

Published in JHEP 12 (2017) 110.

© CERN on behalf of the LHCb collaboration, licence CC-BY-4.0.

---

<sup>†</sup>Authors are listed at the end of this paper.



# 1 Introduction

Studies of heavy quarkonium production play an important role in the development of quantum chromodynamics (QCD) [1, 2]. According to the current theoretical framework, nonrelativistic QCD (NRQCD) [3, 4], the production of heavy quarkonium factorizes into two steps, separated by different time and energy scales. In the first step, a heavy quark-antiquark pair,  $Q\bar{Q}$ , is created in a short time, of order  $\hbar/(2m_Qc^2)$ , where  $m_Q$  is the heavy-quark mass. In the second step, the  $Q\bar{Q}$  pair, being produced in a colour-singlet or colour-octet [5] state, evolves nonperturbatively into a quarkonium state. The nonperturbative transitions from the initially produced  $Q\bar{Q}$  pairs to the observable colourless quarkonium states are described by long-distance matrix elements. According to the NRQCD factorization approach [4], these matrix elements are universal constants which are independent of the short-time production processes, and need to be determined from data. Calculations based on the colour-singlet model [6–8] show good agreement [9–14] with the experimental data [15–22] for production cross-sections and the shapes of the transverse momentum spectra. However, this approach fails to describe the spin-alignment (usually labelled as polarization) of S-wave charmonium states [23, 24]. Leading-order colour-singlet calculations predict a transverse polarization for the S-wave quarkonia, while next-to-leading-order (NLO) calculations predict a longitudinal polarization for these states [10]. An analysis using NLO NRQCD calculations of the short-distance coefficients [14] concludes that the  $\Upsilon(1S)$  and  $\Upsilon(2S)$  bottomonium states should have a very small transverse polarization, almost independent of the transverse momentum, while the  $\Upsilon(3S)$  meson should show a large transverse polarization at high transverse momenta. For the  $\Upsilon(3S)$  meson this analysis neglects the contributions from the cascade decays of higher excited bottomonium states. Accounting for these contributions, *e.g.* from the radiative  $\chi_b(nP) \rightarrow \Upsilon\gamma$  decays<sup>1</sup> [25–29], is important for a correct interpretation of results [30]. The measured fractions of  $\Upsilon$  mesons originating from  $\chi_b$  decays are large, around 30 – 40 % [28], for  $\Upsilon$  mesons with high transverse momenta,  $p_T^\Upsilon \gtrsim 20 \text{ GeV}/c$ .

Experimentally, polarization of  $\Upsilon$  mesons produced in high-energy hadron-hadron interactions was studied by the CDF collaboration in  $p\bar{p}$  collisions at  $\sqrt{s} = 1.8$  and 1.96 TeV [16, 31]. It was found that the angular distributions of muons from  $\Upsilon \rightarrow \mu^+\mu^-$  decays for all three  $\Upsilon$  states are nearly isotropic in the central rapidity region  $|y^\Upsilon| < 0.6$  and  $p_T^\Upsilon < 40 \text{ GeV}/c$  [31]. This result is inconsistent with the measurement performed by the D0 collaboration, where a significant  $p_T^\Upsilon$ -dependent longitudinal polarization was observed for  $\Upsilon(1S)$  mesons produced in  $p\bar{p}$  collisions at  $\sqrt{s} = 1.96 \text{ TeV}$ , for  $|y^\Upsilon| < 1.8$  and  $p_T^\Upsilon < 20 \text{ GeV}/c$  [32]. At the LHC the  $\Upsilon$  polarization was measured by the CMS collaboration [33] using pp collision data at  $\sqrt{s} = 7 \text{ TeV}$ , for the rapidity ranges  $|y^\Upsilon| < 0.6$  and  $0.6 < |y^\Upsilon| < 1.2$ , and for  $10 < p_T^\Upsilon < 50 \text{ GeV}/c$ . No evidence of large transverse or longitudinal polarization was found for any of the three  $\Upsilon$  mesons in the considered kinematic region.

The spin-alignment state of  $\Upsilon$  mesons is measured through the analysis of the angular distribution of muons from the decay  $\Upsilon \rightarrow \mu^+\mu^-$  [34–36]

$$\frac{1}{\sigma} \frac{d\sigma}{d\Omega} = \frac{3}{4\pi} \frac{1}{3 + \lambda_\theta} \left( 1 + \lambda_\theta \cos^2 \theta + \lambda_{\theta\phi} \sin 2\theta \cos \phi + \lambda_\phi \sin^2 \theta \cos 2\phi \right), \quad (1)$$

where the angular quantities  $\Omega = (\cos \theta, \phi)$  denote the direction of the positive

---

<sup>1</sup>Throughout this paper the symbol  $\Upsilon$  represents generically  $\Upsilon(1S)$ ,  $\Upsilon(2S)$  and  $\Upsilon(3S)$  mesons.

muon in the rest frame of the  $\Upsilon$  meson with respect to the chosen reference frame. The spin-alignment parameters  $\boldsymbol{\lambda} \equiv (\lambda_\theta, \lambda_{\theta\phi}, \lambda_\phi)$  are directly related to the spin-1 density-matrix elements [34,37]. Alternatively, these parameters are often denoted as  $(\lambda, \mu, \nu/2)$ . The case  $\boldsymbol{\lambda} = (0, 0, 0)$  corresponds to unpolarized  $\Upsilon$  mesons and for the chosen reference frame transverse (longitudinal) polarization corresponds to  $\lambda_\theta > 0$  ( $< 0$ ).

The parameters  $\boldsymbol{\lambda}$  depend on the choice for the reference system in the rest frame of the  $\Upsilon$  meson. The following three frames are widely used in polarization analyses: helicity (HX), Collins-Soper (CS) and Gottfried-Jackson (GJ). In the HX frame [38], the  $z$  axis is defined as the direction of the  $\Upsilon$  momentum in the centre-of-mass frame of the colliding LHC protons, that is  $\hat{z} \equiv -(\vec{p}_1 + \vec{p}_2) / |\vec{p}_1 + \vec{p}_2|$ , where  $\vec{p}_1$  and  $\vec{p}_2$  are the three-momenta of the colliding protons in the rest frame of the  $\Upsilon$  meson.<sup>2</sup> In the CS frame [40], the  $z$  axis is defined such that it bisects the angle between  $\vec{p}_1$  and  $-\vec{p}_2$  in the rest frame of the  $\Upsilon$  meson. In the GJ frame [41], the  $z$  axis is defined as the direction of  $\vec{p}_1$  in the rest frame of the  $\Upsilon$  meson. In all of these frames, the  $y$  axis is normal to the production plane of the  $\Upsilon$  mesons with the direction along the vector product  $\vec{p}_1 \times \vec{p}_2$  defined in the rest frame of the  $\Upsilon$  meson.<sup>3</sup> The  $x$  axis is defined to complete a right-handed coordinate system.

Since the HX, CS and GJ reference frames are related by rotations around the  $y$  axis, the three polarization parameters measured in one frame can be translated into another [36, 43]. The frame-transformation relations imply the existence of quantities  $\mathcal{F}$  that are invariant under these rotations [44, 45]. These quantities are defined in terms of  $\lambda_\theta$  and  $\lambda_\phi$  as

$$\mathcal{F}(c_1, c_2, c_3) \equiv \frac{(3 + \lambda_\theta) + c_1(1 - \lambda_\phi)}{c_2(3 + \lambda_\theta) + c_3(1 - \lambda_\phi)}$$

for arbitrary numbers  $c_1$ ,  $c_2$  and  $c_3$ . In particular, the frame-invariant polarization parameter  $\tilde{\lambda}$  is defined for the specific choice of constants  $c_1$ ,  $c_2$  and  $c_3$  [44–48]

$$\tilde{\lambda} \equiv \mathcal{F}(-3, 0, 1) = \frac{\lambda_\theta + 3\lambda_\phi}{1 - \lambda_\phi}. \quad (2)$$

This paper presents a full angular analysis performed on  $\Upsilon$  mesons produced in pp collisions at  $\sqrt{s} = 7$  and 8 TeV corresponding to integrated luminosities of 1 and 2 fb<sup>-1</sup>, respectively. The polarization parameters are measured in the HX, CS and GJ frames in the region  $2.2 < y^\Upsilon < 4.5$  as functions of  $p_T^\Upsilon$  and  $y^\Upsilon$  for  $p_T^\Upsilon < 20$  GeV/ $c$  and as functions of  $p_T^\Upsilon$  for  $p_T^\Upsilon < 30$  GeV/ $c$ . The latter range is referred to as the wide  $p_T^\Upsilon$  range in the following.

## 2 LHCb detector and simulation

The LHCb detector [39, 49] is a single-arm forward spectrometer covering the pseudo-rapidity range  $2 < \eta < 5$ , designed for the study of particles containing b or c quarks.

<sup>2</sup>A beam proton travelling in the positive (negative) direction of the  $z$  axis of the coordinate system of the LHCb detector [39] is designated as the first (second).

<sup>3</sup>This definition is adopted from Ref. [36], and is opposite to the Madison convention [42],  $\vec{p}_1 \times \vec{p}_\Upsilon$ , where  $\vec{p}_1$  and  $\vec{p}_\Upsilon$  are the three-momenta of the first beam proton and the  $\Upsilon$  meson in the centre-of-mass frame of the two colliding protons. The two conventions differ by the sign of the  $\lambda_{\theta\phi}$  parameter while keeping the same values for  $\lambda_\theta$  and  $\lambda_\phi$  [36].

The detector includes a high-precision tracking system consisting of a silicon-strip vertex detector surrounding the pp interaction region, a large-area silicon-strip detector located upstream of a dipole magnet with a bending power of about 4 Tm, and three stations of silicon-strip detectors and straw drift tubes placed downstream of the magnet. The tracking system provides a measurement of momentum,  $p$ , of charged particles with a relative uncertainty that varies from 0.5% at low momentum to 1.0% at 200 GeV/ $c$ . The minimum distance of a track to a primary vertex, the impact parameter, is measured with a resolution of  $(15 + 29/p_T) \mu\text{m}$ , where  $p_T$  is in GeV/ $c$ . Different types of charged hadrons are distinguished using information from two ring-imaging Cherenkov detectors. Photons, electrons and hadrons are identified by a calorimeter system consisting of scintillating-pad and preshower detectors, an electromagnetic calorimeter and a hadronic calorimeter. Muons are identified by a system composed of alternating layers of iron and multiwire proportional chambers [50]. The online event selection is performed by a trigger [51], which consists of a hardware stage, based on information from the calorimeter and muon systems, followed by a software stage, which applies a full event reconstruction.

The hardware trigger stage is implemented by requiring the presence of two muon candidates with the product of their  $p_T$  exceeding 1.7 (2.6) (GeV/ $c$ )<sup>2</sup> for data collected at  $\sqrt{s} = 7$  (8) TeV. In the subsequent software stage, the trigger requires the presence of two well-reconstructed tracks with hits in the muon system,  $p_T > 0.5$  GeV/ $c$  and  $p > 6$  GeV/ $c$ . Only events with a pair of tracks identified as oppositely charged muons with a common vertex and a mass  $m_{\mu^+\mu^-} > 4.7$  GeV/ $c^2$  are retained for further analysis.

In Monte Carlo simulation, pp collisions are generated using PYTHIA 6 [52] with a specific LHCb configuration [53]. Decays of hadrons are described by EVTGEN [54] with final-state radiation generated using PHOTOS [55]. The interaction of the generated particles with the detector, and its response, are implemented using the GEANT4 toolkit [56] as described in Ref. [57]. The bottomonium production is simulated according to the leading order colour-singlet and colour-octet mechanisms [53, 58], and the bottomonium states are generated without polarization.

### 3 Data selection

The selection of  $\Upsilon$  candidates is based on the same criteria as used in the previous LHCb analyses [17–20]. The  $\Upsilon$  candidates are formed from pairs of oppositely charged tracks. Each track is required to have a good reconstruction quality [59] and to be identified as a muon [60]. Each muon is then required to satisfy  $1 < p_T < 25$  GeV/ $c$ ,  $10 < p < 400$  GeV/ $c$  and have pseudorapidity within  $2.2 < \eta < 4.5$ . The two muons are required to be consistent with originating from a common vertex. The consistency of the dimuon vertex with a primary vertex is ensured via the quality requirement of a global fit, performed for each dimuon candidate using the primary vertex position as a constraint [61]. This requirement also reduces the background from genuine muons coming from decays of long-lived charm and beauty hadrons. The mass of the muon pair is required to be in the range  $8.8 < m_{\mu^+\mu^-} < 11.0$  GeV/ $c^2$ . A large fraction of the combinatorial background is characterized by a large absolute value of the cosine of the polar angle,  $\cos\theta_{GJ}$ , of the  $\mu^+$  lepton in the GJ frame. The distributions of  $\cos\theta_{GJ}$  for signal and for background components in a typical bin,  $6 < p_T^\Upsilon < 8$  GeV/ $c$  and  $2.2 < y^\Upsilon < 3.0$ , are shown in Fig. 1a. The components are determined using the *sPlot* technique, described

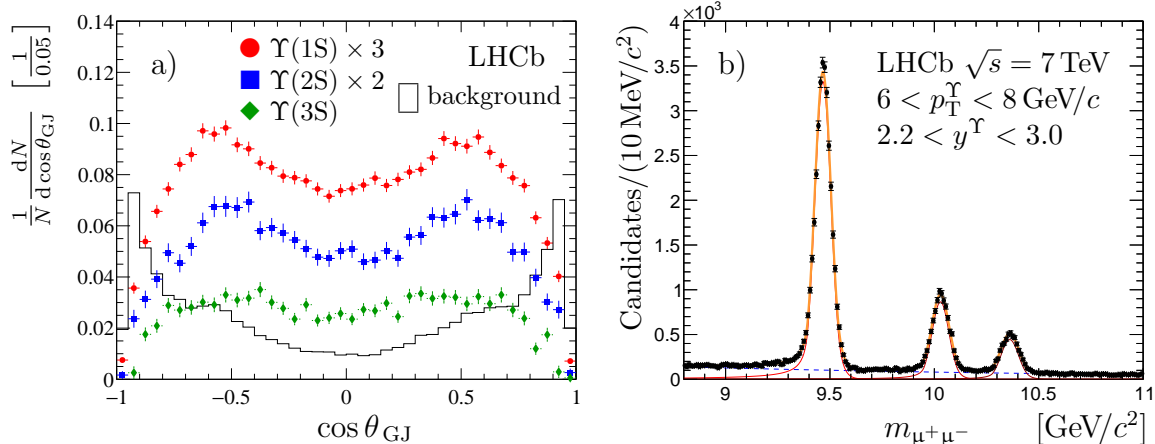


Figure 1: (a) Distributions of  $\cos \theta_{GJ}$  for  $\Upsilon(1S)$  (red circles),  $\Upsilon(2S)$  (blue squares) and  $\Upsilon(3S)$  (green diamonds) signal candidates and the background component (histogram) in the region  $6 < p_T^\Upsilon < 8 \text{ GeV}/c$ ,  $2.2 < y^\Upsilon < 3.0$  for data accumulated at  $\sqrt{s} = 7 \text{ TeV}$ . To improve visibility, the distributions for the  $\Upsilon(1S)$  and  $\Upsilon(2S)$  signals are scaled by factors of 3 and 2, respectively. (b) Dimuon mass distribution in the region  $6 < p_T^\Upsilon < 8 \text{ GeV}/c$ ,  $2.2 < y^\Upsilon < 3.0$  for data accumulated at  $\sqrt{s} = 7 \text{ TeV}$ . The thick dark yellow solid curve shows the result of the fit, as described in the text. The three peaks, shown with thin red solid lines, correspond to the  $\Upsilon(1S)$ ,  $\Upsilon(2S)$  and  $\Upsilon(3S)$  signals (left to right). The background component is indicated with a dashed blue line.

below. To reduce this background, a requirement  $|\cos \theta_{GJ}| < 0.8$  is applied.

Dimuon mass distributions of the  $\Upsilon \rightarrow \mu^+\mu^-$  candidates selected in the region  $6 < p_T^\Upsilon < 8 \text{ GeV}/c$  and  $2.2 < y^\Upsilon < 3.0$  for data collected at  $\sqrt{s} = 7 \text{ TeV}$  are shown in Fig. 1b. In each  $(p_T^\Upsilon, y^\Upsilon)$  bin, the dimuon mass distribution is parametrized by a sum of three double-sided Crystal Ball functions [62, 63], describing the three  $\Upsilon$  meson signals, and an exponential function for the combinatorial background. A double-sided Crystal Ball function is defined as a Gaussian function with power-law tails on both the low- and high-mass sides. The peak position and the resolution parameters of the Crystal Ball function describing the mass distribution of the  $\Upsilon(1S)$  meson are free parameters for the unbinned extended maximum likelihood fit. The peak position parameters of the  $\Upsilon(2S)$  and  $\Upsilon(3S)$  signal components are fixed using the known values of the mass differences of the  $\Upsilon(2S)$  and  $\Upsilon(3S)$  mesons to that of the  $\Upsilon(1S)$  meson [64], while the resolution parameters are fixed to the value of the resolution parameter of the  $\Upsilon(1S)$  signal, scaled by the ratio of the masses of the  $\Upsilon(2S)$  and  $\Upsilon(3S)$  mesons to that of the  $\Upsilon(1S)$  meson. The power-law tail parameters of the three Crystal Ball functions are common for the three  $\Upsilon$  meson signals and left free in the fit.

## 4 Polarization fit

The polarization parameters are determined from unbinned maximum likelihood fits [65] to the two-dimensional  $(\cos \theta, \phi)$  angular distribution of the  $\mu^+$  lepton from the  $\Upsilon \rightarrow \mu^+\mu^-$  decay, described by Eq. 1, following the approach of Refs. [23, 24]. The projections of the two-dimensional  $(\cos \theta, \phi)$  angular distribution in the HX frame are shown in Fig. 2 for data accumulated at  $\sqrt{s} = 7 \text{ TeV}$  in the kinematic region  $6 < p_T^\Upsilon < 8 \text{ GeV}/c$ ,

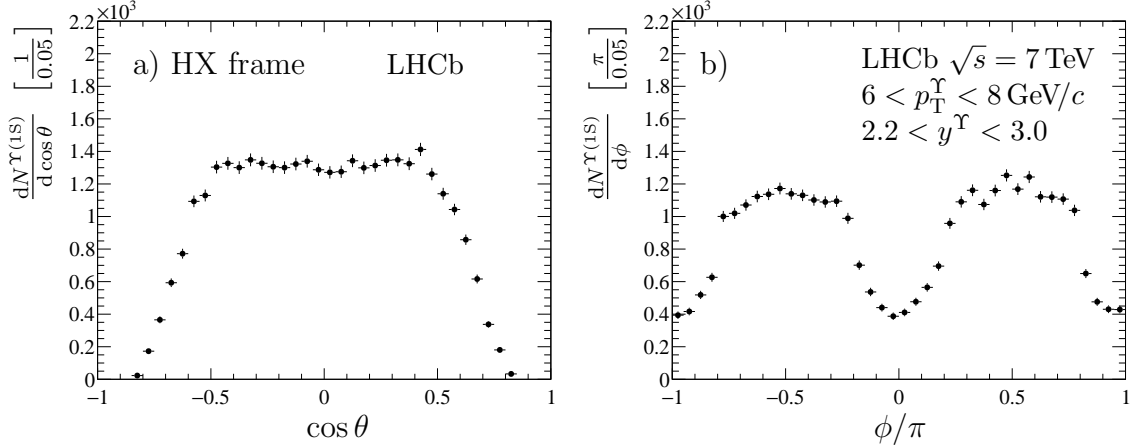


Figure 2: Background-subtracted distributions of (a)  $\cos \theta$  and (b)  $\phi$  for the  $\Upsilon(1S)$  signal candidates in the HX frame, measured in the kinematic region  $6 < p_{\text{T}}^{\Upsilon} < 8 \text{ GeV}/c$  and  $2.2 < y^{\Upsilon} < 3.0$ , for data accumulated at  $\sqrt{s} = 7 \text{ TeV}$ .

$2.2 < y^{\Upsilon} < 3.0$ .

The logarithm of the likelihood function for each  $\Upsilon$  state, in each  $(p_{\text{T}}^{\Upsilon}, y^{\Upsilon})$  bin, is defined as [24]

$$\begin{aligned}
 \log \mathcal{L}^{\Upsilon}(\boldsymbol{\lambda}) &= s_w \sum_i w_i^{\Upsilon} \log \left[ \frac{\mathcal{P}(\Omega_i|\boldsymbol{\lambda}) \varepsilon(\Omega_i)}{\mathcal{N}(\boldsymbol{\lambda})} \right] \\
 &= s_w \sum_i w_i^{\Upsilon} \log \left[ \frac{\mathcal{P}(\Omega_i|\boldsymbol{\lambda})}{\mathcal{N}(\boldsymbol{\lambda})} \right] \\
 &+ s_w \sum_i w_i^{\Upsilon} \log [\varepsilon(\Omega_i)] ,
 \end{aligned} \tag{3}$$

where  $\mathcal{P}(\Omega_i|\boldsymbol{\lambda}) \equiv 1 + \lambda_{\theta} \cos^2 \theta_i + \lambda_{\theta\phi} \sin 2\theta_i \cos \phi_i + \lambda_{\phi} \sin^2 \theta_i \cos 2\phi_i$ ,  $\varepsilon(\Omega_i)$  is the total efficiency for the  $i^{\text{th}}$   $\Upsilon$  candidate and  $\mathcal{N}(\boldsymbol{\lambda})$  is the normalization integral defined below. The weights  $w_i^{\Upsilon}$  are determined from the fit of the dimuon mass distribution using the *sPlot* technique [66], which projects out the corresponding signal component from the combined signal plus background densities. The sum in Eq. 3 runs over all selected  $\Upsilon$  candidates. The constant scale factor  $s_w \equiv \sum_i w_i^{\Upsilon} / \sum_i (w_i^{\Upsilon})^2$  accounts for statistical fluctuations in the background subtraction [24, 67, 68] and was validated using pseudoexperiments. Numerically, it increases by approximately 5% the uncertainties in the polarization parameters. The last term in Eq. 3 is ignored in the fit as it has no dependence on the polarization parameters. The normalization factor  $\mathcal{N}(\boldsymbol{\lambda})$  is defined as

$$\mathcal{N}(\boldsymbol{\lambda}) \equiv \int d\Omega \mathcal{P}(\Omega|\boldsymbol{\lambda}) \varepsilon(\Omega) \tag{4}$$

and is calculated using simulated events. In the simulation, where the  $\Upsilon$  mesons are generated unpolarized, the two-dimensional  $(\cos \theta, \phi)$  distribution of selected candidates is proportional to the total efficiency  $\varepsilon(\Omega)$ , so  $\mathcal{N}(\boldsymbol{\lambda})$  is evaluated by summing  $\mathcal{P}(\Omega_i|\boldsymbol{\lambda})$  over the selected  $\Upsilon$  candidates in the simulated sample

$$\mathcal{N}(\boldsymbol{\lambda}) \propto \sum_i \varepsilon^{\mu^+\mu^-} \mathcal{P}(\Omega_i|\boldsymbol{\lambda}). \tag{5}$$

For simulated events no muon identification requirement is applied when selecting the  $\Upsilon$  candidates. Instead, a muon-pair identification efficiency factor  $\varepsilon^{\mu^+\mu^-}$  is applied for all selected simulated  $\Upsilon \rightarrow \mu^+\mu^-$  decays. This factor is calculated on a per-event basis as

$$\varepsilon^{\mu^+\mu^-} = \varepsilon^{\mu\text{ID}}(\mu^+) \varepsilon^{\mu\text{ID}}(\mu^-), \quad (6)$$

where  $\varepsilon^{\mu\text{ID}}$  is the single-muon identification efficiency, measured in data, using large samples of prompt  $J/\psi$  mesons decaying to muon pairs. Given that the reconstruction and selection efficiencies are taken from simulation, the efficiency  $\varepsilon^{\mu^+\mu^-}$  is further corrected to account for small differences between data and simulation in the track reconstruction efficiency [59, 60] and in the  $p_{\text{T}}^{\Upsilon}$  and  $y^{\Upsilon}$  spectra [52, 53].

## 5 Systematic uncertainties

The sources of systematic uncertainty studied in this analysis are summarized in Table 1. They are considered for the polarization parameters  $\lambda_{\theta}$ ,  $\lambda_{\theta\phi}$ ,  $\lambda_{\phi}$  and for the frame-invariant parameter  $\tilde{\lambda}$  in the HX, CS and GJ frames for each  $(p_{\text{T}}^{\Upsilon}, y^{\Upsilon})$  bin.

The systematic uncertainty related to the signal determination procedure is studied by varying the mass model describing the shape of the dimuon mass distributions. For the signal parametrizations, the power-law tail parameters of the double-sided Crystal Ball functions are fixed to the values obtained in the simulation, and the constraints for the mean values of the Crystal Ball functions describing the  $\Upsilon(2S)$  and  $\Upsilon(3S)$  signals are removed. The variation of the background parametrization is done by replacing the exponential function with the product of an exponential function and a polynomial function. Mass fit ranges are also varied. The maximum differences in each parameter  $\lambda$  and  $\tilde{\lambda}$  with respect to the nominal fit results are taken as systematic uncertainties. For all  $(p_{\text{T}}^{\Upsilon}, y^{\Upsilon})$  bins these uncertainties are around 10 % of the corresponding statistical uncertainties.

For several sources of systematic uncertainty pseudoexperiments are used, whereby an ensemble of pseudodata samples is generated, each with a random value of the appropriate parameter taken from a Gaussian distribution. The fit is then performed for each sample, and the observed variations in the fit parameters are used to assign the corresponding systematic uncertainties.

The single-muon identification efficiency,  $\varepsilon^{\mu\text{ID}}$ , is determined from large samples of  $J/\psi \rightarrow \mu^+\mu^-$  decays. The efficiency  $\varepsilon^{\mu\text{ID}}$  is measured as a function of muon transverse momentum and pseudorapidity. The systematic uncertainty in the  $\lambda$  and  $\tilde{\lambda}$  parameters related to the muon identification is obtained from the uncertainties of the single particle identification efficiency  $\varepsilon^{\mu\text{ID}}$  using pseudoexperiments. This uncertainty is around 2 % of the statistical uncertainty for data in low- $p_{\text{T}}^{\Upsilon}$  bins and rises to 8 % of the statistical uncertainty in high- $p_{\text{T}}^{\Upsilon}$  bins.

The uncertainties in the correction factors for the muon-pair identification efficiency  $\varepsilon^{\mu^+\mu^-}$ , related to small differences in the tracking and muon reconstruction efficiencies between data and simulation, are propagated to the determination of the polarization parameters using pseudoexperiments. These uncertainties are 20 % of the statistical uncertainty for low- $p_{\text{T}}^{\Upsilon}$  bins and decrease to 10 % of the statistical uncertainty for high- $p_{\text{T}}^{\Upsilon}$  bins.

In this analysis the efficiency of the trigger is taken from simulation. The systematic uncertainty associated with a possible small difference in the trigger efficiency between data



Table 1: Ranges of the absolute systematic uncertainties of the parameters  $\boldsymbol{\lambda}$  and  $\tilde{\lambda}$ . The ranges indicate variations depending on the  $(p_{\text{T}}^{\Upsilon}, y^{\Upsilon})$  bin and frame.

Source	$\sigma_{\lambda_{\theta}}$ [ $10^{-3}$ ]	$\sigma_{\lambda_{\theta\phi}}$ [ $10^{-3}$ ]	$\sigma_{\lambda_{\phi}}$ [ $10^{-3}$ ]	$\sigma_{\tilde{\lambda}}$ [ $10^{-3}$ ]
$\Upsilon(1\text{S})$				
Dimuon mass fit	1.0 – 12	0.2 – 10	0.1 – 7	1.8 – 20
Efficiency calculation				
muon identification	0.2 – 10	0.1 – 7	0.1 – 6	0.2 – 17
correction factors for $\varepsilon^{\mu^+\mu^-}$	0.7 – 12	0.4 – 5	0.1 – 4	2.1 – 14
trigger	0.1 – 18	0.1 – 8	0.1 – 5	0.3 – 19
Finite size of simulated samples	6.0 – 82	1.3 – 29	0.9 – 35	6.9 – 95
$\Upsilon(2\text{S})$				
Dimuon mass fit	0.6 – 37	0.2 – 19	0.3 – 16	4.6 – 53
Efficiency calculation				
muon identification	0.2 – 11	0.1 – 6	0.1 – 5	0.2 – 13
correction factors for $\varepsilon^{\mu^+\mu^-}$	0.7 – 12	0.3 – 5	0.1 – 5	2.1 – 13
trigger	0.1 – 17	0.1 – 7	0.1 – 5	0.3 – 18
Finite size of simulated samples	9.8 – 210	2.5 – 98	1.5 – 120	14 – 320
$\Upsilon(3\text{S})$				
Dimuon mass fit model	1.4 – 72	0.2 – 24	0.5 – 21	7.2 – 86
Efficiency calculation				
muon identification	0.2 – 12	0.1 – 7	0.1 – 5	0.3 – 22
correction factors for $\varepsilon^{\mu^+\mu^-}$	0.6 – 14	0.3 – 6	0.1 – 5	2.1 – 18
trigger	0.2 – 17	0.1 – 8	0.1 – 4	0.3 – 19
Finite size of simulated samples	12 – 280	3.5 – 100	2.1 – 110	16 – 350

and simulation is assessed by studying the performance of the dimuon trigger, described in Sect. 2, for events selected using the single-muon high- $p_{\text{T}}$  trigger [51]. The fractions of  $\Upsilon(1\text{S})$  signal candidates selected using both trigger requirements are compared for the data and simulation in  $(p_{\text{T}}^{\Upsilon}, y^{\Upsilon})$  bins and found to agree within 2% [19, 20]. The corresponding systematic uncertainties in the polarization parameters are obtained using pseudoexperiments and found to be between 2% and 4% of the statistical uncertainty.

Good agreement between the data and simulated samples is observed for all variables used to select the  $\Upsilon$  candidates [19, 20]. The discrepancies in the corresponding integrated normalized distributions do not exceed 1% and therefore no systematic uncertainty related to possible mismodelling is assigned to the polarization parameters.

The finite size of the simulated samples introduces a systematic uncertainty related to the normalization factors  $\mathcal{N}(\boldsymbol{\lambda})$  of Eq. 5. This uncertainty is also propagated to the final uncertainty of the polarization results using pseudoexperiments. This systematic uncertainty is dominant for most of the  $(p_{\text{T}}^{\Upsilon}, y^{\Upsilon})$  bins, varying between 30% and 70% of the statistical uncertainty.

The total systematic uncertainty for each polarization parameter is calculated as the quadratic sum of the systematic uncertainties from all the considered sources, assuming

no correlations. The systematic uncertainties of the  $\boldsymbol{\lambda}$  and  $\tilde{\lambda}$  parameters in the different frames are comparable. For the majority of the  $(p_{\text{T}}^{\Upsilon}, y^{\Upsilon})$  bins the total systematic uncertainty is much smaller than the statistical uncertainty. For some high- $p_{\text{T}}^{\Upsilon}$  bins the systematic and statistical uncertainties are comparable.

## 6 Results

The polarization parameters  $\lambda_{\theta}$ ,  $\lambda_{\theta\phi}$ ,  $\lambda_{\phi}$  for the  $\Upsilon$  mesons, measured in the HX, CS and GJ frames for different  $(p_{\text{T}}^{\Upsilon}, y^{\Upsilon})$  bins, for data collected at  $\sqrt{s} = 7$  TeV and 8 TeV, are shown in Figs. 3, 4 and 5 for the  $\Upsilon(1\text{S})$  meson, in Figs. 6, 7 and 8 for the  $\Upsilon(2\text{S})$  meson and in Figs. 9, 10 and 11 for the  $\Upsilon(3\text{S})$  meson. The parameters  $\boldsymbol{\lambda}$  do not show significant variations as a function of  $y^{\Upsilon}$ , in accordance with expectations. Figures 12, 13 and 14 show the polarization parameters measured in the full considered rapidity range  $2.2 < y^{\Upsilon} < 4.5$  and the wide region of transverse momentum up to 30 GeV/ $c$ . All polarization parameters are listed in Appendix A for the  $\Upsilon(1\text{S})$  mesons, Appendix B for the  $\Upsilon(2\text{S})$  mesons and Appendix C for the  $\Upsilon(3\text{S})$  mesons. The correlation coefficients between the different polarization parameters are, in general, small, especially between the  $\lambda_{\theta}$  and  $\lambda_{\phi}$  parameters. The smallest correlation coefficients are obtained in the CS frame.

The values of the parameter  $\lambda_{\theta}$  measured in the HX, CS and GJ frames do not show large transverse or longitudinal polarization over the considered kinematic region. The values of the parameters  $\lambda_{\theta\phi}$  and  $\lambda_{\phi}$  are small in all polarization frames, over all  $(p_{\text{T}}^{\Upsilon}, y^{\Upsilon})$  bins. The  $\Upsilon$  polarization results are in good agreement with those obtained by the CMS collaboration [33]. The polarization results obtained for the two centre-of-mass energies,  $\sqrt{s} = 7$  TeV and 8 TeV, are similar and show a good agreement.

In the rest frame of the  $\Upsilon$  meson, the spin-1 density matrix is proportional to [69, 70]

$$\begin{pmatrix} \frac{1 - \lambda_{\theta}}{2} & \lambda_{\theta\phi} & 0 \\ \lambda_{\theta\phi} & \frac{1 + \lambda_{\theta} - 2\lambda_{\phi}}{2} & 0 \\ 0 & 0 & \frac{1 + \lambda_{\theta} + 2\lambda_{\phi}}{2} \end{pmatrix}.$$

The positivity of the density matrix imposes constraints on the  $\boldsymbol{\lambda}$  parameters as follows [45, 48, 69–72]

$$\begin{aligned} 0 &\leq \mathcal{C}_1 = 1 - |\lambda_{\theta}| \\ 0 &\leq \mathcal{C}_2 = 1 + \lambda_{\theta} - 2|\lambda_{\phi}| \\ 0 &\leq \mathcal{C}_3 = (1 - \lambda_{\theta})(1 + \lambda_{\theta} - 2\lambda_{\phi}) - 4\lambda_{\theta\phi}^2 \\ 0 &\leq \mathcal{C}_4 = (1 - \lambda_{\theta})(1 + \lambda_{\theta} + 2\lambda_{\phi}) \\ 0 &\leq \mathcal{C}_5 = (1 + \lambda_{\theta})^2 - 4\lambda_{\phi}^2 \\ 0 &\leq \mathcal{C}_6 = (1 + \lambda_{\theta} + 2\lambda_{\phi})((1 - \lambda_{\theta})(1 + \lambda_{\theta} - 2\lambda_{\phi}) - 4\lambda_{\theta\phi}^2). \end{aligned}$$

The measured values of the  $\boldsymbol{\lambda}$  parameters satisfy these positivity constraints  $\mathcal{C}_i$  in all frames over all  $(p_{\text{T}}^{\Upsilon}, y^{\Upsilon})$  bins.

The frame-invariant polarization parameter  $\tilde{\lambda}$  measured in the HX, CS and GJ frames is shown in Fig. 15. A possible disagreement between the values of  $\tilde{\lambda}$  measured in

the different frames would indicate an unaccounted systematic uncertainty, *e.g.* related to limitations of the simulation. No such disagreement is found. The rotation angles between the different frames depend on the transverse momentum of the  $\Upsilon$  mesons and vanish for small  $p_T^\Upsilon$ , resulting in a degeneracy between the three frames [36, 43]. Due to this degeneracy, the polarization results for different frames are very similar for low- $p_T^\Upsilon$  bins, see *e.g.* Figs. 12, 13 and 14.

## 7 Summary

A polarization analysis is carried out for the  $\Upsilon(1S)$ ,  $\Upsilon(2S)$  and  $\Upsilon(3S)$  mesons in pp collision data at  $\sqrt{s} = 7$  and 8 TeV at LHCb, corresponding to integrated luminosities of 1 and 2 fb<sup>-1</sup>, respectively. The analysis is performed in the helicity, Collins-Soper and Gottfried-Jackson frames by studying the angular distribution of the  $\mu^+$  lepton in the rest frame of the  $\Upsilon$  meson, in  $\Upsilon \rightarrow \mu^+\mu^-$  decays. The angular distribution parameters  $\lambda_\theta$ ,  $\lambda_{\theta\phi}$  and  $\lambda_\phi$ , as well as the frame-invariant parameter  $\tilde{\lambda}$ , are measured as functions of the  $\Upsilon$  transverse momentum  $p_T^\Upsilon$  and rapidity  $y^\Upsilon$ , in the regions  $p_T^\Upsilon < 30$  GeV/ $c$  and  $2.2 < y^\Upsilon < 4.5$ .

The values of the  $\lambda_\theta$  parameter obtained for all the  $\Upsilon$  mesons show no large transverse or longitudinal polarization in all frames over the accessible phase space domain. The values of the  $\lambda_{\theta\phi}$  and  $\lambda_\phi$  parameters are small in all frames over the accessible kinematic region. The values of the frame-invariant parameter  $\tilde{\lambda}$  measured in the HX, CS and GJ frames are consistent. The polarization results corresponding to  $\sqrt{s} = 7$  and 8 TeV are in good agreement. The  $\Upsilon$  polarization results agree with the results obtained by the CMS collaboration [33].

## Acknowledgements

We would like to thank S. P. Baranov, K.-T. Chao, J.-P. Lansberg, A. K. Likhoded, H.-S. Shao, S. R. Slabospitsky and O. V. Teryaev for interesting and stimulating discussions on quarkonium polarization. We express our gratitude to our colleagues in the CERN accelerator departments for the excellent performance of the LHC. We thank the technical and administrative staff at the LHCb institutes. We acknowledge support from CERN and from the national agencies: CAPES, CNPq, FAPERJ and FINEP (Brazil); MOST and NSFC (China); CNRS/IN2P3 (France); BMBF, DFG and MPG (Germany); INFN (Italy); NWO (The Netherlands); MNiSW and NCN (Poland); MEN/IFA (Romania); MinES and FASO (Russia); MinECo (Spain); SNSF and SER (Switzerland); NASU (Ukraine); STFC (United Kingdom); NSF (USA). We acknowledge the computing resources that are provided by CERN, IN2P3 (France), KIT and DESY (Germany), INFN (Italy), SURF (The Netherlands), PIC (Spain), GridPP (United Kingdom), RRCKI and Yandex LLC (Russia), CSCS (Switzerland), IFIN-HH (Romania), CBPF (Brazil), PL-GRID (Poland) and OSC (USA). We are indebted to the communities behind the multiple open source software packages on which we depend. Individual groups or members have received support from AvH Foundation (Germany), EPLANET, Marie Skłodowska-Curie Actions and ERC (European Union), Conseil Général de Haute-Savoie, Labex ENIGMASS and OCEVU, Région Auvergne (France), RFBR and Yandex LLC (Russia), GVA, XuntaGal and GENCAT (Spain), Herchel Smith Fund,

The Royal Society, Royal Commission for the Exhibition of 1851 and the Leverhulme Trust (United Kingdom).

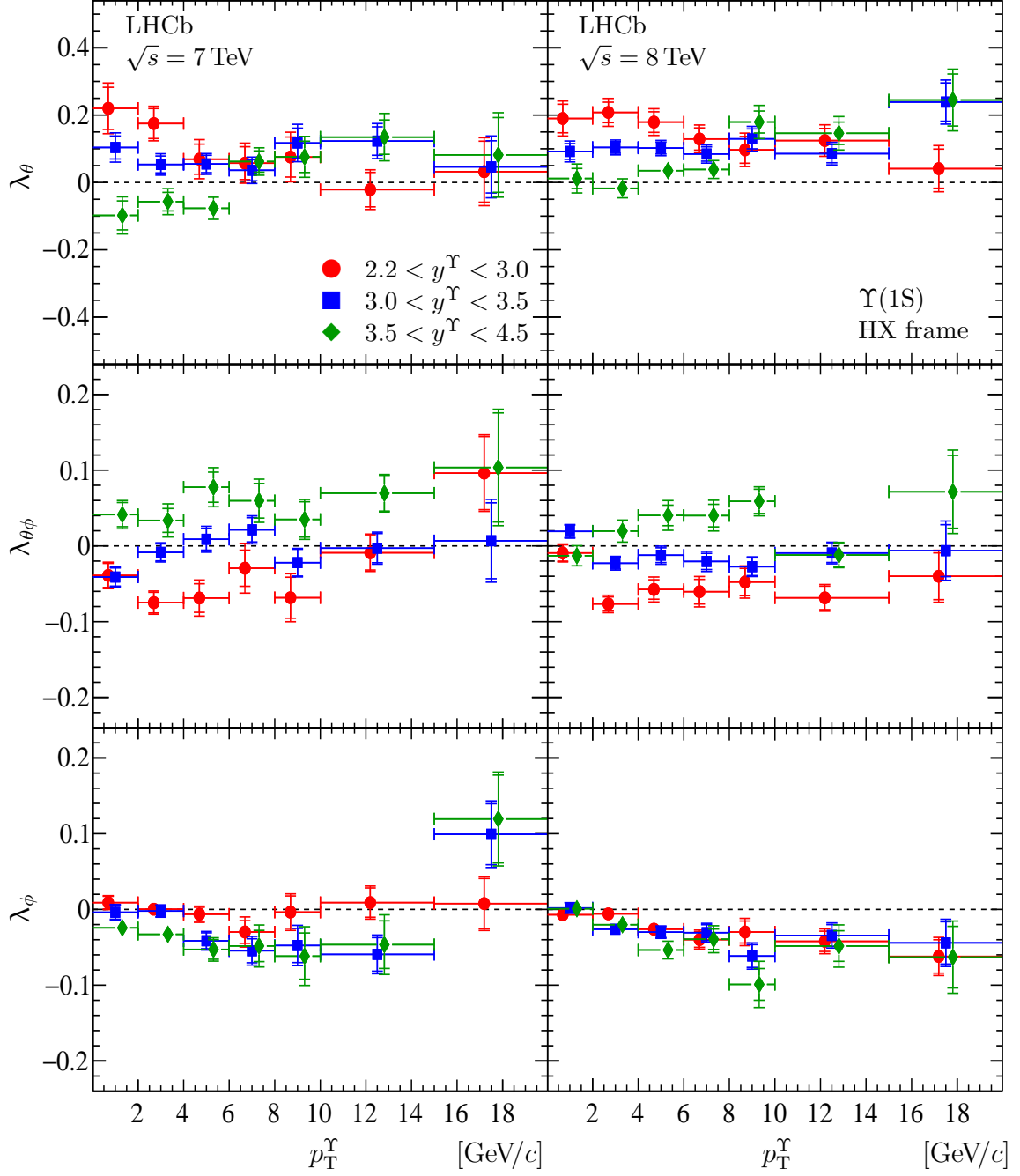


Figure 3: The polarization parameters (top)  $\lambda_\theta$ , (middle)  $\lambda_{\theta\phi}$  and (bottom)  $\lambda_\phi$ , measured in the HX frame for the  $\Upsilon(1S)$  state in different bins of  $p_T^\Upsilon$  and three rapidity ranges, for data collected at (left)  $\sqrt{s} = 7$  TeV and (right)  $\sqrt{s} = 8$  TeV. The results for the rapidity ranges  $2.2 < y^\Upsilon < 3.0$ ,  $3.0 < y^\Upsilon < 3.5$  and  $3.5 < y^\Upsilon < 4.5$  are shown with red circles, blue squares and green diamonds, respectively. The vertical inner error bars indicate the statistical uncertainty, whilst the outer error bars indicate the sum of the statistical and systematic uncertainties added in quadrature. The horizontal error bars indicate the bin width. Some data points are displaced from the bin centers to improve visibility.

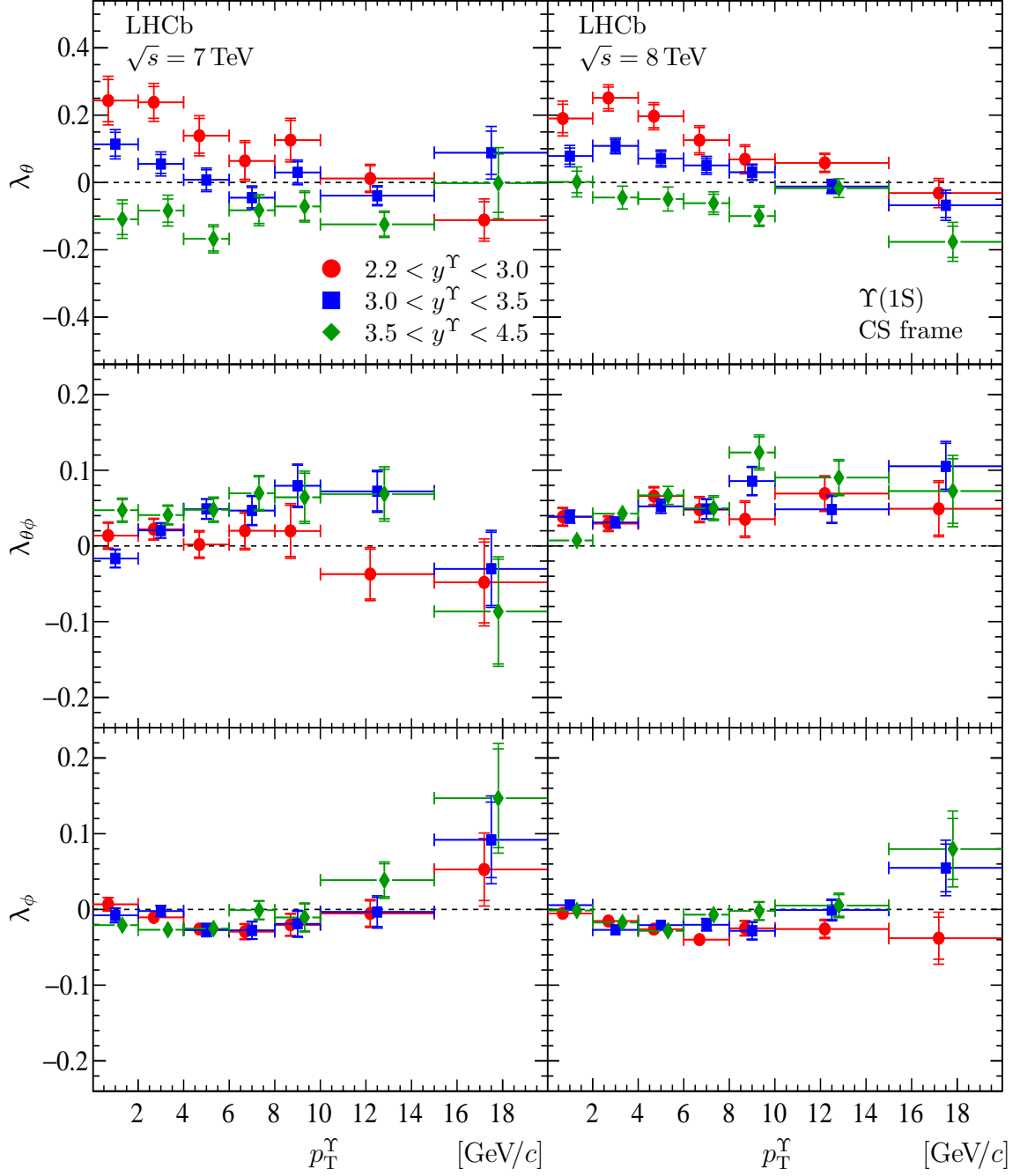


Figure 4: The polarization parameters (top)  $\lambda_\theta$ , (middle)  $\lambda_{\theta\phi}$  and (bottom)  $\lambda_\phi$ , measured in the CS frame for the  $\Upsilon(1S)$  state in different bins of  $p_T^\Upsilon$  and three rapidity ranges, for data collected at (left)  $\sqrt{s} = 7$  TeV and (right)  $\sqrt{s} = 8$  TeV. The results for the rapidity ranges  $2.2 < y^\Upsilon < 3.0$ ,  $3.0 < y^\Upsilon < 3.5$  and  $3.5 < y^\Upsilon < 4.5$  are shown with red circles, blue squares and green diamonds, respectively. The vertical inner error bars indicate the statistical uncertainty, whilst the outer error bars indicate the sum of the statistical and systematic uncertainties added in quadrature. The horizontal error bars indicate the bin width. Some data points are displaced from the bin centers to improve visibility.

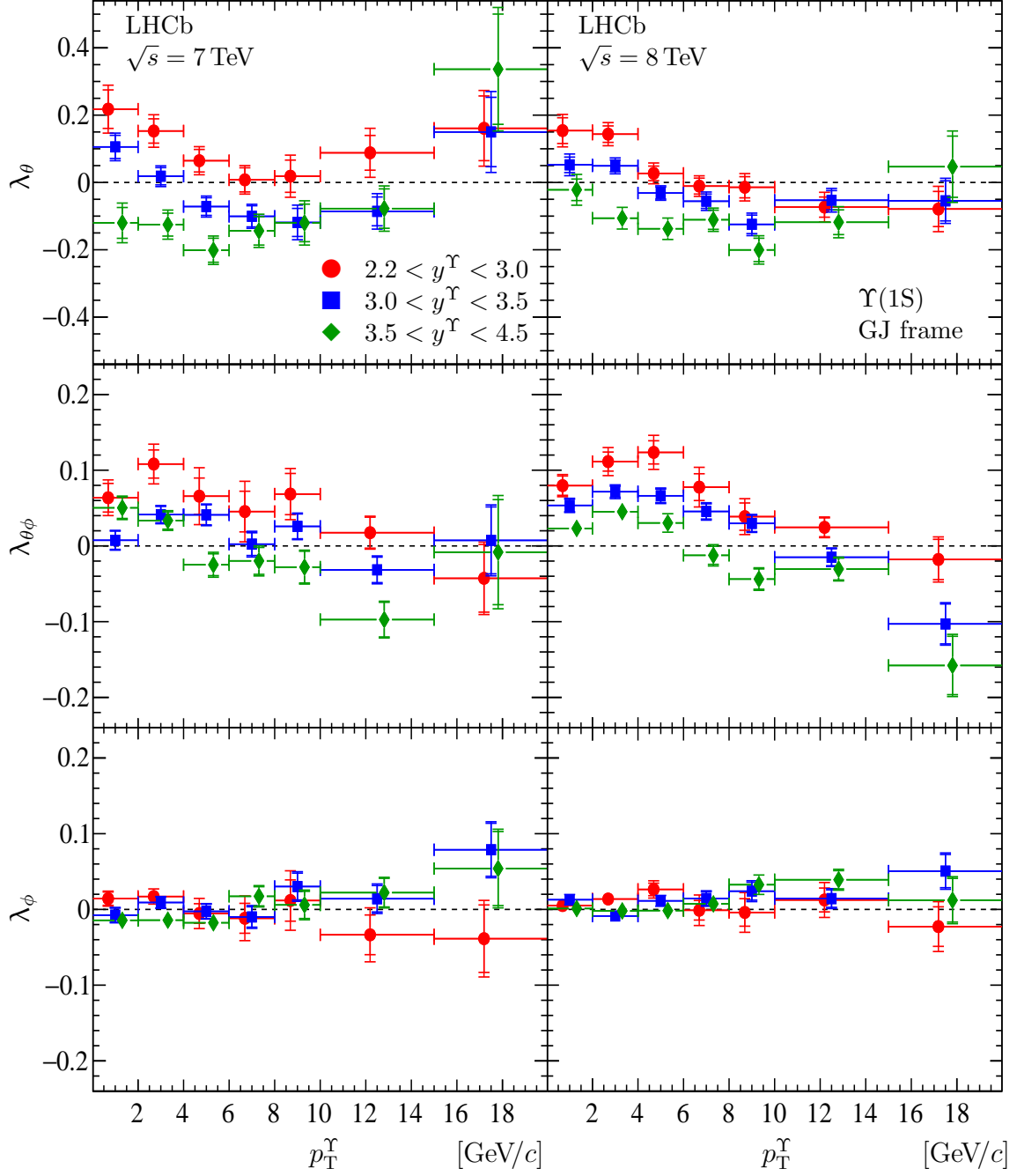


Figure 5: The polarization parameters (top)  $\lambda_\theta$ , (middle)  $\lambda_{\theta\phi}$  and (bottom)  $\lambda_\phi$ , measured in the GJ frame for the  $\Upsilon(1S)$  state in different bins of  $p_T^\Upsilon$  and three rapidity ranges, for data collected at (left)  $\sqrt{s} = 7$  TeV and (right)  $\sqrt{s} = 8$  TeV. The results for the rapidity ranges  $2.2 < y^\Upsilon < 3.0$ ,  $3.0 < y^\Upsilon < 3.5$  and  $3.5 < y^\Upsilon < 4.5$  are shown with red circles, blue squares and green diamonds, respectively. The vertical inner error bars indicate the statistical uncertainty, whilst the outer error bars indicate the sum of the statistical and systematic uncertainties added in quadrature. The horizontal error bars indicate the bin width. Some data points are displaced from the bin centers to improve visibility.

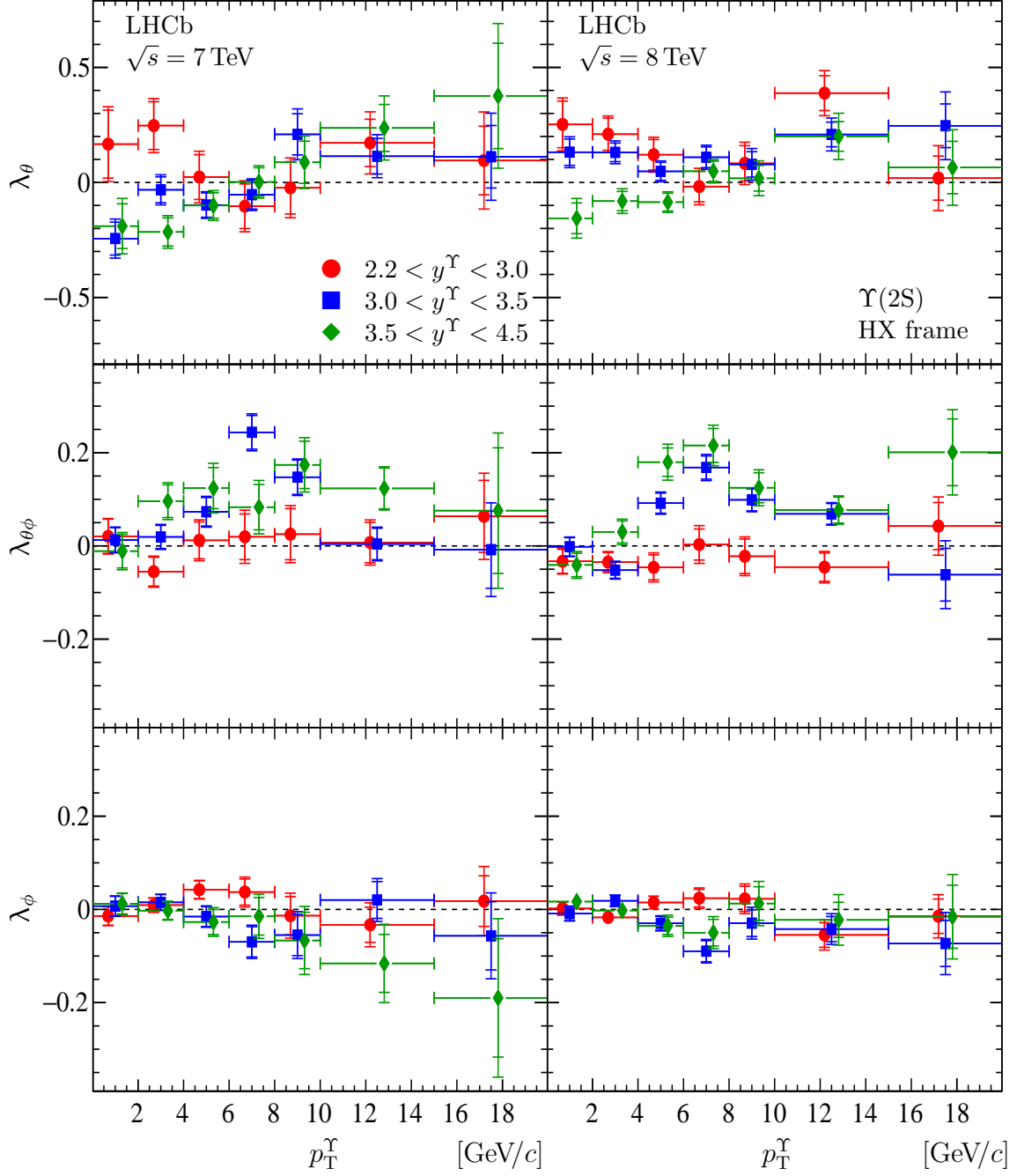


Figure 6: The polarization parameters (top)  $\lambda_\theta$ , (middle)  $\lambda_{\theta\phi}$  and (bottom)  $\lambda_\phi$ , measured in the HX frame for the  $\Upsilon(2S)$  state in different bins of  $p_T^\Upsilon$  and three rapidity ranges, for data collected at (left)  $\sqrt{s} = 7$  TeV and (right)  $\sqrt{s} = 8$  TeV. The results for the rapidity ranges  $2.2 < y^\Upsilon < 3.0$ ,  $3.0 < y^\Upsilon < 3.5$  and  $3.5 < y^\Upsilon < 4.5$  are shown with red circles, blue squares and green diamonds, respectively. The vertical inner error bars indicate the statistical uncertainty, whilst the outer error bars indicate the sum of the statistical and systematic uncertainties added in quadrature. The horizontal error bars indicate the bin width. Some data points are displaced from the bin centers to improve visibility.



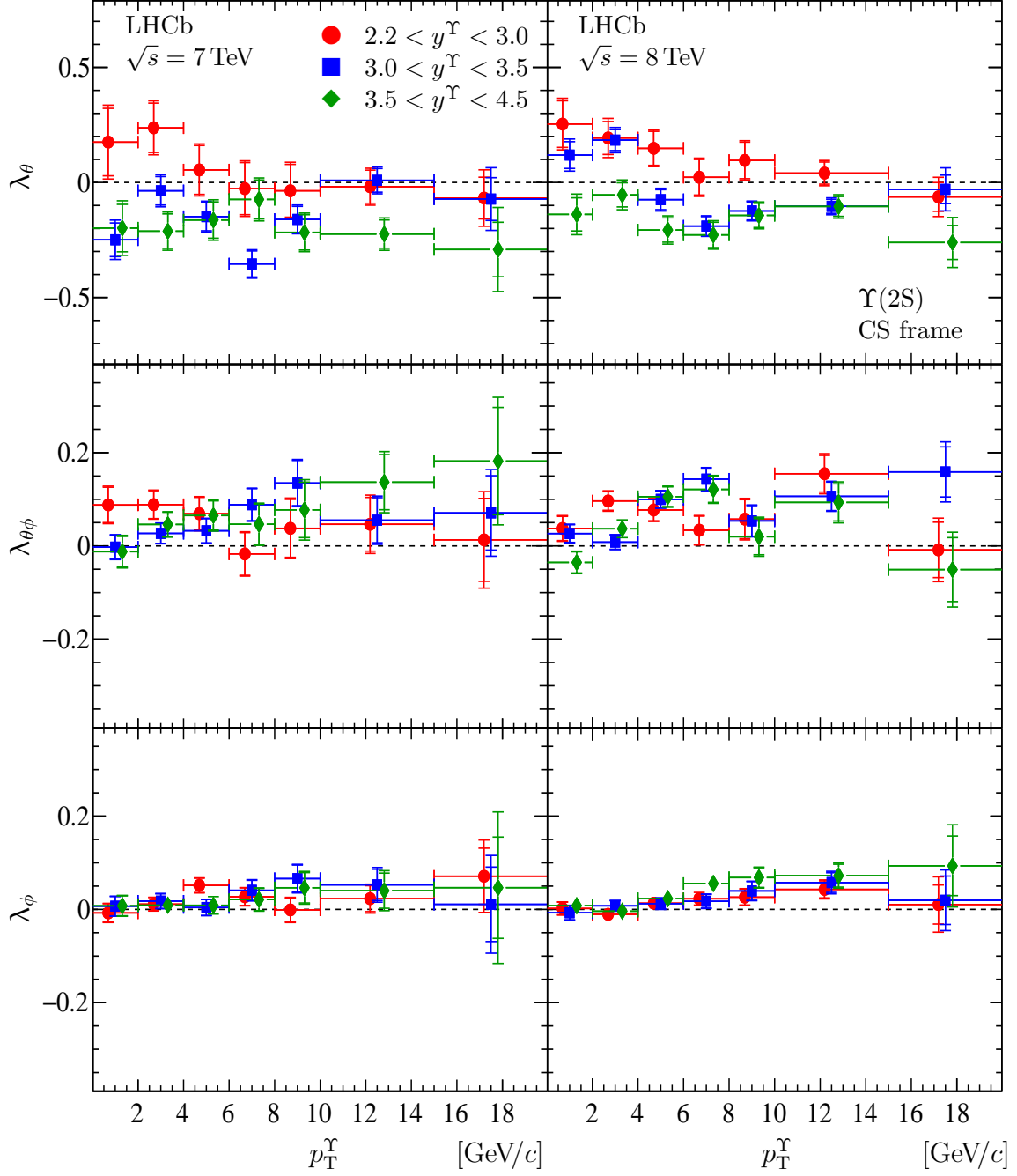


Figure 7: The polarization parameters (top)  $\lambda_\theta$ , (middle)  $\lambda_{\theta\phi}$  and (bottom)  $\lambda_\phi$ , measured in the CS frame for the  $\Upsilon(2S)$  state in different bins of  $p_T^\Upsilon$  and three rapidity ranges, for data collected at (left)  $\sqrt{s} = 7$  TeV and (right)  $\sqrt{s} = 8$  TeV. The results for the rapidity ranges  $2.2 < y^\Upsilon < 3.0$ ,  $3.0 < y^\Upsilon < 3.5$  and  $3.5 < y^\Upsilon < 4.5$  are shown with red circles, blue squares and green diamonds, respectively. The vertical inner error bars indicate the statistical uncertainty, whilst the outer error bars indicate the sum of the statistical and systematic uncertainties added in quadrature. The horizontal error bars indicate the bin width. Some data points are displaced from the bin centers to improve visibility.

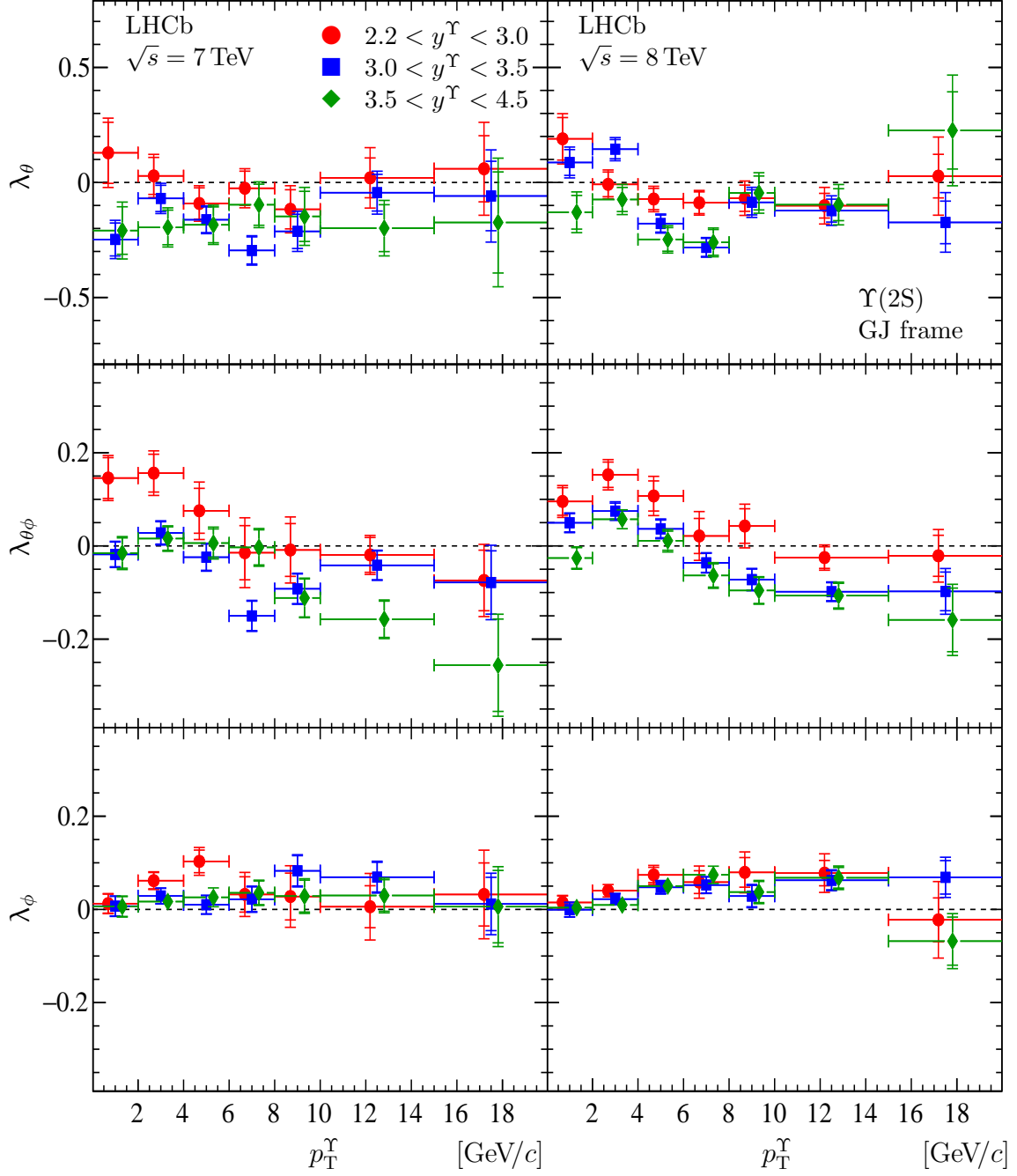


Figure 8: The polarization parameters (top)  $\lambda_\theta$ , (middle)  $\lambda_{\theta\phi}$  and (bottom)  $\lambda_\phi$ , measured in the GJ frame for the  $\Upsilon(2S)$  state in different bins of  $p_T^\Upsilon$  and three rapidity ranges, for data collected at (left)  $\sqrt{s} = 7$  TeV and (right)  $\sqrt{s} = 8$  TeV. The results for the rapidity ranges  $2.2 < y^\Upsilon < 3.0$ ,  $3.0 < y^\Upsilon < 3.5$  and  $3.5 < y^\Upsilon < 4.5$  are shown with red circles, blue squares and green diamonds, respectively. The vertical inner error bars indicate the statistical uncertainty, whilst the outer error bars indicate the sum of the statistical and systematic uncertainties added in quadrature. The horizontal error bars indicate the bin width. Some data points are displaced from the bin centers to improve visibility.

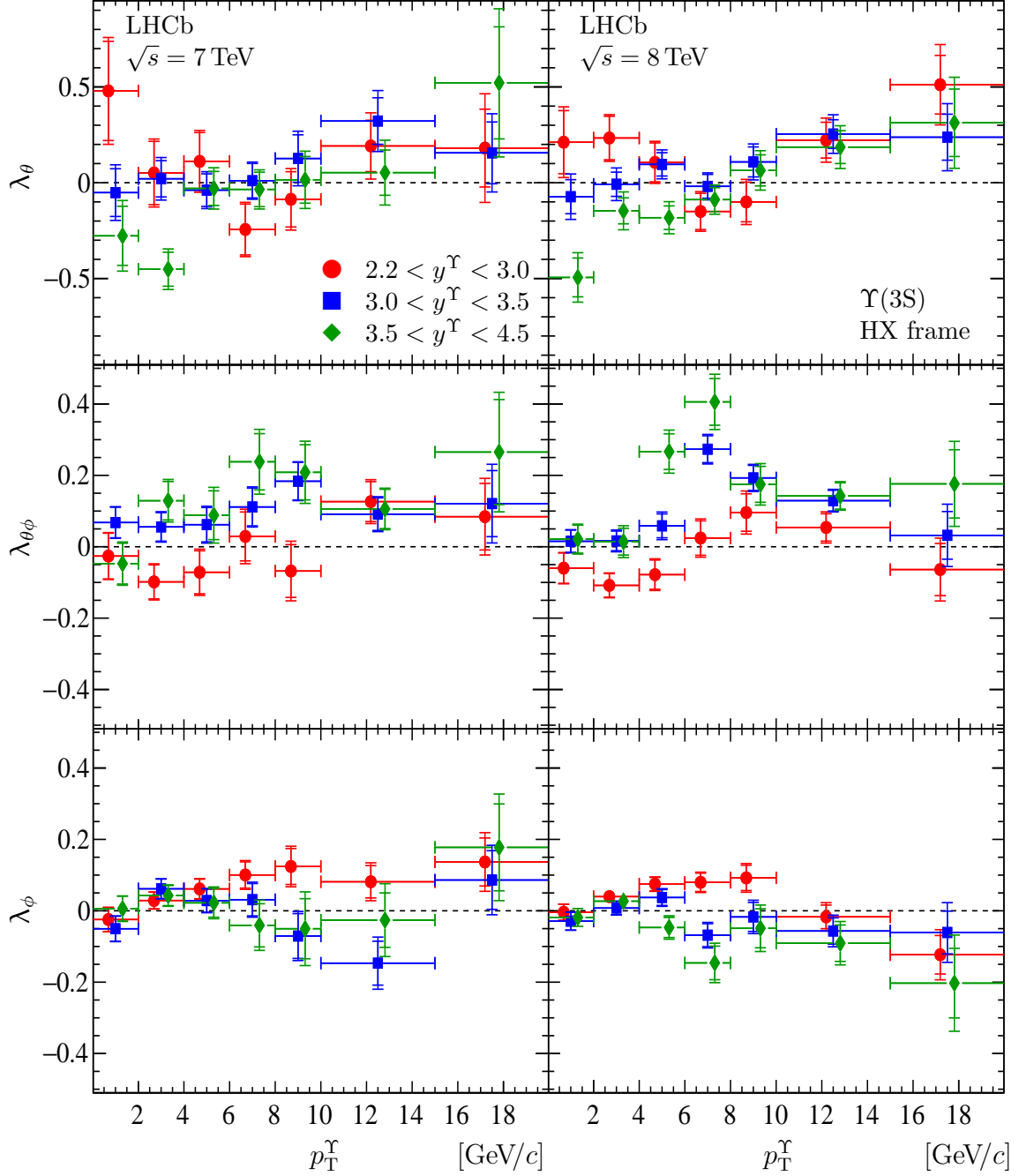


Figure 9: The polarization parameters (top)  $\lambda_\theta$ , (middle)  $\lambda_{\theta\phi}$  and (bottom)  $\lambda_\phi$ , measured in the HX frame for the  $\Upsilon(3S)$  state in different bins of  $p_T^\Upsilon$  and three rapidity ranges, for data collected at (left)  $\sqrt{s} = 7$  TeV and (right)  $\sqrt{s} = 8$  TeV. The results for the rapidity ranges  $2.2 < y^\Upsilon < 3.0$ ,  $3.0 < y^\Upsilon < 3.5$  and  $3.5 < y^\Upsilon < 4.5$  are shown with red circles, blue squares and green diamonds, respectively. The vertical inner error bars indicate the statistical uncertainty, whilst the outer error bars indicate the sum of the statistical and systematic uncertainties added in quadrature. The horizontal error bars indicate the bin width. Some data points are displaced from the bin centers to improve visibility.

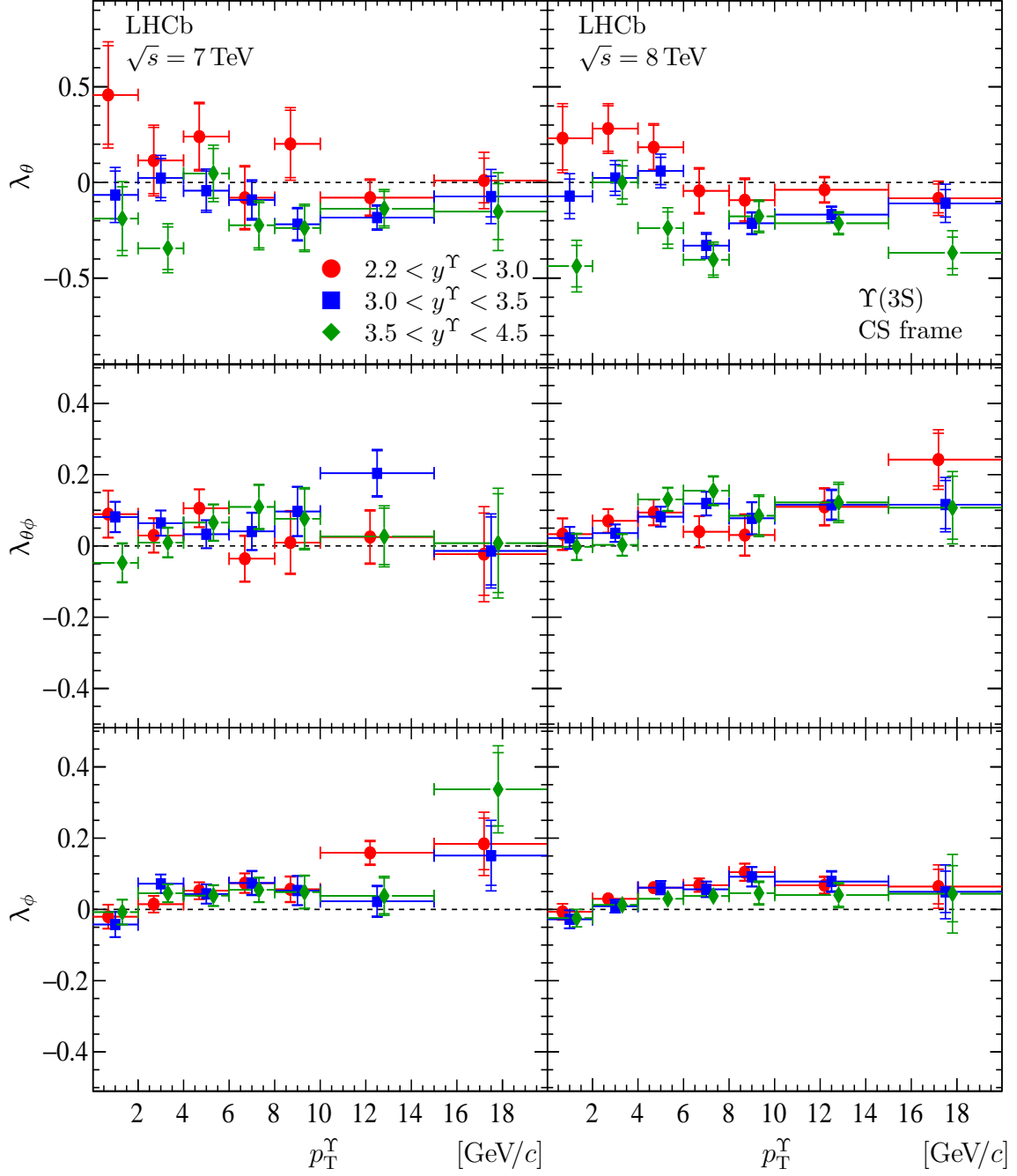


Figure 10: The polarization parameters  $\lambda_\theta$  (top),  $\lambda_{\theta\phi}$  (middle) and  $\lambda_\phi$  (bottom), measured in the CS frame for the  $\Upsilon(3S)$  state in different bins of  $p_T^\Upsilon$  and three rapidity ranges, for data collected at  $\sqrt{s} = 7$  TeV (left) and  $\sqrt{s} = 8$  TeV (right). The results for the rapidity ranges  $2.2 < y^\Upsilon < 3.0$ ,  $3.0 < y^\Upsilon < 3.5$  and  $3.5 < y^\Upsilon < 4.5$  are shown with red circles, blue squares and green diamonds, respectively. The vertical inner error bars indicate the statistical uncertainty, whilst the outer error bars indicate the sum of the statistical and systematic uncertainties added in quadrature. The horizontal error bars indicate the bin width. Some data points are displaced from the bin centers to improve visibility.

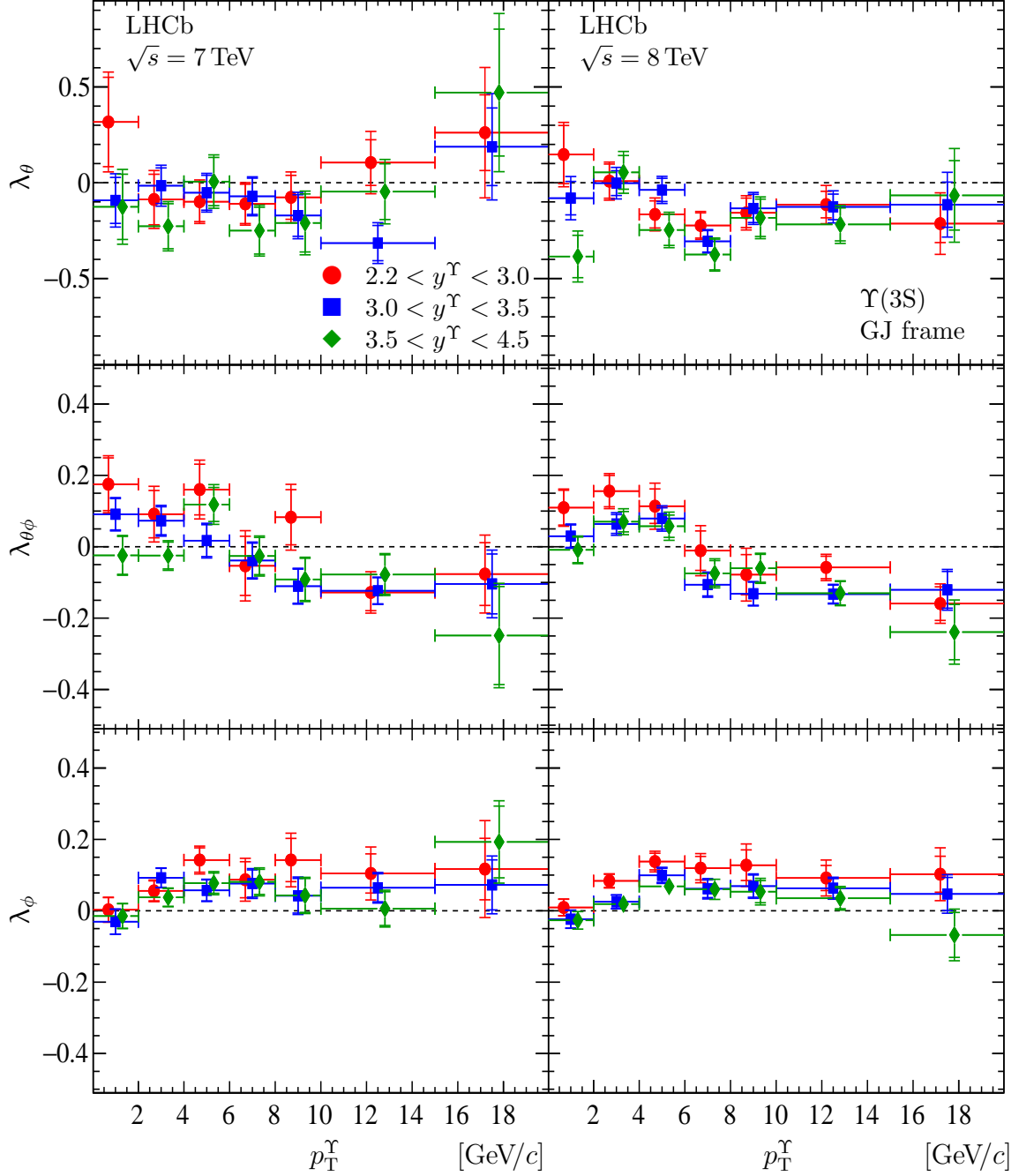


Figure 11: The polarization parameters  $\lambda_\theta$  (top),  $\lambda_{\theta\phi}$  (middle) and  $\lambda_\phi$  (bottom), measured in the GJ frame for the  $\Upsilon(3S)$  state in different bins of  $p_T^\Upsilon$  and three rapidity ranges, for data collected at  $\sqrt{s} = 7$  TeV (left) and  $\sqrt{s} = 8$  TeV (right). The results for the rapidity ranges  $2.2 < y^\Upsilon < 3.0$ ,  $3.0 < y^\Upsilon < 3.5$  and  $3.5 < y^\Upsilon < 4.5$  are shown with red circles, blue squares and green diamonds, respectively. The vertical inner error bars indicate the statistical uncertainty, whilst the outer error bars indicate the sum of the statistical and systematic uncertainties added in quadrature. The horizontal error bars indicate the bin width. Some data points are displaced from the bin centers to improve visibility.

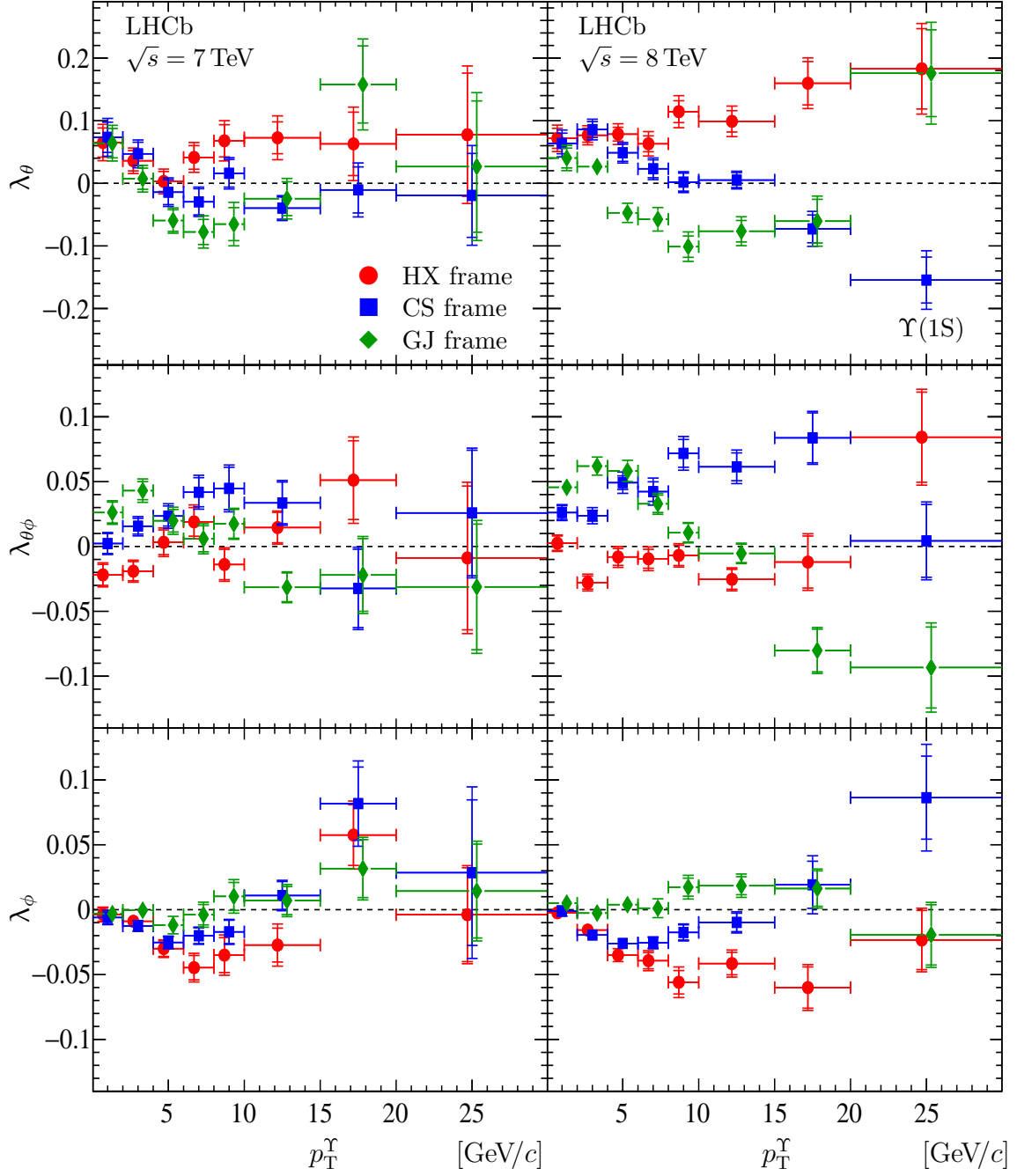


Figure 12: The polarization parameters (top)  $\lambda_\theta$ , (middle)  $\lambda_{\theta\phi}$  and (bottom)  $\lambda_\phi$ , for  $\Upsilon(1S)$  mesons as a function of  $p_T^\Upsilon$ , for the rapidity range  $2.2 < y^\Upsilon < 4.5$ , for data collected at (left)  $\sqrt{s} = 7 \text{ TeV}$  and (right)  $\sqrt{s} = 8 \text{ TeV}$ . The results for the HX, CS and GJ frames are shown with red circles, blue squares and green diamonds, respectively. The inner error bars indicate the statistical uncertainty, whilst the outer error bars indicate the sum of the statistical and systematic uncertainties added in quadrature. Some data points are displaced from the bin centers to improve visibility.

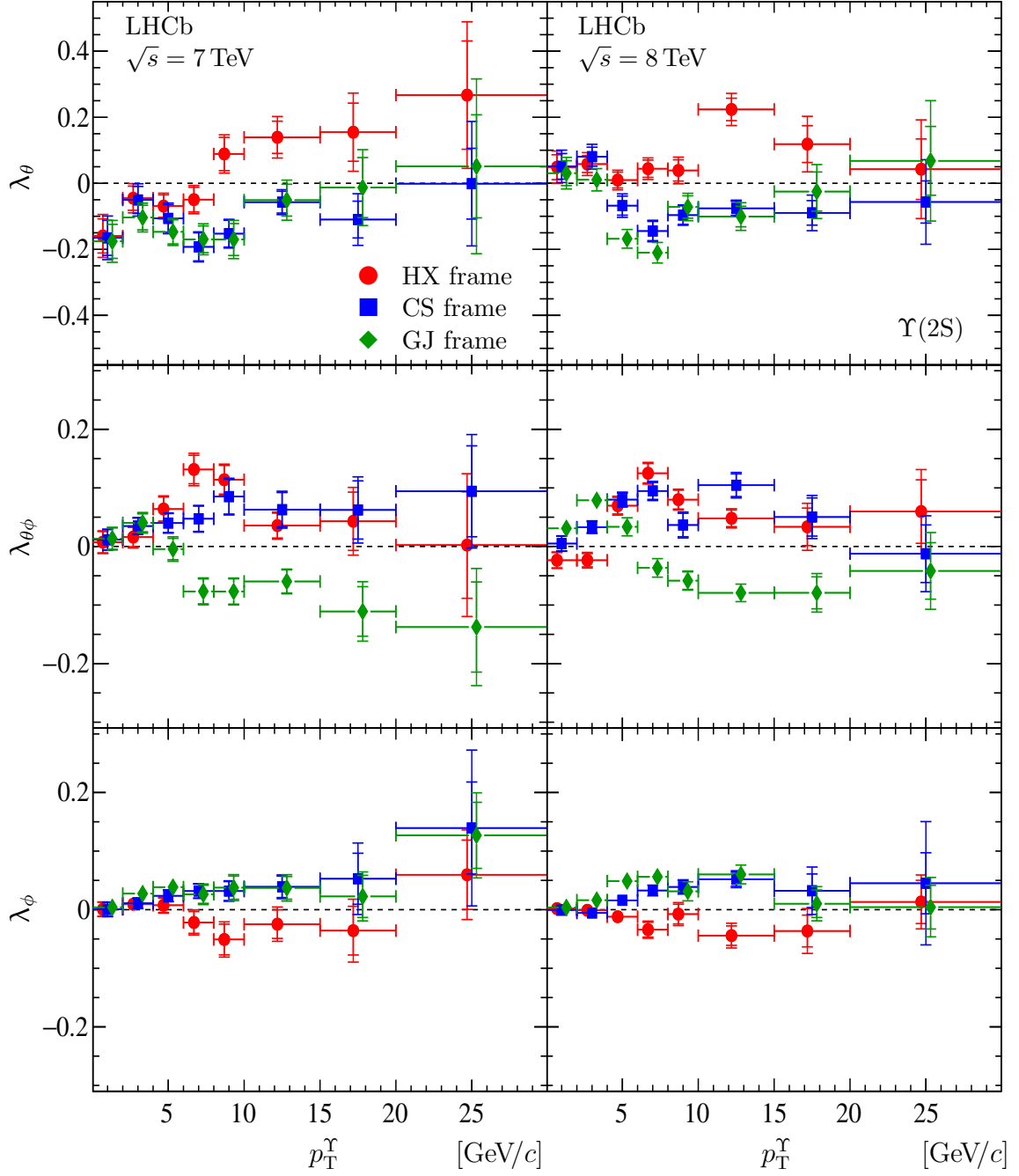


Figure 13: The polarization parameters (top)  $\lambda_\theta$ , (middle)  $\lambda_{\theta\phi}$  and (bottom)  $\lambda_\phi$ , for  $\Upsilon(2S)$  mesons as a function of  $p_T^\Upsilon$ , for the rapidity range  $2.2 < y^\Upsilon < 4.5$ , for data collected at (left)  $\sqrt{s} = 7$  TeV and (right)  $\sqrt{s} = 8$  TeV. The results for the HX, CS and GJ frames are shown with red circles, blue squares and green diamonds, respectively. The inner error bars indicate the statistical uncertainty, whilst the outer error bars indicate the sum of the statistical and systematic uncertainties added in quadrature. Some data points are displaced from the bin centers to improve visibility.

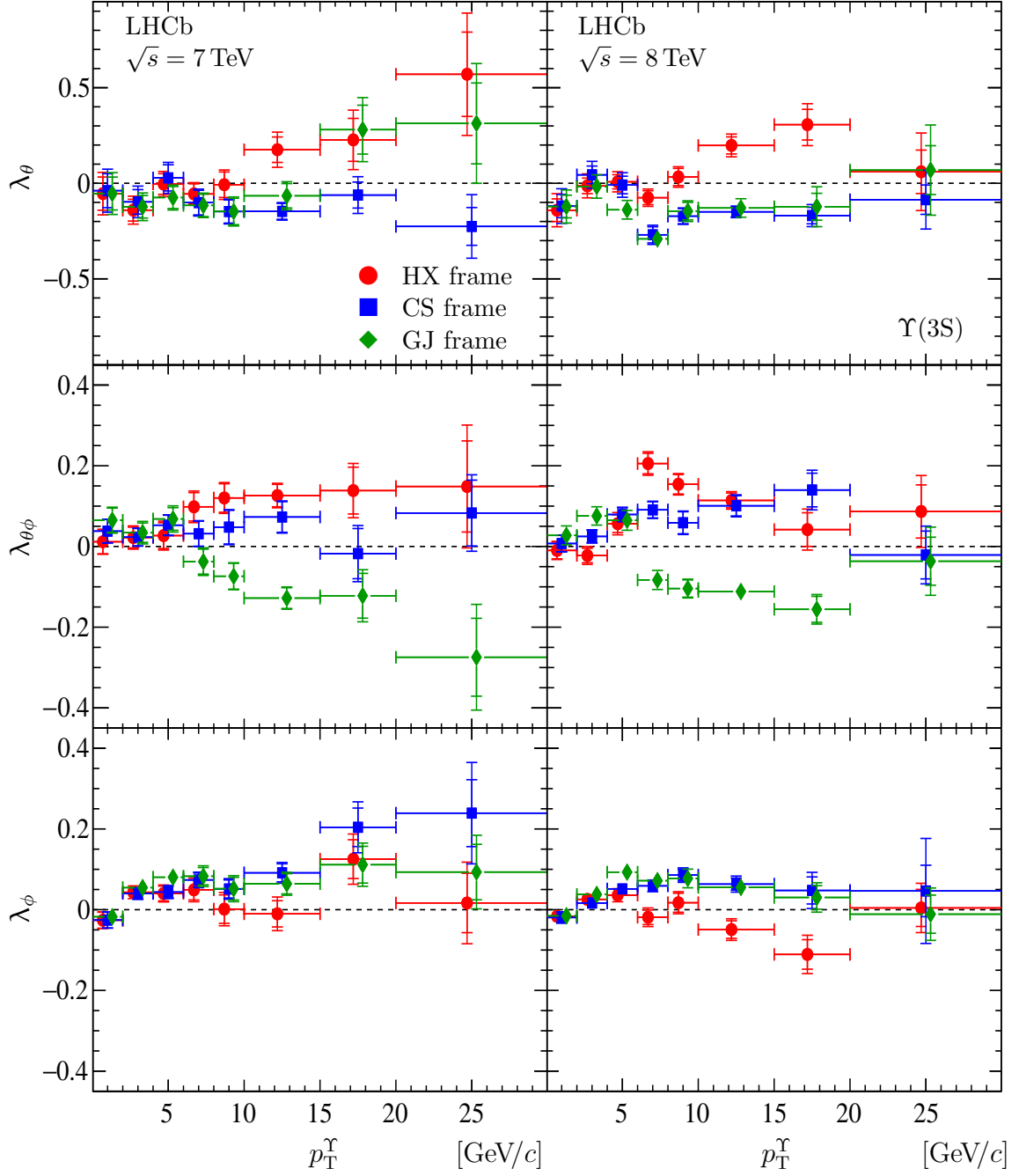


Figure 14: The polarization parameters (top)  $\lambda_\theta$ , (middle)  $\lambda_{\theta\phi}$  and (bottom)  $\lambda_\phi$ , for  $\Upsilon(3S)$  mesons as a function of  $p_T^\Upsilon$ , for the rapidity range  $2.2 < y^\Upsilon < 4.5$ , for data collected at (left)  $\sqrt{s} = 7$  TeV and (right)  $\sqrt{s} = 8$  TeV. The results for the HX, CS and GJ frames are shown with red circles, blue squares and green diamonds, respectively. The inner error bars indicate the statistical uncertainty, whilst the outer error bars indicate the sum of the statistical and systematic uncertainties added in quadrature. Some data points are displaced from the bin centers to improve visibility.



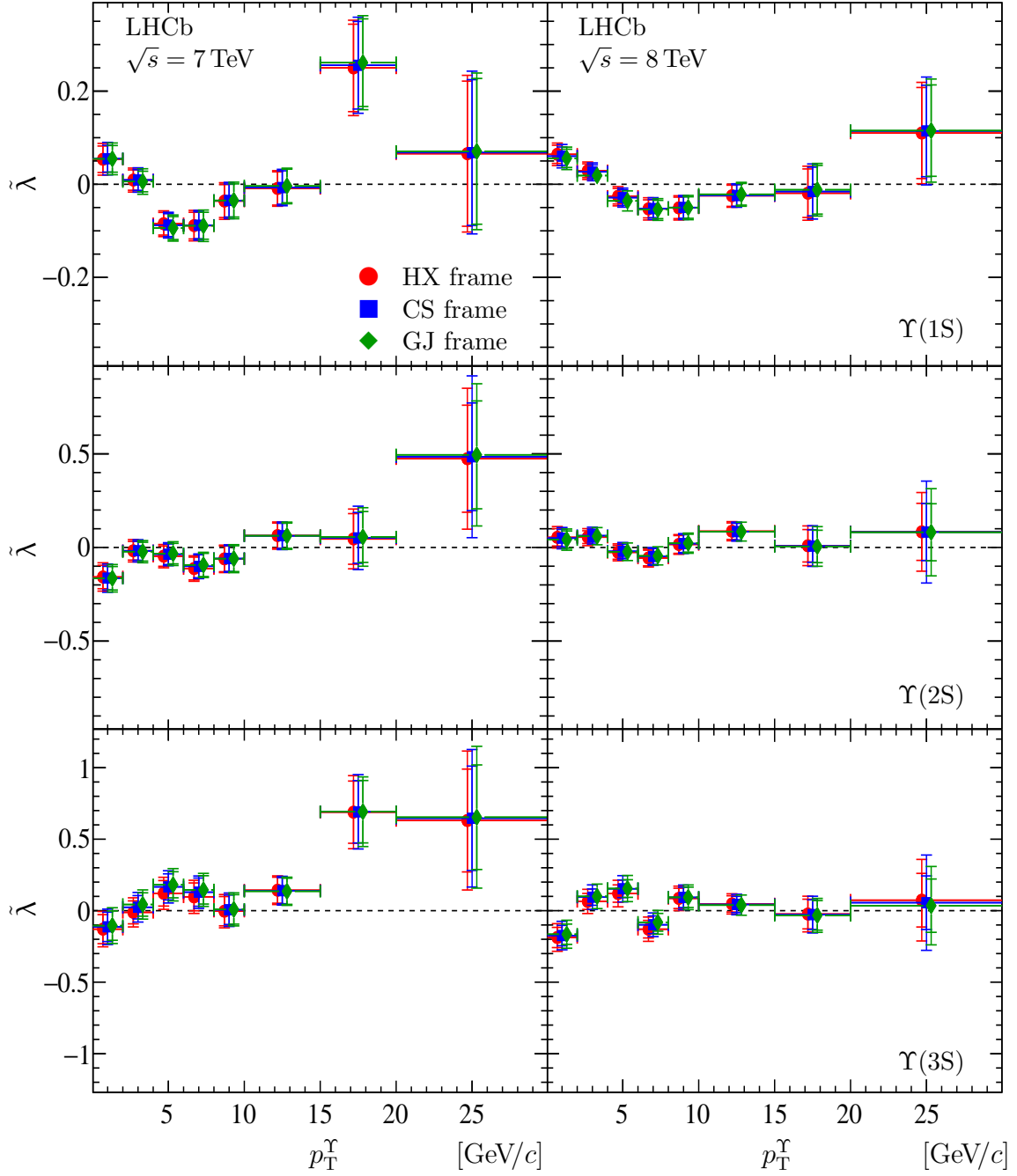


Figure 15: The polarization parameter  $\tilde{\lambda}$  for (top)  $\Upsilon(1S)$  mesons, (middle)  $\Upsilon(2S)$  mesons and (bottom)  $\Upsilon(3S)$  mesons as a function of  $p_T^\Upsilon$ , for the rapidity range  $2.2 < y^\Upsilon < 4.5$ , for data collected at (left)  $\sqrt{s} = 7$  TeV and (right)  $\sqrt{s} = 8$  TeV. The results for the HX, CS and GJ frames are shown with red circles, blue squares and green diamonds, respectively. The inner error bars indicate the statistical uncertainty, whilst the outer error bars indicate the sum of the statistical and systematic uncertainties added in quadrature. Some data points are displaced from the bin centers to improve visibility.

# Appendices

## A Polarization results for the $\Upsilon(1S)$ state

Values of the polarization parameters  $\lambda$  and  $\tilde{\lambda}$  for the  $\Upsilon(1S)$  meson are presented in Tables 2 and 3 for the HX frame, in Tables 4 and 5 for the CS frame and in Tables 6 and 7 for the GJ frame for  $\sqrt{s} = 7$  and 8 TeV, respectively. The polarization parameters  $\lambda$  measured in the wide rapidity bin  $2.2 < y^\Upsilon < 4.5$  are presented in Tables 8 and 9, while the parameters  $\tilde{\lambda}$  are listed in Table 10.

Table 2: Values of  $\lambda_\theta$ ,  $\lambda_{\theta\phi}$ ,  $\lambda_\phi$  and  $\tilde{\lambda}$  measured in the HX frame for the  $\Upsilon(1S)$  produced at  $\sqrt{s} = 7$  TeV. The first uncertainty is statistical and the second systematic.

$p_T^\Upsilon$ [GeV/c]	$\lambda$	$2.2 < y < 3.0$	$3.0 < y < 3.5$	$3.5 < y < 4.5$
0 – 2	$\lambda_\theta$	$0.220 \pm 0.063 \pm 0.042$	$0.104 \pm 0.034 \pm 0.027$	$-0.098 \pm 0.043 \pm 0.035$
	$\lambda_{\theta\phi}$	$-0.039 \pm 0.016 \pm 0.007$	$-0.041 \pm 0.012 \pm 0.006$	$0.041 \pm 0.016 \pm 0.010$
	$\lambda_\phi$	$0.009 \pm 0.008 \pm 0.004$	$-0.004 \pm 0.009 \pm 0.005$	$-0.024 \pm 0.009 \pm 0.004$
	$\tilde{\lambda}$	$0.249 \pm 0.069 \pm 0.045$	$0.092 \pm 0.045 \pm 0.032$	$-0.167 \pm 0.051 \pm 0.036$
2 – 4	$\lambda_\theta$	$0.175 \pm 0.045 \pm 0.025$	$0.053 \pm 0.025 \pm 0.020$	$-0.057 \pm 0.028 \pm 0.027$
	$\lambda_{\theta\phi}$	$-0.075 \pm 0.014 \pm 0.007$	$-0.009 \pm 0.011 \pm 0.006$	$0.034 \pm 0.016 \pm 0.015$
	$\lambda_\phi$	$0.000 \pm 0.007 \pm 0.002$	$-0.002 \pm 0.007 \pm 0.003$	$-0.033 \pm 0.009 \pm 0.005$
	$\tilde{\lambda}$	$0.176 \pm 0.051 \pm 0.029$	$0.047 \pm 0.036 \pm 0.026$	$-0.151 \pm 0.039 \pm 0.036$
4 – 6	$\lambda_\theta$	$0.069 \pm 0.045 \pm 0.037$	$0.055 \pm 0.026 \pm 0.017$	$-0.077 \pm 0.025 \pm 0.021$
	$\lambda_{\theta\phi}$	$-0.069 \pm 0.019 \pm 0.015$	$0.009 \pm 0.014 \pm 0.009$	$0.078 \pm 0.020 \pm 0.016$
	$\lambda_\phi$	$-0.006 \pm 0.009 \pm 0.005$	$-0.041 \pm 0.011 \pm 0.006$	$-0.053 \pm 0.013 \pm 0.008$
	$\tilde{\lambda}$	$0.050 \pm 0.057 \pm 0.045$	$-0.066 \pm 0.040 \pm 0.025$	$-0.223 \pm 0.044 \pm 0.035$
6 – 8	$\lambda_\theta$	$0.057 \pm 0.049 \pm 0.034$	$0.036 \pm 0.031 \pm 0.024$	$0.062 \pm 0.032 \pm 0.026$
	$\lambda_{\theta\phi}$	$-0.029 \pm 0.024 \pm 0.023$	$0.021 \pm 0.016 \pm 0.009$	$0.060 \pm 0.023 \pm 0.017$
	$\lambda_\phi$	$-0.030 \pm 0.015 \pm 0.013$	$-0.055 \pm 0.016 \pm 0.010$	$-0.048 \pm 0.021 \pm 0.019$
	$\tilde{\lambda}$	$-0.031 \pm 0.064 \pm 0.054$	$-0.121 \pm 0.047 \pm 0.025$	$-0.079 \pm 0.056 \pm 0.041$
8 – 10	$\lambda_\theta$	$0.076 \pm 0.059 \pm 0.044$	$0.117 \pm 0.044 \pm 0.034$	$0.076 \pm 0.047 \pm 0.039$
	$\lambda_{\theta\phi}$	$-0.068 \pm 0.027 \pm 0.016$	$-0.022 \pm 0.018 \pm 0.006$	$0.035 \pm 0.023 \pm 0.012$
	$\lambda_\phi$	$-0.004 \pm 0.021 \pm 0.011$	$-0.048 \pm 0.023 \pm 0.014$	$-0.062 \pm 0.031 \pm 0.024$
	$\tilde{\lambda}$	$0.065 \pm 0.077 \pm 0.045$	$-0.024 \pm 0.059 \pm 0.024$	$-0.103 \pm 0.070 \pm 0.038$
10 – 15	$\lambda_\theta$	$-0.021 \pm 0.051 \pm 0.029$	$0.123 \pm 0.042 \pm 0.030$	$0.135 \pm 0.051 \pm 0.048$
	$\lambda_{\theta\phi}$	$-0.009 \pm 0.023 \pm 0.010$	$-0.003 \pm 0.019 \pm 0.009$	$0.070 \pm 0.024 \pm 0.007$
	$\lambda_\phi$	$0.009 \pm 0.019 \pm 0.010$	$-0.059 \pm 0.022 \pm 0.013$	$-0.047 \pm 0.031 \pm 0.024$
	$\tilde{\lambda}$	$0.006 \pm 0.064 \pm 0.026$	$-0.052 \pm 0.060 \pm 0.026$	$-0.005 \pm 0.076 \pm 0.033$
15 – 20	$\lambda_\theta$	$0.032 \pm 0.091 \pm 0.045$	$0.046 \pm 0.077 \pm 0.049$	$0.082 \pm 0.111 \pm 0.058$
	$\lambda_{\theta\phi}$	$0.096 \pm 0.048 \pm 0.015$	$0.007 \pm 0.050 \pm 0.022$	$0.104 \pm 0.072 \pm 0.027$
	$\lambda_\phi$	$0.008 \pm 0.033 \pm 0.013$	$0.099 \pm 0.040 \pm 0.018$	$0.119 \pm 0.058 \pm 0.022$
	$\tilde{\lambda}$	$0.055 \pm 0.130 \pm 0.044$	$0.382 \pm 0.175 \pm 0.083$	$0.500 \pm 0.252 \pm 0.094$

Table 3: Values of  $\lambda_\theta$ ,  $\lambda_{\theta\phi}$ ,  $\lambda_\phi$  and  $\tilde{\lambda}$  measured in the HX frame for the  $\Upsilon(1S)$  produced at  $\sqrt{s} = 8$  TeV. The first uncertainty is statistical and the second systematic.

$p_T^\Upsilon$ [GeV/c]	$\lambda$	$2.2 < y < 3.0$	$3.0 < y < 3.5$	$3.5 < y < 4.5$
0 – 2	$\lambda_\theta$	$0.190 \pm 0.042 \pm 0.030$	$0.092 \pm 0.023 \pm 0.020$	$0.012 \pm 0.030 \pm 0.031$
	$\lambda_{\theta\phi}$	$-0.009 \pm 0.011 \pm 0.005$	$0.019 \pm 0.008 \pm 0.004$	$-0.013 \pm 0.011 \pm 0.007$
	$\lambda_\phi$	$-0.007 \pm 0.006 \pm 0.003$	$0.002 \pm 0.006 \pm 0.003$	$0.001 \pm 0.006 \pm 0.003$
	$\tilde{\lambda}$	$0.168 \pm 0.046 \pm 0.032$	$0.098 \pm 0.031 \pm 0.023$	$0.014 \pm 0.037 \pm 0.033$
2 – 4	$\lambda_\theta$	$0.208 \pm 0.030 \pm 0.028$	$0.104 \pm 0.017 \pm 0.014$	$-0.017 \pm 0.019 \pm 0.021$
	$\lambda_{\theta\phi}$	$-0.077 \pm 0.009 \pm 0.007$	$-0.023 \pm 0.008 \pm 0.005$	$0.020 \pm 0.011 \pm 0.010$
	$\lambda_\phi$	$-0.006 \pm 0.004 \pm 0.002$	$-0.026 \pm 0.005 \pm 0.003$	$-0.020 \pm 0.006 \pm 0.004$
	$\tilde{\lambda}$	$0.189 \pm 0.035 \pm 0.030$	$0.025 \pm 0.024 \pm 0.017$	$-0.076 \pm 0.027 \pm 0.028$
4 – 6	$\lambda_\theta$	$0.179 \pm 0.031 \pm 0.025$	$0.102 \pm 0.018 \pm 0.014$	$0.035 \pm 0.018 \pm 0.017$
	$\lambda_{\theta\phi}$	$-0.057 \pm 0.013 \pm 0.010$	$-0.012 \pm 0.010 \pm 0.007$	$0.040 \pm 0.014 \pm 0.014$
	$\lambda_\phi$	$-0.026 \pm 0.006 \pm 0.004$	$-0.030 \pm 0.007 \pm 0.004$	$-0.054 \pm 0.009 \pm 0.008$
	$\tilde{\lambda}$	$0.098 \pm 0.038 \pm 0.031$	$0.012 \pm 0.028 \pm 0.020$	$-0.119 \pm 0.031 \pm 0.030$
6 – 8	$\lambda_\theta$	$0.129 \pm 0.033 \pm 0.025$	$0.084 \pm 0.021 \pm 0.017$	$0.038 \pm 0.021 \pm 0.017$
	$\lambda_{\theta\phi}$	$-0.060 \pm 0.016 \pm 0.012$	$-0.020 \pm 0.011 \pm 0.008$	$0.040 \pm 0.015 \pm 0.014$
	$\lambda_\phi$	$-0.040 \pm 0.010 \pm 0.007$	$-0.031 \pm 0.011 \pm 0.007$	$-0.039 \pm 0.013 \pm 0.012$
	$\tilde{\lambda}$	$0.009 \pm 0.044 \pm 0.030$	$-0.007 \pm 0.033 \pm 0.020$	$-0.077 \pm 0.037 \pm 0.029$
8 – 10	$\lambda_\theta$	$0.097 \pm 0.040 \pm 0.030$	$0.129 \pm 0.030 \pm 0.022$	$0.180 \pm 0.033 \pm 0.037$
	$\lambda_{\theta\phi}$	$-0.048 \pm 0.018 \pm 0.011$	$-0.027 \pm 0.012 \pm 0.006$	$0.059 \pm 0.016 \pm 0.010$
	$\lambda_\phi$	$-0.030 \pm 0.015 \pm 0.011$	$-0.062 \pm 0.015 \pm 0.009$	$-0.099 \pm 0.021 \pm 0.022$
	$\tilde{\lambda}$	$0.007 \pm 0.050 \pm 0.030$	$-0.052 \pm 0.039 \pm 0.015$	$-0.107 \pm 0.045 \pm 0.033$
10 – 15	$\lambda_\theta$	$0.124 \pm 0.036 \pm 0.030$	$0.086 \pm 0.027 \pm 0.020$	$0.146 \pm 0.033 \pm 0.037$
	$\lambda_{\theta\phi}$	$-0.069 \pm 0.016 \pm 0.008$	$-0.009 \pm 0.013 \pm 0.007$	$-0.012 \pm 0.015 \pm 0.007$
	$\lambda_\phi$	$-0.042 \pm 0.013 \pm 0.009$	$-0.034 \pm 0.014 \pm 0.008$	$-0.048 \pm 0.020 \pm 0.019$
	$\tilde{\lambda}$	$-0.002 \pm 0.041 \pm 0.022$	$-0.017 \pm 0.040 \pm 0.018$	$0.001 \pm 0.049 \pm 0.031$
15 – 20	$\lambda_\theta$	$0.041 \pm 0.058 \pm 0.036$	$0.239 \pm 0.057 \pm 0.032$	$0.245 \pm 0.077 \pm 0.049$
	$\lambda_{\theta\phi}$	$-0.040 \pm 0.031 \pm 0.015$	$-0.006 \pm 0.034 \pm 0.019$	$0.071 \pm 0.048 \pm 0.027$
	$\lambda_\phi$	$-0.062 \pm 0.022 \pm 0.012$	$-0.044 \pm 0.028 \pm 0.014$	$-0.063 \pm 0.041 \pm 0.025$
	$\tilde{\lambda}$	$-0.137 \pm 0.075 \pm 0.036$	$0.102 \pm 0.098 \pm 0.045$	$0.052 \pm 0.126 \pm 0.067$

Table 4: Values of  $\lambda_\theta$ ,  $\lambda_{\theta\phi}$ ,  $\lambda_\phi$  and  $\tilde{\lambda}$  measured in the CS frame for the  $\Upsilon(1S)$  produced at  $\sqrt{s} = 7$  TeV. The first uncertainty is statistical and the second systematic.

$p_T^\Upsilon$ [GeV/c]	$\lambda$	$2.2 < y < 3.0$	$3.0 < y < 3.5$	$3.5 < y < 4.5$
0 – 2	$\lambda_\theta$	$0.243 \pm 0.063 \pm 0.036$	$0.114 \pm 0.035 \pm 0.026$	$-0.109 \pm 0.046 \pm 0.034$
	$\lambda_{\theta\phi}$	$0.014 \pm 0.016 \pm 0.008$	$-0.017 \pm 0.012 \pm 0.004$	$0.047 \pm 0.014 \pm 0.007$
	$\lambda_\phi$	$0.007 \pm 0.008 \pm 0.003$	$-0.008 \pm 0.009 \pm 0.003$	$-0.021 \pm 0.009 \pm 0.004$
	$\tilde{\lambda}$	$0.265 \pm 0.069 \pm 0.038$	$0.089 \pm 0.046 \pm 0.028$	$-0.168 \pm 0.052 \pm 0.036$
2 – 4	$\lambda_\theta$	$0.238 \pm 0.047 \pm 0.031$	$0.055 \pm 0.028 \pm 0.022$	$-0.084 \pm 0.034 \pm 0.030$
	$\lambda_{\theta\phi}$	$0.022 \pm 0.013 \pm 0.006$	$0.020 \pm 0.010 \pm 0.003$	$0.041 \pm 0.012 \pm 0.006$
	$\lambda_\phi$	$-0.011 \pm 0.006 \pm 0.003$	$-0.002 \pm 0.007 \pm 0.003$	$-0.027 \pm 0.007 \pm 0.003$
	$\tilde{\lambda}$	$0.204 \pm 0.052 \pm 0.033$	$0.048 \pm 0.037 \pm 0.024$	$-0.160 \pm 0.040 \pm 0.033$
4 – 6	$\lambda_\theta$	$0.139 \pm 0.052 \pm 0.030$	$0.008 \pm 0.030 \pm 0.018$	$-0.168 \pm 0.036 \pm 0.021$
	$\lambda_{\theta\phi}$	$0.002 \pm 0.017 \pm 0.008$	$0.049 \pm 0.013 \pm 0.005$	$0.048 \pm 0.015 \pm 0.008$
	$\lambda_\phi$	$-0.026 \pm 0.007 \pm 0.003$	$-0.027 \pm 0.008 \pm 0.003$	$-0.025 \pm 0.008 \pm 0.003$
	$\tilde{\lambda}$	$0.059 \pm 0.058 \pm 0.033$	$-0.072 \pm 0.041 \pm 0.021$	$-0.238 \pm 0.045 \pm 0.024$
6 – 8	$\lambda_\theta$	$0.064 \pm 0.055 \pm 0.025$	$-0.045 \pm 0.030 \pm 0.018$	$-0.083 \pm 0.039 \pm 0.024$
	$\lambda_{\theta\phi}$	$0.020 \pm 0.023 \pm 0.010$	$0.047 \pm 0.019 \pm 0.007$	$0.070 \pm 0.022 \pm 0.009$
	$\lambda_\phi$	$-0.029 \pm 0.010 \pm 0.004$	$-0.028 \pm 0.011 \pm 0.004$	$-0.001 \pm 0.012 \pm 0.005$
	$\tilde{\lambda}$	$-0.023 \pm 0.065 \pm 0.031$	$-0.125 \pm 0.047 \pm 0.022$	$-0.086 \pm 0.057 \pm 0.032$
8 – 10	$\lambda_\theta$	$0.126 \pm 0.059 \pm 0.027$	$0.030 \pm 0.032 \pm 0.018$	$-0.071 \pm 0.041 \pm 0.020$
	$\lambda_{\theta\phi}$	$0.020 \pm 0.034 \pm 0.012$	$0.079 \pm 0.027 \pm 0.009$	$0.064 \pm 0.032 \pm 0.014$
	$\lambda_\phi$	$-0.020 \pm 0.014 \pm 0.005$	$-0.019 \pm 0.016 \pm 0.007$	$-0.011 \pm 0.018 \pm 0.007$
	$\tilde{\lambda}$	$0.063 \pm 0.078 \pm 0.035$	$-0.027 \pm 0.059 \pm 0.026$	$-0.102 \pm 0.070 \pm 0.029$
10 – 15	$\lambda_\theta$	$0.012 \pm 0.038 \pm 0.018$	$-0.039 \pm 0.026 \pm 0.014$	$-0.124 \pm 0.035 \pm 0.017$
	$\lambda_{\theta\phi}$	$-0.037 \pm 0.033 \pm 0.012$	$0.072 \pm 0.026 \pm 0.010$	$0.069 \pm 0.033 \pm 0.015$
	$\lambda_\phi$	$-0.005 \pm 0.017 \pm 0.008$	$-0.003 \pm 0.019 \pm 0.009$	$0.039 \pm 0.022 \pm 0.010$
	$\tilde{\lambda}$	$-0.004 \pm 0.063 \pm 0.022$	$-0.049 \pm 0.060 \pm 0.024$	$-0.009 \pm 0.077 \pm 0.035$
15 – 20	$\lambda_\theta$	$-0.112 \pm 0.054 \pm 0.031$	$0.088 \pm 0.064 \pm 0.044$	$-0.002 \pm 0.087 \pm 0.060$
	$\lambda_{\theta\phi}$	$-0.048 \pm 0.053 \pm 0.021$	$-0.030 \pm 0.048 \pm 0.016$	$-0.087 \pm 0.069 \pm 0.021$
	$\lambda_\phi$	$0.053 \pm 0.041 \pm 0.025$	$0.092 \pm 0.050 \pm 0.030$	$0.147 \pm 0.065 \pm 0.032$
	$\tilde{\lambda}$	$0.049 \pm 0.129 \pm 0.061$	$0.401 \pm 0.176 \pm 0.079$	$0.514 \pm 0.253 \pm 0.090$

Table 5: Values of  $\lambda_\theta$ ,  $\lambda_{\theta\phi}$ ,  $\lambda_\phi$  and  $\tilde{\lambda}$  measured in the CS frame for the  $\Upsilon(1S)$  produced at  $\sqrt{s} = 8$  TeV. The first uncertainty is statistical and the second systematic.

$p_T^\Upsilon$ [GeV/c]	$\lambda$	$2.2 < y < 3.0$	$3.0 < y < 3.5$	$3.5 < y < 4.5$
0 – 2	$\lambda_\theta$	$0.190 \pm 0.042 \pm 0.030$	$0.078 \pm 0.024 \pm 0.021$	$0.002 \pm 0.032 \pm 0.031$
	$\lambda_{\theta\phi}$	$0.038 \pm 0.011 \pm 0.006$	$0.039 \pm 0.008 \pm 0.004$	$0.007 \pm 0.010 \pm 0.005$
	$\lambda_\phi$	$-0.005 \pm 0.006 \pm 0.002$	$0.006 \pm 0.006 \pm 0.003$	$-0.001 \pm 0.006 \pm 0.003$
	$\tilde{\lambda}$	$0.173 \pm 0.046 \pm 0.031$	$0.096 \pm 0.031 \pm 0.024$	$-0.003 \pm 0.037 \pm 0.033$
2 – 4	$\lambda_\theta$	$0.251 \pm 0.032 \pm 0.022$	$0.109 \pm 0.019 \pm 0.014$	$-0.045 \pm 0.024 \pm 0.024$
	$\lambda_{\theta\phi}$	$0.029 \pm 0.009 \pm 0.006$	$0.031 \pm 0.007 \pm 0.003$	$0.043 \pm 0.008 \pm 0.005$
	$\lambda_\phi$	$-0.015 \pm 0.004 \pm 0.002$	$-0.027 \pm 0.005 \pm 0.002$	$-0.017 \pm 0.005 \pm 0.002$
	$\tilde{\lambda}$	$0.202 \pm 0.035 \pm 0.023$	$0.027 \pm 0.024 \pm 0.017$	$-0.095 \pm 0.028 \pm 0.025$
4 – 6	$\lambda_\theta$	$0.197 \pm 0.034 \pm 0.021$	$0.071 \pm 0.021 \pm 0.015$	$-0.049 \pm 0.025 \pm 0.025$
	$\lambda_{\theta\phi}$	$0.066 \pm 0.011 \pm 0.006$	$0.052 \pm 0.009 \pm 0.004$	$0.067 \pm 0.010 \pm 0.006$
	$\lambda_\phi$	$-0.026 \pm 0.005 \pm 0.003$	$-0.021 \pm 0.006 \pm 0.003$	$-0.028 \pm 0.006 \pm 0.003$
	$\tilde{\lambda}$	$0.116 \pm 0.039 \pm 0.026$	$0.008 \pm 0.028 \pm 0.018$	$-0.130 \pm 0.031 \pm 0.027$
6 – 8	$\lambda_\theta$	$0.125 \pm 0.038 \pm 0.021$	$0.051 \pm 0.021 \pm 0.017$	$-0.062 \pm 0.026 \pm 0.021$
	$\lambda_{\theta\phi}$	$0.048 \pm 0.016 \pm 0.008$	$0.049 \pm 0.013 \pm 0.004$	$0.050 \pm 0.014 \pm 0.008$
	$\lambda_\phi$	$-0.040 \pm 0.007 \pm 0.003$	$-0.020 \pm 0.008 \pm 0.003$	$-0.007 \pm 0.008 \pm 0.004$
	$\tilde{\lambda}$	$0.006 \pm 0.044 \pm 0.026$	$-0.010 \pm 0.033 \pm 0.021$	$-0.082 \pm 0.038 \pm 0.027$
8 – 10	$\lambda_\theta$	$0.069 \pm 0.038 \pm 0.020$	$0.030 \pm 0.021 \pm 0.012$	$-0.100 \pm 0.027 \pm 0.015$
	$\lambda_{\theta\phi}$	$0.035 \pm 0.022 \pm 0.010$	$0.086 \pm 0.018 \pm 0.007$	$0.123 \pm 0.021 \pm 0.011$
	$\lambda_\phi$	$-0.025 \pm 0.009 \pm 0.004$	$-0.028 \pm 0.011 \pm 0.005$	$-0.002 \pm 0.011 \pm 0.005$
	$\tilde{\lambda}$	$-0.006 \pm 0.050 \pm 0.027$	$-0.053 \pm 0.039 \pm 0.018$	$-0.106 \pm 0.045 \pm 0.024$
10 – 15	$\lambda_\theta$	$0.058 \pm 0.025 \pm 0.014$	$-0.012 \pm 0.018 \pm 0.011$	$-0.017 \pm 0.024 \pm 0.014$
	$\lambda_{\theta\phi}$	$0.069 \pm 0.022 \pm 0.009$	$0.048 \pm 0.017 \pm 0.007$	$0.090 \pm 0.022 \pm 0.009$
	$\lambda_\phi$	$-0.026 \pm 0.011 \pm 0.006$	$-0.001 \pm 0.013 \pm 0.007$	$0.005 \pm 0.014 \pm 0.008$
	$\tilde{\lambda}$	$-0.019 \pm 0.040 \pm 0.022$	$-0.014 \pm 0.040 \pm 0.019$	$-0.001 \pm 0.049 \pm 0.028$
15 – 20	$\lambda_\theta$	$-0.032 \pm 0.037 \pm 0.023$	$-0.068 \pm 0.036 \pm 0.027$	$-0.176 \pm 0.046 \pm 0.035$
	$\lambda_{\theta\phi}$	$0.049 \pm 0.035 \pm 0.013$	$0.105 \pm 0.030 \pm 0.013$	$0.072 \pm 0.043 \pm 0.020$
	$\lambda_\phi$	$-0.038 \pm 0.028 \pm 0.020$	$0.055 \pm 0.031 \pm 0.019$	$0.080 \pm 0.040 \pm 0.030$
	$\tilde{\lambda}$	$-0.140 \pm 0.075 \pm 0.043$	$0.102 \pm 0.098 \pm 0.046$	$0.068 \pm 0.127 \pm 0.071$

Table 6: Values of  $\lambda_\theta$ ,  $\lambda_{\theta\phi}$ ,  $\lambda_\phi$  and  $\tilde{\lambda}$  measured in the GJ frame for the  $\Upsilon(1S)$  produced at  $\sqrt{s} = 7$  TeV. The first uncertainty is statistical and the second systematic.

$p_T^\Upsilon$ [GeV/c]	$\lambda$	$2.2 < y < 3.0$	$3.0 < y < 3.5$	$3.5 < y < 4.5$
0 – 2	$\lambda_\theta$	$0.218 \pm 0.057 \pm 0.042$	$0.106 \pm 0.034 \pm 0.022$	$-0.120 \pm 0.046 \pm 0.037$
	$\lambda_{\theta\phi}$	$0.064 \pm 0.019 \pm 0.014$	$0.007 \pm 0.012 \pm 0.005$	$0.050 \pm 0.014 \pm 0.007$
	$\lambda_\phi$	$0.014 \pm 0.009 \pm 0.005$	$-0.008 \pm 0.009 \pm 0.004$	$-0.014 \pm 0.009 \pm 0.004$
	$\tilde{\lambda}$	$0.264 \pm 0.067 \pm 0.048$	$0.082 \pm 0.045 \pm 0.025$	$-0.161 \pm 0.052 \pm 0.040$
2 – 4	$\lambda_\theta$	$0.153 \pm 0.036 \pm 0.032$	$0.018 \pm 0.026 \pm 0.017$	$-0.125 \pm 0.034 \pm 0.027$
	$\lambda_{\theta\phi}$	$0.108 \pm 0.019 \pm 0.019$	$0.041 \pm 0.011 \pm 0.005$	$0.034 \pm 0.011 \pm 0.006$
	$\lambda_\phi$	$0.017 \pm 0.008 \pm 0.006$	$0.009 \pm 0.007 \pm 0.003$	$-0.014 \pm 0.007 \pm 0.003$
	$\tilde{\lambda}$	$0.208 \pm 0.052 \pm 0.049$	$0.046 \pm 0.037 \pm 0.022$	$-0.166 \pm 0.040 \pm 0.030$
4 – 6	$\lambda_\theta$	$0.065 \pm 0.033 \pm 0.025$	$-0.072 \pm 0.026 \pm 0.017$	$-0.201 \pm 0.036 \pm 0.023$
	$\lambda_{\theta\phi}$	$0.066 \pm 0.024 \pm 0.029$	$0.041 \pm 0.013 \pm 0.005$	$-0.025 \pm 0.014 \pm 0.008$
	$\lambda_\phi$	$-0.005 \pm 0.013 \pm 0.015$	$-0.003 \pm 0.009 \pm 0.004$	$-0.018 \pm 0.009 \pm 0.004$
	$\tilde{\lambda}$	$0.048 \pm 0.058 \pm 0.064$	$-0.079 \pm 0.041 \pm 0.021$	$-0.250 \pm 0.045 \pm 0.027$
6 – 8	$\lambda_\theta$	$0.008 \pm 0.036 \pm 0.022$	$-0.101 \pm 0.031 \pm 0.017$	$-0.144 \pm 0.042 \pm 0.026$
	$\lambda_{\theta\phi}$	$0.045 \pm 0.027 \pm 0.030$	$0.002 \pm 0.015 \pm 0.008$	$-0.020 \pm 0.018 \pm 0.009$
	$\lambda_\phi$	$-0.012 \pm 0.020 \pm 0.022$	$-0.010 \pm 0.013 \pm 0.007$	$0.017 \pm 0.013 \pm 0.006$
	$\tilde{\lambda}$	$-0.027 \pm 0.066 \pm 0.063$	$-0.129 \pm 0.047 \pm 0.022$	$-0.093 \pm 0.057 \pm 0.031$
8 – 10	$\lambda_\theta$	$0.019 \pm 0.048 \pm 0.040$	$-0.119 \pm 0.042 \pm 0.030$	$-0.120 \pm 0.056 \pm 0.035$
	$\lambda_{\theta\phi}$	$0.068 \pm 0.027 \pm 0.020$	$0.026 \pm 0.016 \pm 0.006$	$-0.028 \pm 0.021 \pm 0.008$
	$\lambda_\phi$	$0.012 \pm 0.027 \pm 0.028$	$0.030 \pm 0.018 \pm 0.008$	$0.006 \pm 0.018 \pm 0.008$
	$\tilde{\lambda}$	$0.054 \pm 0.077 \pm 0.059$	$-0.029 \pm 0.060 \pm 0.021$	$-0.103 \pm 0.070 \pm 0.029$
10 – 15	$\lambda_\theta$	$0.088 \pm 0.052 \pm 0.051$	$-0.086 \pm 0.043 \pm 0.031$	$-0.078 \pm 0.059 \pm 0.033$
	$\lambda_{\theta\phi}$	$0.018 \pm 0.020 \pm 0.007$	$-0.032 \pm 0.017 \pm 0.008$	$-0.097 \pm 0.023 \pm 0.008$
	$\lambda_\phi$	$-0.034 \pm 0.026 \pm 0.024$	$0.014 \pm 0.017 \pm 0.009$	$0.022 \pm 0.019 \pm 0.007$
	$\tilde{\lambda}$	$-0.012 \pm 0.062 \pm 0.029$	$-0.044 \pm 0.060 \pm 0.028$	$-0.011 \pm 0.077 \pm 0.031$
15 – 20	$\lambda_\theta$	$0.161 \pm 0.096 \pm 0.058$	$0.150 \pm 0.103 \pm 0.062$	$0.336 \pm 0.164 \pm 0.083$
	$\lambda_{\theta\phi}$	$-0.043 \pm 0.045 \pm 0.017$	$0.007 \pm 0.044 \pm 0.015$	$-0.008 \pm 0.069 \pm 0.028$
	$\lambda_\phi$	$-0.039 \pm 0.045 \pm 0.024$	$0.079 \pm 0.035 \pm 0.012$	$0.054 \pm 0.049 \pm 0.017$
	$\tilde{\lambda}$	$0.043 \pm 0.129 \pm 0.051$	$0.419 \pm 0.177 \pm 0.078$	$0.527 \pm 0.254 \pm 0.101$

Table 7: Values of  $\lambda_\theta$ ,  $\lambda_{\theta\phi}$ ,  $\lambda_\phi$  and  $\tilde{\lambda}$  measured in the GJ frame for the  $\Upsilon(1S)$  produced at  $\sqrt{s} = 8$  TeV. The first uncertainty is statistical and the second systematic.

$p_T^\Upsilon$ [GeV/c]	$\lambda$	$2.2 < y < 3.0$	$3.0 < y < 3.5$	$3.5 < y < 4.5$
0 – 2	$\lambda_\theta$	$0.154 \pm 0.038 \pm 0.029$	$0.052 \pm 0.023 \pm 0.023$	$-0.022 \pm 0.032 \pm 0.033$
	$\lambda_{\theta\phi}$	$0.080 \pm 0.013 \pm 0.007$	$0.054 \pm 0.008 \pm 0.004$	$0.023 \pm 0.010 \pm 0.005$
	$\lambda_\phi$	$0.005 \pm 0.006 \pm 0.003$	$0.013 \pm 0.006 \pm 0.003$	$0.001 \pm 0.006 \pm 0.003$
	$\tilde{\lambda}$	$0.170 \pm 0.045 \pm 0.034$	$0.092 \pm 0.031 \pm 0.025$	$-0.018 \pm 0.037 \pm 0.034$
2 – 4	$\lambda_\theta$	$0.144 \pm 0.024 \pm 0.024$	$0.049 \pm 0.017 \pm 0.016$	$-0.106 \pm 0.023 \pm 0.023$
	$\lambda_{\theta\phi}$	$0.111 \pm 0.013 \pm 0.014$	$0.072 \pm 0.007 \pm 0.005$	$0.045 \pm 0.008 \pm 0.006$
	$\lambda_\phi$	$0.014 \pm 0.005 \pm 0.004$	$-0.009 \pm 0.005 \pm 0.003$	$-0.002 \pm 0.005 \pm 0.002$
	$\tilde{\lambda}$	$0.187 \pm 0.035 \pm 0.036$	$0.023 \pm 0.024 \pm 0.023$	$-0.112 \pm 0.028 \pm 0.025$
4 – 6	$\lambda_\theta$	$0.027 \pm 0.022 \pm 0.022$	$-0.031 \pm 0.018 \pm 0.012$	$-0.138 \pm 0.024 \pm 0.021$
	$\lambda_{\theta\phi}$	$0.124 \pm 0.015 \pm 0.016$	$0.066 \pm 0.009 \pm 0.005$	$0.030 \pm 0.010 \pm 0.007$
	$\lambda_\phi$	$0.026 \pm 0.008 \pm 0.008$	$0.011 \pm 0.006 \pm 0.003$	$-0.002 \pm 0.006 \pm 0.003$
	$\tilde{\lambda}$	$0.109 \pm 0.039 \pm 0.042$	$0.002 \pm 0.028 \pm 0.018$	$-0.142 \pm 0.031 \pm 0.024$
6 – 8	$\lambda_\theta$	$-0.011 \pm 0.024 \pm 0.019$	$-0.056 \pm 0.021 \pm 0.017$	$-0.111 \pm 0.028 \pm 0.020$
	$\lambda_{\theta\phi}$	$0.078 \pm 0.018 \pm 0.019$	$0.046 \pm 0.010 \pm 0.006$	$-0.012 \pm 0.012 \pm 0.007$
	$\lambda_\phi$	$-0.001 \pm 0.013 \pm 0.015$	$0.014 \pm 0.009 \pm 0.005$	$0.007 \pm 0.008 \pm 0.004$
	$\tilde{\lambda}$	$-0.014 \pm 0.044 \pm 0.045$	$-0.013 \pm 0.033 \pm 0.020$	$-0.090 \pm 0.038 \pm 0.025$
8 – 10	$\lambda_\theta$	$-0.014 \pm 0.031 \pm 0.026$	$-0.125 \pm 0.028 \pm 0.019$	$-0.200 \pm 0.035 \pm 0.024$
	$\lambda_{\theta\phi}$	$0.039 \pm 0.018 \pm 0.015$	$0.030 \pm 0.011 \pm 0.005$	$-0.044 \pm 0.013 \pm 0.006$
	$\lambda_\phi$	$-0.004 \pm 0.018 \pm 0.019$	$0.024 \pm 0.012 \pm 0.007$	$0.033 \pm 0.011 \pm 0.006$
	$\tilde{\lambda}$	$-0.026 \pm 0.049 \pm 0.043$	$-0.054 \pm 0.039 \pm 0.017$	$-0.106 \pm 0.046 \pm 0.024$
10 – 15	$\lambda_\theta$	$-0.073 \pm 0.030 \pm 0.032$	$-0.053 \pm 0.029 \pm 0.020$	$-0.118 \pm 0.037 \pm 0.028$
	$\lambda_{\theta\phi}$	$0.025 \pm 0.012 \pm 0.006$	$-0.015 \pm 0.011 \pm 0.005$	$-0.031 \pm 0.014 \pm 0.006$
	$\lambda_\phi$	$0.012 \pm 0.016 \pm 0.017$	$0.014 \pm 0.012 \pm 0.006$	$0.039 \pm 0.012 \pm 0.007$
	$\tilde{\lambda}$	$-0.036 \pm 0.040 \pm 0.025$	$-0.010 \pm 0.040 \pm 0.021$	$-0.001 \pm 0.050 \pm 0.030$
15 – 20	$\lambda_\theta$	$-0.079 \pm 0.052 \pm 0.043$	$-0.055 \pm 0.060 \pm 0.031$	$0.047 \pm 0.091 \pm 0.055$
	$\lambda_{\theta\phi}$	$-0.018 \pm 0.027 \pm 0.013$	$-0.103 \pm 0.026 \pm 0.010$	$-0.158 \pm 0.039 \pm 0.014$
	$\lambda_\phi$	$-0.023 \pm 0.026 \pm 0.020$	$0.051 \pm 0.022 \pm 0.010$	$0.012 \pm 0.029 \pm 0.011$
	$\tilde{\lambda}$	$-0.144 \pm 0.075 \pm 0.039$	$0.102 \pm 0.098 \pm 0.044$	$0.084 \pm 0.128 \pm 0.060$

Table 8: Values of  $\lambda_\theta$ ,  $\lambda_{\theta\phi}$  and  $\lambda_\phi$  measured in the HX, CS and GJ frames for the  $\Upsilon(1S)$  produced at  $\sqrt{s} = 7$  TeV in the rapidity range  $2.2 < y^\Upsilon < 4.5$ . The first uncertainty is statistical and the second systematic.

$p_T^\Upsilon$ [GeV/c]		$\lambda_\theta$	$\lambda_{\theta\phi}$	$\lambda_\phi$
0 – 2	HX	$0.065 \pm 0.023 \pm 0.017$	$-0.022 \pm 0.008 \pm 0.005$	$-0.004 \pm 0.005 \pm 0.002$
	CS	$0.073 \pm 0.024 \pm 0.018$	$0.002 \pm 0.008 \pm 0.004$	$-0.006 \pm 0.005 \pm 0.002$
	GJ	$0.064 \pm 0.023 \pm 0.016$	$0.026 \pm 0.008 \pm 0.004$	$-0.003 \pm 0.005 \pm 0.002$
2 – 4	HX	$0.036 \pm 0.016 \pm 0.012$	$-0.019 \pm 0.007 \pm 0.004$	$-0.009 \pm 0.004 \pm 0.002$
	CS	$0.047 \pm 0.019 \pm 0.012$	$0.016 \pm 0.006 \pm 0.004$	$-0.013 \pm 0.004 \pm 0.002$
	GJ	$0.007 \pm 0.017 \pm 0.013$	$0.043 \pm 0.007 \pm 0.006$	$0.000 \pm 0.004 \pm 0.003$
4 – 6	HX	$0.003 \pm 0.016 \pm 0.012$	$0.003 \pm 0.010 \pm 0.006$	$-0.030 \pm 0.006 \pm 0.003$
	CS	$-0.014 \pm 0.020 \pm 0.011$	$0.023 \pm 0.008 \pm 0.005$	$-0.025 \pm 0.004 \pm 0.002$
	GJ	$-0.060 \pm 0.017 \pm 0.010$	$0.020 \pm 0.009 \pm 0.006$	$-0.012 \pm 0.005 \pm 0.004$
6 – 8	HX	$0.041 \pm 0.019 \pm 0.015$	$0.019 \pm 0.011 \pm 0.007$	$-0.045 \pm 0.009 \pm 0.006$
	CS	$-0.030 \pm 0.021 \pm 0.011$	$0.042 \pm 0.011 \pm 0.007$	$-0.020 \pm 0.006 \pm 0.003$
	GJ	$-0.078 \pm 0.020 \pm 0.016$	$0.006 \pm 0.010 \pm 0.006$	$-0.004 \pm 0.008 \pm 0.006$
8 – 10	HX	$0.068 \pm 0.026 \pm 0.019$	$-0.014 \pm 0.012 \pm 0.005$	$-0.035 \pm 0.013 \pm 0.008$
	CS	$0.016 \pm 0.022 \pm 0.012$	$0.045 \pm 0.016 \pm 0.008$	$-0.017 \pm 0.009 \pm 0.003$
	GJ	$-0.065 \pm 0.026 \pm 0.023$	$0.017 \pm 0.011 \pm 0.004$	$0.010 \pm 0.011 \pm 0.007$
10 – 15	HX	$0.073 \pm 0.025 \pm 0.024$	$0.015 \pm 0.012 \pm 0.005$	$-0.027 \pm 0.013 \pm 0.010$
	CS	$-0.040 \pm 0.018 \pm 0.009$	$0.034 \pm 0.016 \pm 0.006$	$0.011 \pm 0.011 \pm 0.005$
	GJ	$-0.025 \pm 0.027 \pm 0.018$	$-0.031 \pm 0.011 \pm 0.004$	$0.007 \pm 0.011 \pm 0.006$
15 – 20	HX	$0.063 \pm 0.051 \pm 0.030$	$0.051 \pm 0.030 \pm 0.014$	$0.058 \pm 0.023 \pm 0.012$
	CS	$-0.011 \pm 0.037 \pm 0.023$	$-0.032 \pm 0.030 \pm 0.010$	$0.082 \pm 0.028 \pm 0.017$
	GJ	$0.158 \pm 0.062 \pm 0.039$	$-0.022 \pm 0.028 \pm 0.010$	$0.032 \pm 0.022 \pm 0.009$
20 – 30	HX	$0.077 \pm 0.098 \pm 0.049$	$-0.009 \pm 0.055 \pm 0.018$	$-0.004 \pm 0.036 \pm 0.011$
	CS	$-0.019 \pm 0.067 \pm 0.043$	$0.026 \pm 0.048 \pm 0.013$	$0.029 \pm 0.056 \pm 0.035$
	GJ	$0.027 \pm 0.105 \pm 0.054$	$-0.031 \pm 0.048 \pm 0.017$	$0.014 \pm 0.036 \pm 0.013$



Table 9: Values of  $\lambda_\theta$ ,  $\lambda_{\theta\phi}$  and  $\lambda_\phi$  measured in the HX, CS and GJ frames for the  $\Upsilon(1S)$  produced at  $\sqrt{s} = 8$  TeV in the rapidity range  $2.2 < y^\Upsilon < 4.5$ . The first uncertainty is statistical and the second systematic.

$p_T^\Upsilon$ [GeV/c]		$\lambda_\theta$	$\lambda_{\theta\phi}$	$\lambda_\phi$
0 – 2	HX	$0.072 \pm 0.016 \pm 0.014$	$0.003 \pm 0.006 \pm 0.003$	$-0.002 \pm 0.004 \pm 0.001$
	CS	$0.064 \pm 0.016 \pm 0.014$	$0.026 \pm 0.005 \pm 0.003$	$-0.001 \pm 0.003 \pm 0.002$
	GJ	$0.040 \pm 0.016 \pm 0.012$	$0.046 \pm 0.005 \pm 0.004$	$0.005 \pm 0.004 \pm 0.001$
2 – 4	HX	$0.077 \pm 0.011 \pm 0.011$	$-0.028 \pm 0.005 \pm 0.004$	$-0.016 \pm 0.003 \pm 0.002$
	CS	$0.086 \pm 0.013 \pm 0.010$	$0.024 \pm 0.004 \pm 0.005$	$-0.020 \pm 0.003 \pm 0.001$
	GJ	$0.027 \pm 0.011 \pm 0.007$	$0.062 \pm 0.005 \pm 0.005$	$-0.003 \pm 0.003 \pm 0.002$
4 – 6	HX	$0.078 \pm 0.011 \pm 0.012$	$-0.008 \pm 0.006 \pm 0.005$	$-0.035 \pm 0.004 \pm 0.003$
	CS	$0.049 \pm 0.014 \pm 0.009$	$0.049 \pm 0.005 \pm 0.006$	$-0.026 \pm 0.003 \pm 0.002$
	GJ	$-0.047 \pm 0.012 \pm 0.010$	$0.058 \pm 0.006 \pm 0.006$	$0.004 \pm 0.004 \pm 0.004$
6 – 8	HX	$0.063 \pm 0.013 \pm 0.015$	$-0.010 \pm 0.007 \pm 0.005$	$-0.039 \pm 0.006 \pm 0.005$
	CS	$0.023 \pm 0.014 \pm 0.010$	$0.042 \pm 0.008 \pm 0.007$	$-0.026 \pm 0.004 \pm 0.002$
	GJ	$-0.058 \pm 0.013 \pm 0.013$	$0.033 \pm 0.007 \pm 0.005$	$0.001 \pm 0.005 \pm 0.005$
8 – 10	HX	$0.114 \pm 0.017 \pm 0.019$	$-0.007 \pm 0.008 \pm 0.004$	$-0.056 \pm 0.009 \pm 0.008$
	CS	$0.002 \pm 0.014 \pm 0.008$	$0.072 \pm 0.011 \pm 0.007$	$-0.018 \pm 0.006 \pm 0.003$
	GJ	$-0.101 \pm 0.017 \pm 0.016$	$0.011 \pm 0.007 \pm 0.003$	$0.017 \pm 0.007 \pm 0.006$
10 – 15	HX	$0.099 \pm 0.017 \pm 0.017$	$-0.025 \pm 0.008 \pm 0.004$	$-0.042 \pm 0.009 \pm 0.006$
	CS	$0.005 \pm 0.012 \pm 0.008$	$0.061 \pm 0.011 \pm 0.007$	$-0.010 \pm 0.007 \pm 0.004$
	GJ	$-0.077 \pm 0.017 \pm 0.016$	$-0.005 \pm 0.007 \pm 0.003$	$0.018 \pm 0.007 \pm 0.006$
15 – 20	HX	$0.160 \pm 0.035 \pm 0.021$	$-0.012 \pm 0.020 \pm 0.009$	$-0.060 \pm 0.016 \pm 0.008$
	CS	$-0.073 \pm 0.022 \pm 0.017$	$0.084 \pm 0.019 \pm 0.007$	$0.019 \pm 0.018 \pm 0.013$
	GJ	$-0.060 \pm 0.035 \pm 0.020$	$-0.080 \pm 0.016 \pm 0.007$	$0.016 \pm 0.014 \pm 0.006$
20 – 30	HX	$0.183 \pm 0.064 \pm 0.033$	$0.084 \pm 0.035 \pm 0.013$	$-0.023 \pm 0.023 \pm 0.009$
	CS	$-0.155 \pm 0.037 \pm 0.029$	$0.004 \pm 0.028 \pm 0.011$	$0.086 \pm 0.032 \pm 0.026$
	GJ	$0.176 \pm 0.069 \pm 0.043$	$-0.093 \pm 0.031 \pm 0.014$	$-0.019 \pm 0.023 \pm 0.009$

Table 10: Values of  $\tilde{\lambda}$  measured in the HX, CS and GJ frames for the  $\Upsilon(1S)$  produced at  $\sqrt{s} = 7$  and 8 TeV in the rapidity range  $2.2 < y^\Upsilon < 4.5$ . The first uncertainty is statistical and the second systematic.

$p_T^\Upsilon$ [GeV/c]	$\tilde{\lambda}$	$\sqrt{s} = 7$ TeV	$\sqrt{s} = 8$ TeV
0 – 2	HX	$0.054 \pm 0.028 \pm 0.019$	$0.064 \pm 0.020 \pm 0.014$
	CS	$0.055 \pm 0.029 \pm 0.020$	$0.060 \pm 0.020 \pm 0.016$
	GJ	$0.055 \pm 0.029 \pm 0.018$	$0.056 \pm 0.020 \pm 0.014$
2 – 4	HX	$0.009 \pm 0.022 \pm 0.014$	$0.029 \pm 0.015 \pm 0.011$
	CS	$0.009 \pm 0.022 \pm 0.014$	$0.027 \pm 0.015 \pm 0.012$
	GJ	$0.006 \pm 0.022 \pm 0.016$	$0.019 \pm 0.015 \pm 0.010$
4 – 6	HX	$-0.085 \pm 0.024 \pm 0.013$	$-0.026 \pm 0.017 \pm 0.012$
	CS	$-0.088 \pm 0.025 \pm 0.013$	$-0.029 \pm 0.017 \pm 0.012$
	GJ	$-0.094 \pm 0.025 \pm 0.013$	$-0.036 \pm 0.017 \pm 0.013$
6 – 8	HX	$-0.089 \pm 0.029 \pm 0.016$	$-0.053 \pm 0.019 \pm 0.014$
	CS	$-0.088 \pm 0.029 \pm 0.014$	$-0.052 \pm 0.020 \pm 0.013$
	GJ	$-0.089 \pm 0.029 \pm 0.017$	$-0.054 \pm 0.020 \pm 0.013$
8 – 10	HX	$-0.036 \pm 0.035 \pm 0.017$	$-0.051 \pm 0.023 \pm 0.012$
	CS	$-0.035 \pm 0.035 \pm 0.016$	$-0.050 \pm 0.023 \pm 0.012$
	GJ	$-0.035 \pm 0.036 \pm 0.017$	$-0.050 \pm 0.023 \pm 0.012$
10 – 15	HX	$-0.009 \pm 0.036 \pm 0.014$	$-0.025 \pm 0.023 \pm 0.010$
	CS	$-0.007 \pm 0.036 \pm 0.016$	$-0.024 \pm 0.023 \pm 0.010$
	GJ	$-0.004 \pm 0.036 \pm 0.013$	$-0.022 \pm 0.023 \pm 0.011$
15 – 20	HX	$0.250 \pm 0.094 \pm 0.041$	$-0.019 \pm 0.052 \pm 0.025$
	CS	$0.256 \pm 0.094 \pm 0.042$	$-0.016 \pm 0.052 \pm 0.028$
	GJ	$0.261 \pm 0.094 \pm 0.036$	$-0.012 \pm 0.052 \pm 0.022$
20 – 30	HX	$0.066 \pm 0.156 \pm 0.063$	$0.110 \pm 0.098 \pm 0.048$
	CS	$0.068 \pm 0.156 \pm 0.078$	$0.114 \pm 0.098 \pm 0.061$
	GJ	$0.071 \pm 0.157 \pm 0.061$	$0.115 \pm 0.098 \pm 0.051$

## B Polarization results for the $\Upsilon(2S)$ state

Values of the polarization parameters  $\lambda$  and  $\tilde{\lambda}$  for the  $\Upsilon(2S)$  meson are presented in Tables 11 and 12 for the HX frame, in Tables 13 and 14 for the CS frame and in Tables 15 and 16 for the GJ frame for  $\sqrt{s} = 7$  and 8 TeV, respectively. The polarization parameters  $\lambda$  measured in the wide rapidity bin  $2.2 < y^r < 4.5$  are presented in Tables 17 and 18, while the parameters  $\tilde{\lambda}$  are listed in Table 19.

Table 11: Values of  $\lambda_\theta$ ,  $\lambda_{\theta\phi}$ ,  $\lambda_\phi$  and  $\tilde{\lambda}$  measured in the HX frame for the  $\Upsilon(2S)$  produced at  $\sqrt{s} = 7$  TeV. The first uncertainty is statistical and the second systematic.

$p_T^r$ [GeV/c]	$\lambda$	$2.2 < y < 3.0$	$3.0 < y < 3.5$	$3.5 < y < 4.5$
0 – 2	$\lambda_\theta$	$0.167 \pm 0.148 \pm 0.068$	$-0.244 \pm 0.072 \pm 0.046$	$-0.190 \pm 0.097 \pm 0.071$
	$\lambda_{\theta\phi}$	$0.021 \pm 0.037 \pm 0.010$	$0.013 \pm 0.026 \pm 0.009$	$-0.011 \pm 0.036 \pm 0.017$
	$\lambda_\phi$	$-0.014 \pm 0.020 \pm 0.006$	$0.007 \pm 0.021 \pm 0.007$	$0.012 \pm 0.022 \pm 0.007$
	$\tilde{\lambda}$	$0.123 \pm 0.158 \pm 0.071$	$-0.224 \pm 0.095 \pm 0.052$	$-0.155 \pm 0.119 \pm 0.074$
2 – 4	$\lambda_\theta$	$0.247 \pm 0.104 \pm 0.055$	$-0.032 \pm 0.056 \pm 0.033$	$-0.215 \pm 0.061 \pm 0.036$
	$\lambda_{\theta\phi}$	$-0.055 \pm 0.031 \pm 0.012$	$0.019 \pm 0.025 \pm 0.010$	$0.096 \pm 0.035 \pm 0.018$
	$\lambda_\phi$	$0.009 \pm 0.015 \pm 0.004$	$0.015 \pm 0.017 \pm 0.005$	$-0.003 \pm 0.019 \pm 0.008$
	$\tilde{\lambda}$	$0.278 \pm 0.120 \pm 0.062$	$0.014 \pm 0.082 \pm 0.042$	$-0.223 \pm 0.088 \pm 0.051$
4 – 6	$\lambda_\theta$	$0.023 \pm 0.097 \pm 0.056$	$-0.098 \pm 0.053 \pm 0.024$	$-0.100 \pm 0.055 \pm 0.034$
	$\lambda_{\theta\phi}$	$0.012 \pm 0.040 \pm 0.019$	$0.073 \pm 0.031 \pm 0.012$	$0.124 \pm 0.044 \pm 0.030$
	$\lambda_\phi$	$0.042 \pm 0.019 \pm 0.007$	$-0.015 \pm 0.021 \pm 0.008$	$-0.027 \pm 0.027 \pm 0.015$
	$\tilde{\lambda}$	$0.157 \pm 0.129 \pm 0.070$	$-0.142 \pm 0.085 \pm 0.032$	$-0.176 \pm 0.099 \pm 0.063$
6 – 8	$\lambda_\theta$	$-0.103 \pm 0.097 \pm 0.054$	$-0.053 \pm 0.063 \pm 0.029$	$0.002 \pm 0.062 \pm 0.033$
	$\lambda_{\theta\phi}$	$0.020 \pm 0.049 \pm 0.030$	$0.244 \pm 0.036 \pm 0.016$	$0.083 \pm 0.049 \pm 0.030$
	$\lambda_\phi$	$0.037 \pm 0.028 \pm 0.016$	$-0.070 \pm 0.032 \pm 0.015$	$-0.015 \pm 0.040 \pm 0.025$
	$\tilde{\lambda}$	$0.009 \pm 0.140 \pm 0.079$	$-0.245 \pm 0.095 \pm 0.032$	$-0.042 \pm 0.121 \pm 0.069$
8 – 10	$\lambda_\theta$	$-0.023 \pm 0.114 \pm 0.063$	$0.209 \pm 0.090 \pm 0.065$	$0.088 \pm 0.092 \pm 0.068$
	$\lambda_{\theta\phi}$	$0.025 \pm 0.055 \pm 0.027$	$0.147 \pm 0.037 \pm 0.013$	$0.174 \pm 0.051 \pm 0.029$
	$\lambda_\phi$	$-0.013 \pm 0.041 \pm 0.026$	$-0.055 \pm 0.044 \pm 0.024$	$-0.067 \pm 0.060 \pm 0.041$
	$\tilde{\lambda}$	$-0.063 \pm 0.148 \pm 0.072$	$0.042 \pm 0.119 \pm 0.037$	$-0.105 \pm 0.138 \pm 0.061$
10 – 15	$\lambda_\theta$	$0.172 \pm 0.103 \pm 0.087$	$0.114 \pm 0.077 \pm 0.053$	$0.237 \pm 0.102 \pm 0.095$
	$\lambda_{\theta\phi}$	$0.007 \pm 0.043 \pm 0.022$	$0.004 \pm 0.034 \pm 0.013$	$0.123 \pm 0.044 \pm 0.015$
	$\lambda_\phi$	$-0.033 \pm 0.038 \pm 0.028$	$0.020 \pm 0.039 \pm 0.024$	$-0.116 \pm 0.062 \pm 0.057$
	$\tilde{\lambda}$	$0.071 \pm 0.119 \pm 0.057$	$0.178 \pm 0.123 \pm 0.055$	$-0.099 \pm 0.131 \pm 0.080$
15 – 20	$\lambda_\theta$	$0.095 \pm 0.149 \pm 0.150$	$0.112 \pm 0.136 \pm 0.132$	$0.376 \pm 0.229 \pm 0.216$
	$\lambda_{\theta\phi}$	$0.063 \pm 0.077 \pm 0.051$	$-0.008 \pm 0.083 \pm 0.057$	$0.076 \pm 0.135 \pm 0.098$
	$\lambda_\phi$	$0.018 \pm 0.054 \pm 0.050$	$-0.057 \pm 0.073 \pm 0.056$	$-0.190 \pm 0.127 \pm 0.113$
	$\tilde{\lambda}$	$0.152 \pm 0.207 \pm 0.162$	$-0.055 \pm 0.229 \pm 0.164$	$-0.163 \pm 0.312 \pm 0.191$

Table 12: Values of  $\lambda_\theta$ ,  $\lambda_{\theta\phi}$ ,  $\lambda_\phi$  and  $\tilde{\lambda}$  measured in the HX frame for the  $\Upsilon(2S)$  produced at  $\sqrt{s} = 8$  TeV. The first uncertainty is statistical and the second systematic.

$p_T^\Upsilon$ [GeV/c]	$\lambda$	$2.2 < y < 3.0$	$3.0 < y < 3.5$	$3.5 < y < 4.5$
0 – 2	$\lambda_\theta$	$0.252 \pm 0.101 \pm 0.054$	$0.131 \pm 0.057 \pm 0.035$	$-0.156 \pm 0.067 \pm 0.054$
	$\lambda_{\theta\phi}$	$-0.033 \pm 0.026 \pm 0.009$	$-0.002 \pm 0.020 \pm 0.007$	$-0.041 \pm 0.025 \pm 0.014$
	$\lambda_\phi$	$0.002 \pm 0.014 \pm 0.004$	$-0.009 \pm 0.015 \pm 0.005$	$0.017 \pm 0.015 \pm 0.005$
	$\tilde{\lambda}$	$0.259 \pm 0.111 \pm 0.061$	$0.104 \pm 0.075 \pm 0.039$	$-0.107 \pm 0.083 \pm 0.059$
2 – 4	$\lambda_\theta$	$0.210 \pm 0.070 \pm 0.037$	$0.131 \pm 0.040 \pm 0.029$	$-0.081 \pm 0.042 \pm 0.033$
	$\lambda_{\theta\phi}$	$-0.035 \pm 0.021 \pm 0.009$	$-0.052 \pm 0.018 \pm 0.008$	$0.030 \pm 0.024 \pm 0.014$
	$\lambda_\phi$	$-0.017 \pm 0.010 \pm 0.004$	$0.018 \pm 0.012 \pm 0.004$	$-0.002 \pm 0.013 \pm 0.005$
	$\tilde{\lambda}$	$0.156 \pm 0.078 \pm 0.040$	$0.190 \pm 0.060 \pm 0.037$	$-0.088 \pm 0.061 \pm 0.042$
4 – 6	$\lambda_\theta$	$0.121 \pm 0.066 \pm 0.037$	$0.048 \pm 0.039 \pm 0.023$	$-0.086 \pm 0.039 \pm 0.022$
	$\lambda_{\theta\phi}$	$-0.046 \pm 0.027 \pm 0.016$	$0.092 \pm 0.022 \pm 0.010$	$0.180 \pm 0.030 \pm 0.024$
	$\lambda_\phi$	$0.015 \pm 0.013 \pm 0.005$	$-0.030 \pm 0.015 \pm 0.006$	$-0.035 \pm 0.019 \pm 0.013$
	$\tilde{\lambda}$	$0.168 \pm 0.085 \pm 0.049$	$-0.040 \pm 0.061 \pm 0.034$	$-0.185 \pm 0.067 \pm 0.048$
6 – 8	$\lambda_\theta$	$-0.018 \pm 0.066 \pm 0.043$	$0.109 \pm 0.045 \pm 0.027$	$0.049 \pm 0.044 \pm 0.026$
	$\lambda_{\theta\phi}$	$0.003 \pm 0.033 \pm 0.023$	$0.168 \pm 0.025 \pm 0.013$	$0.216 \pm 0.036 \pm 0.024$
	$\lambda_\phi$	$0.024 \pm 0.019 \pm 0.011$	$-0.090 \pm 0.023 \pm 0.011$	$-0.050 \pm 0.029 \pm 0.019$
	$\tilde{\lambda}$	$0.056 \pm 0.095 \pm 0.062$	$-0.146 \pm 0.066 \pm 0.029$	$-0.096 \pm 0.082 \pm 0.044$
8 – 10	$\lambda_\theta$	$0.083 \pm 0.077 \pm 0.050$	$0.078 \pm 0.055 \pm 0.041$	$0.018 \pm 0.055 \pm 0.051$
	$\lambda_{\theta\phi}$	$-0.022 \pm 0.037 \pm 0.019$	$0.099 \pm 0.024 \pm 0.010$	$0.125 \pm 0.032 \pm 0.021$
	$\lambda_\phi$	$0.023 \pm 0.027 \pm 0.017$	$-0.029 \pm 0.029 \pm 0.019$	$0.013 \pm 0.036 \pm 0.031$
	$\tilde{\lambda}$	$0.155 \pm 0.107 \pm 0.049$	$-0.010 \pm 0.078 \pm 0.026$	$0.057 \pm 0.096 \pm 0.058$
10 – 15	$\lambda_\theta$	$0.388 \pm 0.076 \pm 0.062$	$0.209 \pm 0.054 \pm 0.047$	$0.200 \pm 0.065 \pm 0.077$
	$\lambda_{\theta\phi}$	$-0.045 \pm 0.030 \pm 0.015$	$0.069 \pm 0.022 \pm 0.009$	$0.077 \pm 0.028 \pm 0.012$
	$\lambda_\phi$	$-0.055 \pm 0.026 \pm 0.019$	$-0.042 \pm 0.027 \pm 0.019$	$-0.022 \pm 0.038 \pm 0.039$
	$\tilde{\lambda}$	$0.212 \pm 0.082 \pm 0.033$	$0.079 \pm 0.075 \pm 0.028$	$0.130 \pm 0.095 \pm 0.058$
15 – 20	$\lambda_\theta$	$0.019 \pm 0.096 \pm 0.103$	$0.246 \pm 0.095 \pm 0.113$	$0.065 \pm 0.114 \pm 0.118$
	$\lambda_{\theta\phi}$	$0.043 \pm 0.051 \pm 0.037$	$-0.062 \pm 0.057 \pm 0.046$	$0.201 \pm 0.072 \pm 0.057$
	$\lambda_\phi$	$-0.015 \pm 0.037 \pm 0.028$	$-0.073 \pm 0.049 \pm 0.045$	$-0.016 \pm 0.068 \pm 0.060$
	$\tilde{\lambda}$	$-0.025 \pm 0.129 \pm 0.083$	$0.025 \pm 0.155 \pm 0.118$	$0.018 \pm 0.208 \pm 0.167$

Table 13: Values of  $\lambda_\theta$ ,  $\lambda_{\theta\phi}$ ,  $\lambda_\phi$  and  $\tilde{\lambda}$  measured in the CS frame for the  $\Upsilon(2S)$  produced at  $\sqrt{s} = 7$  TeV. The first uncertainty is statistical and the second systematic.

$p_T^\Upsilon$ [GeV/c]	$\lambda$	$2.2 < y < 3.0$	$3.0 < y < 3.5$	$3.5 < y < 4.5$
0 – 2	$\lambda_\theta$	$0.175 \pm 0.146 \pm 0.066$	$-0.249 \pm 0.073 \pm 0.045$	$-0.198 \pm 0.103 \pm 0.059$
	$\lambda_{\theta\phi}$	$0.088 \pm 0.038 \pm 0.013$	$-0.003 \pm 0.025 \pm 0.008$	$-0.012 \pm 0.033 \pm 0.012$
	$\lambda_\phi$	$-0.008 \pm 0.020 \pm 0.006$	$0.007 \pm 0.021 \pm 0.006$	$0.008 \pm 0.021 \pm 0.007$
	$\tilde{\lambda}$	$0.152 \pm 0.159 \pm 0.070$	$-0.230 \pm 0.095 \pm 0.050$	$-0.177 \pm 0.120 \pm 0.059$
2 – 4	$\lambda_\theta$	$0.237 \pm 0.107 \pm 0.048$	$-0.036 \pm 0.062 \pm 0.032$	$-0.212 \pm 0.075 \pm 0.036$
	$\lambda_{\theta\phi}$	$0.089 \pm 0.030 \pm 0.009$	$0.027 \pm 0.021 \pm 0.006$	$0.046 \pm 0.026 \pm 0.008$
	$\lambda_\phi$	$0.011 \pm 0.014 \pm 0.004$	$0.018 \pm 0.016 \pm 0.004$	$0.009 \pm 0.016 \pm 0.005$
	$\tilde{\lambda}$	$0.274 \pm 0.122 \pm 0.052$	$0.017 \pm 0.083 \pm 0.040$	$-0.186 \pm 0.091 \pm 0.043$
4 – 6	$\lambda_\theta$	$0.054 \pm 0.106 \pm 0.039$	$-0.148 \pm 0.062 \pm 0.026$	$-0.163 \pm 0.079 \pm 0.039$
	$\lambda_{\theta\phi}$	$0.069 \pm 0.035 \pm 0.011$	$0.032 \pm 0.026 \pm 0.007$	$0.065 \pm 0.031 \pm 0.012$
	$\lambda_\phi$	$0.052 \pm 0.015 \pm 0.004$	$0.004 \pm 0.017 \pm 0.004$	$0.009 \pm 0.018 \pm 0.006$
	$\tilde{\lambda}$	$0.220 \pm 0.133 \pm 0.049$	$-0.137 \pm 0.086 \pm 0.031$	$-0.138 \pm 0.101 \pm 0.048$
6 – 8	$\lambda_\theta$	$-0.027 \pm 0.113 \pm 0.042$	$-0.354 \pm 0.057 \pm 0.025$	$-0.074 \pm 0.085 \pm 0.039$
	$\lambda_{\theta\phi}$	$-0.017 \pm 0.046 \pm 0.013$	$0.088 \pm 0.034 \pm 0.009$	$0.046 \pm 0.043 \pm 0.014$
	$\lambda_\phi$	$0.027 \pm 0.019 \pm 0.005$	$0.041 \pm 0.021 \pm 0.008$	$0.021 \pm 0.024 \pm 0.008$
	$\tilde{\lambda}$	$0.056 \pm 0.143 \pm 0.052$	$-0.241 \pm 0.095 \pm 0.043$	$-0.011 \pm 0.123 \pm 0.052$
8 – 10	$\lambda_\theta$	$-0.036 \pm 0.115 \pm 0.047$	$-0.161 \pm 0.057 \pm 0.026$	$-0.217 \pm 0.077 \pm 0.034$
	$\lambda_{\theta\phi}$	$0.038 \pm 0.062 \pm 0.019$	$0.135 \pm 0.048 \pm 0.015$	$0.077 \pm 0.059 \pm 0.026$
	$\lambda_\phi$	$-0.001 \pm 0.025 \pm 0.010$	$0.066 \pm 0.029 \pm 0.010$	$0.046 \pm 0.033 \pm 0.013$
	$\tilde{\lambda}$	$-0.040 \pm 0.150 \pm 0.059$	$0.040 \pm 0.119 \pm 0.046$	$-0.081 \pm 0.139 \pm 0.059$
10 – 15	$\lambda_\theta$	$-0.019 \pm 0.072 \pm 0.036$	$0.009 \pm 0.051 \pm 0.028$	$-0.224 \pm 0.062 \pm 0.035$
	$\lambda_{\theta\phi}$	$0.046 \pm 0.058 \pm 0.024$	$0.055 \pm 0.048 \pm 0.018$	$0.137 \pm 0.059 \pm 0.028$
	$\lambda_\phi$	$0.023 \pm 0.028 \pm 0.014$	$0.053 \pm 0.033 \pm 0.016$	$0.040 \pm 0.038 \pm 0.021$
	$\tilde{\lambda}$	$0.052 \pm 0.118 \pm 0.055$	$0.177 \pm 0.123 \pm 0.053$	$-0.108 \pm 0.133 \pm 0.063$
15 – 20	$\lambda_\theta$	$-0.068 \pm 0.091 \pm 0.083$	$-0.072 \pm 0.093 \pm 0.100$	$-0.291 \pm 0.118 \pm 0.139$
	$\lambda_{\theta\phi}$	$0.013 \pm 0.089 \pm 0.053$	$0.071 \pm 0.080 \pm 0.048$	$0.182 \pm 0.115 \pm 0.074$
	$\lambda_\phi$	$0.071 \pm 0.060 \pm 0.049$	$0.011 \pm 0.080 \pm 0.068$	$0.047 \pm 0.109 \pm 0.121$
	$\tilde{\lambda}$	$0.157 \pm 0.208 \pm 0.167$	$-0.040 \pm 0.230 \pm 0.154$	$-0.159 \pm 0.315 \pm 0.290$

Table 14: Values of  $\lambda_\theta$ ,  $\lambda_{\theta\phi}$ ,  $\lambda_\phi$  and  $\tilde{\lambda}$  measured in the CS frame for the  $\Upsilon(2S)$  produced at  $\sqrt{s} = 8$  TeV. The first uncertainty is statistical and the second systematic.

$p_T^\Upsilon$ [GeV/c]	$\lambda$	$2.2 < y < 3.0$	$3.0 < y < 3.5$	$3.5 < y < 4.5$
0 – 2	$\lambda_\theta$	$0.254 \pm 0.101 \pm 0.048$	$0.119 \pm 0.058 \pm 0.038$	$-0.139 \pm 0.072 \pm 0.051$
	$\lambda_{\theta\phi}$	$0.037 \pm 0.026 \pm 0.010$	$0.026 \pm 0.019 \pm 0.007$	$-0.035 \pm 0.023 \pm 0.008$
	$\lambda_\phi$	$0.002 \pm 0.014 \pm 0.004$	$-0.007 \pm 0.015 \pm 0.005$	$0.008 \pm 0.015 \pm 0.005$
	$\tilde{\lambda}$	$0.260 \pm 0.111 \pm 0.047$	$0.097 \pm 0.075 \pm 0.042$	$-0.116 \pm 0.084 \pm 0.058$
2 – 4	$\lambda_\theta$	$0.193 \pm 0.072 \pm 0.046$	$0.184 \pm 0.045 \pm 0.030$	$-0.054 \pm 0.053 \pm 0.038$
	$\lambda_{\theta\phi}$	$0.096 \pm 0.020 \pm 0.009$	$0.008 \pm 0.015 \pm 0.005$	$0.037 \pm 0.018 \pm 0.006$
	$\lambda_\phi$	$-0.011 \pm 0.010 \pm 0.003$	$0.008 \pm 0.011 \pm 0.004$	$-0.004 \pm 0.011 \pm 0.003$
	$\tilde{\lambda}$	$0.160 \pm 0.079 \pm 0.051$	$0.209 \pm 0.061 \pm 0.038$	$-0.065 \pm 0.063 \pm 0.040$
4 – 6	$\lambda_\theta$	$0.148 \pm 0.074 \pm 0.029$	$-0.075 \pm 0.043 \pm 0.024$	$-0.207 \pm 0.053 \pm 0.031$
	$\lambda_{\theta\phi}$	$0.077 \pm 0.023 \pm 0.008$	$0.100 \pm 0.018 \pm 0.006$	$0.106 \pm 0.021 \pm 0.008$
	$\lambda_\phi$	$0.013 \pm 0.010 \pm 0.003$	$0.012 \pm 0.012 \pm 0.004$	$0.023 \pm 0.012 \pm 0.004$
	$\tilde{\lambda}$	$0.191 \pm 0.088 \pm 0.034$	$-0.038 \pm 0.062 \pm 0.033$	$-0.141 \pm 0.069 \pm 0.038$
6 – 8	$\lambda_\theta$	$0.023 \pm 0.077 \pm 0.031$	$-0.190 \pm 0.041 \pm 0.018$	$-0.228 \pm 0.055 \pm 0.028$
	$\lambda_{\theta\phi}$	$0.034 \pm 0.030 \pm 0.009$	$0.143 \pm 0.024 \pm 0.007$	$0.121 \pm 0.028 \pm 0.011$
	$\lambda_\phi$	$0.023 \pm 0.013 \pm 0.005$	$0.017 \pm 0.015 \pm 0.005$	$0.056 \pm 0.015 \pm 0.005$
	$\tilde{\lambda}$	$0.093 \pm 0.097 \pm 0.040$	$-0.140 \pm 0.066 \pm 0.027$	$-0.065 \pm 0.083 \pm 0.038$
8 – 10	$\lambda_\theta$	$0.096 \pm 0.080 \pm 0.032$	$-0.124 \pm 0.039 \pm 0.017$	$-0.143 \pm 0.053 \pm 0.025$
	$\lambda_{\theta\phi}$	$0.057 \pm 0.042 \pm 0.015$	$0.054 \pm 0.033 \pm 0.010$	$0.020 \pm 0.039 \pm 0.016$
	$\lambda_\phi$	$0.026 \pm 0.017 \pm 0.007$	$0.040 \pm 0.020 \pm 0.006$	$0.068 \pm 0.021 \pm 0.008$
	$\tilde{\lambda}$	$0.180 \pm 0.108 \pm 0.041$	$-0.005 \pm 0.079 \pm 0.024$	$0.066 \pm 0.097 \pm 0.042$
10 – 15	$\lambda_\theta$	$0.041 \pm 0.048 \pm 0.027$	$-0.104 \pm 0.030 \pm 0.020$	$-0.104 \pm 0.043 \pm 0.027$
	$\lambda_{\theta\phi}$	$0.155 \pm 0.039 \pm 0.018$	$0.106 \pm 0.031 \pm 0.010$	$0.093 \pm 0.040 \pm 0.019$
	$\lambda_\phi$	$0.043 \pm 0.018 \pm 0.009$	$0.058 \pm 0.021 \pm 0.012$	$0.072 \pm 0.025 \pm 0.011$
	$\tilde{\lambda}$	$0.177 \pm 0.081 \pm 0.036$	$0.073 \pm 0.075 \pm 0.039$	$0.122 \pm 0.096 \pm 0.044$
15 – 20	$\lambda_\theta$	$-0.063 \pm 0.063 \pm 0.058$	$-0.030 \pm 0.062 \pm 0.070$	$-0.261 \pm 0.074 \pm 0.080$
	$\lambda_{\theta\phi}$	$-0.008 \pm 0.059 \pm 0.033$	$0.159 \pm 0.054 \pm 0.036$	$-0.051 \pm 0.069 \pm 0.042$
	$\lambda_\phi$	$0.010 \pm 0.042 \pm 0.042$	$0.020 \pm 0.052 \pm 0.039$	$0.093 \pm 0.064 \pm 0.061$
	$\tilde{\lambda}$	$-0.032 \pm 0.129 \pm 0.096$	$0.029 \pm 0.155 \pm 0.081$	$0.022 \pm 0.209 \pm 0.171$

Table 15: Values of  $\lambda_\theta$ ,  $\lambda_{\theta\phi}$ ,  $\lambda_\phi$  and  $\tilde{\lambda}$  measured in the GJ frame for the  $\Upsilon(2S)$  produced at  $\sqrt{s} = 7$  TeV. The first uncertainty is statistical and the second systematic.

$p_T^\Upsilon$ [GeV/c]	$\lambda$	$2.2 < y < 3.0$	$3.0 < y < 3.5$	$3.5 < y < 4.5$
0 – 2	$\lambda_\theta$	$0.129 \pm 0.133 \pm 0.071$	$-0.248 \pm 0.072 \pm 0.043$	$-0.209 \pm 0.103 \pm 0.068$
	$\lambda_{\theta\phi}$	$0.146 \pm 0.044 \pm 0.021$	$-0.018 \pm 0.027 \pm 0.009$	$-0.015 \pm 0.033 \pm 0.014$
	$\lambda_\phi$	$0.012 \pm 0.020 \pm 0.007$	$0.007 \pm 0.021 \pm 0.007$	$0.006 \pm 0.021 \pm 0.007$
	$\tilde{\lambda}$	$0.168 \pm 0.156 \pm 0.085$	$-0.229 \pm 0.095 \pm 0.052$	$-0.192 \pm 0.120 \pm 0.071$
2 – 4	$\lambda_\theta$	$0.028 \pm 0.080 \pm 0.048$	$-0.069 \pm 0.057 \pm 0.033$	$-0.195 \pm 0.075 \pm 0.040$
	$\lambda_{\theta\phi}$	$0.156 \pm 0.041 \pm 0.025$	$0.028 \pm 0.024 \pm 0.010$	$0.016 \pm 0.025 \pm 0.011$
	$\lambda_\phi$	$0.062 \pm 0.017 \pm 0.008$	$0.029 \pm 0.016 \pm 0.005$	$0.017 \pm 0.016 \pm 0.005$
	$\tilde{\lambda}$	$0.228 \pm 0.120 \pm 0.071$	$0.018 \pm 0.083 \pm 0.042$	$-0.147 \pm 0.091 \pm 0.048$
4 – 6	$\lambda_\theta$	$-0.091 \pm 0.068 \pm 0.036$	$-0.162 \pm 0.056 \pm 0.023$	$-0.184 \pm 0.078 \pm 0.035$
	$\lambda_{\theta\phi}$	$0.075 \pm 0.048 \pm 0.038$	$-0.024 \pm 0.028 \pm 0.010$	$0.006 \pm 0.030 \pm 0.016$
	$\lambda_\phi$	$0.103 \pm 0.024 \pm 0.017$	$0.010 \pm 0.019 \pm 0.006$	$0.026 \pm 0.018 \pm 0.008$
	$\tilde{\lambda}$	$0.243 \pm 0.133 \pm 0.093$	$-0.133 \pm 0.086 \pm 0.034$	$-0.109 \pm 0.102 \pm 0.049$
6 – 8	$\lambda_\theta$	$-0.025 \pm 0.074 \pm 0.041$	$-0.296 \pm 0.059 \pm 0.025$	$-0.097 \pm 0.089 \pm 0.044$
	$\lambda_{\theta\phi}$	$-0.015 \pm 0.058 \pm 0.047$	$-0.150 \pm 0.032 \pm 0.011$	$-0.003 \pm 0.038 \pm 0.015$
	$\lambda_\phi$	$0.032 \pm 0.038 \pm 0.028$	$0.022 \pm 0.026 \pm 0.009$	$0.036 \pm 0.025 \pm 0.010$
	$\tilde{\lambda}$	$0.074 \pm 0.144 \pm 0.109$	$-0.235 \pm 0.096 \pm 0.033$	$0.010 \pm 0.125 \pm 0.058$
8 – 10	$\lambda_\theta$	$-0.117 \pm 0.085 \pm 0.057$	$-0.213 \pm 0.075 \pm 0.045$	$-0.148 \pm 0.109 \pm 0.063$
	$\lambda_{\theta\phi}$	$-0.009 \pm 0.057 \pm 0.043$	$-0.092 \pm 0.032 \pm 0.010$	$-0.112 \pm 0.041 \pm 0.012$
	$\lambda_\phi$	$0.028 \pm 0.050 \pm 0.043$	$0.083 \pm 0.032 \pm 0.012$	$0.029 \pm 0.034 \pm 0.014$
	$\tilde{\lambda}$	$-0.035 \pm 0.150 \pm 0.102$	$0.039 \pm 0.120 \pm 0.044$	$-0.064 \pm 0.141 \pm 0.058$
10 – 15	$\lambda_\theta$	$0.020 \pm 0.087 \pm 0.099$	$-0.044 \pm 0.080 \pm 0.048$	$-0.199 \pm 0.102 \pm 0.064$
	$\lambda_{\theta\phi}$	$-0.019 \pm 0.037 \pm 0.019$	$-0.042 \pm 0.031 \pm 0.010$	$-0.157 \pm 0.039 \pm 0.014$
	$\lambda_\phi$	$0.006 \pm 0.045 \pm 0.055$	$0.069 \pm 0.032 \pm 0.012$	$0.030 \pm 0.034 \pm 0.016$
	$\tilde{\lambda}$	$0.038 \pm 0.116 \pm 0.081$	$0.175 \pm 0.123 \pm 0.053$	$-0.112 \pm 0.134 \pm 0.058$
15 – 20	$\lambda_\theta$	$0.059 \pm 0.144 \pm 0.142$	$-0.059 \pm 0.151 \pm 0.132$	$-0.174 \pm 0.220 \pm 0.173$
	$\lambda_{\theta\phi}$	$-0.074 \pm 0.065 \pm 0.042$	$-0.078 \pm 0.068 \pm 0.042$	$-0.256 \pm 0.099 \pm 0.047$
	$\lambda_\phi$	$0.032 \pm 0.068 \pm 0.067$	$0.012 \pm 0.057 \pm 0.033$	$0.006 \pm 0.078 \pm 0.036$
	$\tilde{\lambda}$	$0.161 \pm 0.207 \pm 0.142$	$-0.024 \pm 0.231 \pm 0.157$	$-0.157 \pm 0.315 \pm 0.194$

Table 16: Values of  $\lambda_\theta$ ,  $\lambda_{\theta\phi}$ ,  $\lambda_\phi$  and  $\tilde{\lambda}$  measured in the GJ frame for the  $\Upsilon(2S)$  produced at  $\sqrt{s} = 8$  TeV. The first uncertainty is statistical and the second systematic.

$p_T^\Upsilon$ [GeV/c]	$\lambda$	$2.2 < y < 3.0$	$3.0 < y < 3.5$	$3.5 < y < 4.5$
0 – 2	$\lambda_\theta$	$0.190 \pm 0.092 \pm 0.058$	$0.087 \pm 0.056 \pm 0.037$	$-0.130 \pm 0.073 \pm 0.050$
	$\lambda_{\theta\phi}$	$0.095 \pm 0.030 \pm 0.017$	$0.050 \pm 0.020 \pm 0.008$	$-0.026 \pm 0.022 \pm 0.009$
	$\lambda_\phi$	$0.015 \pm 0.014 \pm 0.006$	$-0.001 \pm 0.015 \pm 0.006$	$0.004 \pm 0.015 \pm 0.005$
	$\tilde{\lambda}$	$0.238 \pm 0.108 \pm 0.068$	$0.085 \pm 0.075 \pm 0.043$	$-0.119 \pm 0.085 \pm 0.053$
2 – 4	$\lambda_\theta$	$-0.008 \pm 0.054 \pm 0.032$	$0.145 \pm 0.042 \pm 0.028$	$-0.074 \pm 0.052 \pm 0.039$
	$\lambda_{\theta\phi}$	$0.153 \pm 0.027 \pm 0.018$	$0.075 \pm 0.017 \pm 0.010$	$0.057 \pm 0.017 \pm 0.010$
	$\lambda_\phi$	$0.040 \pm 0.012 \pm 0.006$	$0.022 \pm 0.011 \pm 0.005$	$0.010 \pm 0.011 \pm 0.004$
	$\tilde{\lambda}$	$0.117 \pm 0.077 \pm 0.049$	$0.216 \pm 0.061 \pm 0.040$	$-0.046 \pm 0.063 \pm 0.047$
4 – 6	$\lambda_\theta$	$-0.072 \pm 0.046 \pm 0.030$	$-0.179 \pm 0.037 \pm 0.018$	$-0.248 \pm 0.051 \pm 0.030$
	$\lambda_{\theta\phi}$	$0.107 \pm 0.032 \pm 0.027$	$0.037 \pm 0.019 \pm 0.010$	$0.011 \pm 0.021 \pm 0.013$
	$\lambda_\phi$	$0.074 \pm 0.016 \pm 0.012$	$0.047 \pm 0.013 \pm 0.006$	$0.050 \pm 0.012 \pm 0.006$
	$\tilde{\lambda}$	$0.162 \pm 0.087 \pm 0.067$	$-0.038 \pm 0.062 \pm 0.031$	$-0.102 \pm 0.070 \pm 0.043$
6 – 8	$\lambda_\theta$	$-0.088 \pm 0.047 \pm 0.025$	$-0.282 \pm 0.039 \pm 0.017$	$-0.261 \pm 0.056 \pm 0.028$
	$\lambda_{\theta\phi}$	$0.021 \pm 0.038 \pm 0.036$	$-0.036 \pm 0.020 \pm 0.007$	$-0.063 \pm 0.025 \pm 0.012$
	$\lambda_\phi$	$0.059 \pm 0.024 \pm 0.024$	$0.052 \pm 0.017 \pm 0.006$	$0.074 \pm 0.017 \pm 0.008$
	$\tilde{\lambda}$	$0.093 \pm 0.097 \pm 0.087$	$-0.132 \pm 0.067 \pm 0.024$	$-0.041 \pm 0.084 \pm 0.041$
8 – 10	$\lambda_\theta$	$-0.069 \pm 0.057 \pm 0.048$	$-0.087 \pm 0.055 \pm 0.036$	$-0.046 \pm 0.074 \pm 0.048$
	$\lambda_{\theta\phi}$	$0.043 \pm 0.037 \pm 0.029$	$-0.072 \pm 0.023 \pm 0.008$	$-0.096 \pm 0.028 \pm 0.010$
	$\lambda_\phi$	$0.079 \pm 0.032 \pm 0.030$	$0.029 \pm 0.023 \pm 0.010$	$0.037 \pm 0.023 \pm 0.010$
	$\tilde{\lambda}$	$0.185 \pm 0.109 \pm 0.077$	$-0.001 \pm 0.079 \pm 0.028$	$0.069 \pm 0.097 \pm 0.049$
10 – 15	$\lambda_\theta$	$-0.101 \pm 0.054 \pm 0.059$	$-0.122 \pm 0.050 \pm 0.041$	$-0.097 \pm 0.069 \pm 0.054$
	$\lambda_{\theta\phi}$	$-0.025 \pm 0.023 \pm 0.014$	$-0.098 \pm 0.019 \pm 0.008$	$-0.107 \pm 0.026 \pm 0.012$
	$\lambda_\phi$	$0.078 \pm 0.027 \pm 0.031$	$0.063 \pm 0.020 \pm 0.009$	$0.068 \pm 0.022 \pm 0.012$
	$\tilde{\lambda}$	$0.144 \pm 0.080 \pm 0.055$	$0.070 \pm 0.075 \pm 0.035$	$0.115 \pm 0.097 \pm 0.046$
15 – 20	$\lambda_\theta$	$0.028 \pm 0.095 \pm 0.141$	$-0.174 \pm 0.093 \pm 0.091$	$0.226 \pm 0.168 \pm 0.172$
	$\lambda_{\theta\phi}$	$-0.021 \pm 0.044 \pm 0.035$	$-0.098 \pm 0.041 \pm 0.026$	$-0.159 \pm 0.068 \pm 0.034$
	$\lambda_\phi$	$-0.022 \pm 0.047 \pm 0.067$	$0.069 \pm 0.036 \pm 0.024$	$-0.068 \pm 0.052 \pm 0.029$
	$\tilde{\lambda}$	$-0.039 \pm 0.128 \pm 0.109$	$0.035 \pm 0.155 \pm 0.118$	$0.020 \pm 0.209 \pm 0.174$



Table 17: Values of  $\lambda_\theta$ ,  $\lambda_{\theta\phi}$  and  $\lambda_\phi$  measured in the HX, CS and GJ frames for the  $\Upsilon(2S)$  produced at  $\sqrt{s} = 7$  TeV in the rapidity range  $2.2 < y^\Upsilon < 4.5$ . The first uncertainty is statistical and the second systematic.

$p_T^\Upsilon$ [GeV/c]		$\lambda_\theta$	$\lambda_{\theta\phi}$	$\lambda_\phi$
0 – 2	HX	$-0.160 \pm 0.052 \pm 0.039$	$0.007 \pm 0.018 \pm 0.007$	$0.001 \pm 0.012 \pm 0.004$
	CS	$-0.165 \pm 0.053 \pm 0.039$	$0.011 \pm 0.017 \pm 0.005$	$0.000 \pm 0.012 \pm 0.004$
	GJ	$-0.176 \pm 0.051 \pm 0.037$	$0.013 \pm 0.018 \pm 0.007$	$0.004 \pm 0.012 \pm 0.004$
2 – 4	HX	$-0.045 \pm 0.037 \pm 0.025$	$0.016 \pm 0.016 \pm 0.009$	$0.009 \pm 0.009 \pm 0.004$
	CS	$-0.051 \pm 0.041 \pm 0.027$	$0.035 \pm 0.014 \pm 0.005$	$0.011 \pm 0.009 \pm 0.003$
	GJ	$-0.104 \pm 0.037 \pm 0.022$	$0.040 \pm 0.015 \pm 0.009$	$0.027 \pm 0.009 \pm 0.004$
4 – 6	HX	$-0.069 \pm 0.034 \pm 0.019$	$0.064 \pm 0.021 \pm 0.009$	$0.008 \pm 0.012 \pm 0.006$
	CS	$-0.106 \pm 0.042 \pm 0.020$	$0.040 \pm 0.016 \pm 0.006$	$0.024 \pm 0.009 \pm 0.004$
	GJ	$-0.147 \pm 0.037 \pm 0.019$	$-0.004 \pm 0.018 \pm 0.010$	$0.039 \pm 0.011 \pm 0.007$
6 – 8	HX	$-0.050 \pm 0.037 \pm 0.021$	$0.131 \pm 0.024 \pm 0.013$	$-0.022 \pm 0.019 \pm 0.010$
	CS	$-0.193 \pm 0.042 \pm 0.016$	$0.047 \pm 0.022 \pm 0.007$	$0.032 \pm 0.012 \pm 0.004$
	GJ	$-0.170 \pm 0.040 \pm 0.024$	$-0.077 \pm 0.021 \pm 0.009$	$0.026 \pm 0.015 \pm 0.008$
8 – 10	HX	$0.089 \pm 0.050 \pm 0.028$	$0.114 \pm 0.025 \pm 0.010$	$-0.051 \pm 0.026 \pm 0.015$
	CS	$-0.153 \pm 0.041 \pm 0.016$	$0.085 \pm 0.030 \pm 0.010$	$0.032 \pm 0.016 \pm 0.007$
	GJ	$-0.170 \pm 0.048 \pm 0.032$	$-0.077 \pm 0.022 \pm 0.008$	$0.038 \pm 0.020 \pm 0.010$
10 – 15	HX	$0.139 \pm 0.049 \pm 0.040$	$0.036 \pm 0.021 \pm 0.009$	$-0.025 \pm 0.024 \pm 0.016$
	CS	$-0.057 \pm 0.033 \pm 0.018$	$0.063 \pm 0.029 \pm 0.012$	$0.039 \pm 0.018 \pm 0.009$
	GJ	$-0.051 \pm 0.048 \pm 0.037$	$-0.060 \pm 0.020 \pm 0.007$	$0.037 \pm 0.019 \pm 0.012$
15 – 20	HX	$0.155 \pm 0.088 \pm 0.079$	$0.043 \pm 0.050 \pm 0.029$	$-0.036 \pm 0.042 \pm 0.034$
	CS	$-0.110 \pm 0.056 \pm 0.055$	$0.062 \pm 0.050 \pm 0.027$	$0.053 \pm 0.044 \pm 0.043$
	GJ	$-0.013 \pm 0.091 \pm 0.070$	$-0.111 \pm 0.042 \pm 0.028$	$0.023 \pm 0.036 \pm 0.021$
20 – 30	HX	$0.267 \pm 0.164 \pm 0.149$	$0.002 \pm 0.091 \pm 0.081$	$0.060 \pm 0.059 \pm 0.048$
	CS	$-0.001 \pm 0.107 \pm 0.155$	$0.094 \pm 0.078 \pm 0.058$	$0.139 \pm 0.079 \pm 0.107$
	GJ	$0.051 \pm 0.156 \pm 0.214$	$-0.138 \pm 0.077 \pm 0.064$	$0.127 \pm 0.056 \pm 0.046$

Table 18: Values of  $\lambda_\theta$ ,  $\lambda_{\theta\phi}$  and  $\lambda_\phi$  measured in the HX, CS and GJ frames for the  $\Upsilon(2S)$  produced at  $\sqrt{s} = 8$  TeV in the rapidity range  $2.2 < y^\Upsilon < 4.5$ . The first uncertainty is statistical and the second systematic.

$p_T^\Upsilon$ [GeV/c]		$\lambda_\theta$	$\lambda_{\theta\phi}$	$\lambda_\phi$
0 – 2	HX	$0.049 \pm 0.038 \pm 0.031$	$-0.023 \pm 0.013 \pm 0.005$	$0.002 \pm 0.008 \pm 0.003$
	CS	$0.051 \pm 0.039 \pm 0.030$	$0.005 \pm 0.012 \pm 0.004$	$0.000 \pm 0.008 \pm 0.003$
	GJ	$0.031 \pm 0.038 \pm 0.030$	$0.031 \pm 0.013 \pm 0.007$	$0.004 \pm 0.008 \pm 0.003$
2 – 4	HX	$0.058 \pm 0.025 \pm 0.024$	$-0.023 \pm 0.011 \pm 0.007$	$-0.001 \pm 0.006 \pm 0.003$
	CS	$0.080 \pm 0.029 \pm 0.024$	$0.033 \pm 0.009 \pm 0.005$	$-0.006 \pm 0.006 \pm 0.002$
	GJ	$0.011 \pm 0.026 \pm 0.022$	$0.079 \pm 0.011 \pm 0.009$	$0.016 \pm 0.006 \pm 0.004$
4 – 6	HX	$0.010 \pm 0.024 \pm 0.018$	$0.070 \pm 0.014 \pm 0.008$	$-0.012 \pm 0.008 \pm 0.005$
	CS	$-0.068 \pm 0.029 \pm 0.021$	$0.080 \pm 0.011 \pm 0.007$	$0.016 \pm 0.006 \pm 0.003$
	GJ	$-0.168 \pm 0.024 \pm 0.015$	$0.034 \pm 0.012 \pm 0.009$	$0.049 \pm 0.007 \pm 0.006$
6 – 8	HX	$0.044 \pm 0.026 \pm 0.019$	$0.125 \pm 0.017 \pm 0.008$	$-0.034 \pm 0.013 \pm 0.007$
	CS	$-0.145 \pm 0.029 \pm 0.014$	$0.095 \pm 0.014 \pm 0.008$	$0.033 \pm 0.008 \pm 0.004$
	GJ	$-0.210 \pm 0.026 \pm 0.017$	$-0.037 \pm 0.014 \pm 0.007$	$0.056 \pm 0.010 \pm 0.008$
8 – 10	HX	$0.039 \pm 0.032 \pm 0.024$	$0.080 \pm 0.016 \pm 0.008$	$-0.008 \pm 0.017 \pm 0.010$
	CS	$-0.096 \pm 0.028 \pm 0.013$	$0.037 \pm 0.020 \pm 0.009$	$0.039 \pm 0.011 \pm 0.006$
	GJ	$-0.072 \pm 0.034 \pm 0.024$	$-0.058 \pm 0.015 \pm 0.006$	$0.031 \pm 0.013 \pm 0.009$
10 – 15	HX	$0.224 \pm 0.034 \pm 0.035$	$0.048 \pm 0.014 \pm 0.008$	$-0.044 \pm 0.017 \pm 0.013$
	CS	$-0.076 \pm 0.021 \pm 0.013$	$0.105 \pm 0.019 \pm 0.010$	$0.052 \pm 0.012 \pm 0.008$
	GJ	$-0.101 \pm 0.031 \pm 0.028$	$-0.079 \pm 0.013 \pm 0.008$	$0.060 \pm 0.012 \pm 0.010$
15 – 20	HX	$0.119 \pm 0.056 \pm 0.063$	$0.034 \pm 0.032 \pm 0.024$	$-0.036 \pm 0.027 \pm 0.027$
	CS	$-0.090 \pm 0.037 \pm 0.039$	$0.050 \pm 0.033 \pm 0.017$	$0.032 \pm 0.029 \pm 0.029$
	GJ	$-0.025 \pm 0.059 \pm 0.056$	$-0.079 \pm 0.027 \pm 0.018$	$0.010 \pm 0.023 \pm 0.017$
20 – 30	HX	$0.043 \pm 0.092 \pm 0.118$	$0.060 \pm 0.054 \pm 0.047$	$0.013 \pm 0.037 \pm 0.027$
	CS	$-0.057 \pm 0.064 \pm 0.111$	$-0.012 \pm 0.049 \pm 0.042$	$0.045 \pm 0.052 \pm 0.091$
	GJ	$0.068 \pm 0.104 \pm 0.150$	$-0.042 \pm 0.048 \pm 0.044$	$0.004 \pm 0.037 \pm 0.034$

Table 19: Values of  $\tilde{\lambda}$  measured in the HX, CS and GJ frames for the  $\Upsilon(2S)$  produced at  $\sqrt{s} = 7$  and 8 TeV in the rapidity range  $2.2 < y^\Upsilon < 4.5$ . The first uncertainty is statistical and the second systematic.

$p_T^\Upsilon$ [GeV/c]	$\tilde{\lambda}$	$\sqrt{s} = 7$ TeV	$\sqrt{s} = 8$ TeV
0 – 2	HX	$-0.158 \pm 0.063 \pm 0.042$	$0.054 \pm 0.046 \pm 0.034$
	CS	$-0.164 \pm 0.063 \pm 0.042$	$0.050 \pm 0.047 \pm 0.033$
	GJ	$-0.164 \pm 0.063 \pm 0.038$	$0.042 \pm 0.046 \pm 0.033$
2 – 4	HX	$-0.018 \pm 0.050 \pm 0.033$	$0.055 \pm 0.034 \pm 0.030$
	CS	$-0.018 \pm 0.050 \pm 0.031$	$0.063 \pm 0.035 \pm 0.029$
	GJ	$-0.022 \pm 0.050 \pm 0.031$	$0.060 \pm 0.034 \pm 0.030$
4 – 6	HX	$-0.046 \pm 0.054 \pm 0.031$	$-0.026 \pm 0.037 \pm 0.026$
	CS	$-0.036 \pm 0.055 \pm 0.028$	$-0.020 \pm 0.037 \pm 0.028$
	GJ	$-0.033 \pm 0.055 \pm 0.032$	$-0.023 \pm 0.037 \pm 0.029$
6 – 8	HX	$-0.112 \pm 0.061 \pm 0.030$	$-0.056 \pm 0.042 \pm 0.023$
	CS	$-0.100 \pm 0.061 \pm 0.024$	$-0.048 \pm 0.042 \pm 0.022$
	GJ	$-0.093 \pm 0.062 \pm 0.027$	$-0.045 \pm 0.042 \pm 0.024$
8 – 10	HX	$-0.061 \pm 0.069 \pm 0.026$	$0.016 \pm 0.047 \pm 0.023$
	CS	$-0.059 \pm 0.069 \pm 0.026$	$0.021 \pm 0.048 \pm 0.024$
	GJ	$-0.060 \pm 0.069 \pm 0.029$	$0.023 \pm 0.048 \pm 0.025$
10 – 15	HX	$0.063 \pm 0.067 \pm 0.028$	$0.087 \pm 0.044 \pm 0.026$
	CS	$0.062 \pm 0.067 \pm 0.031$	$0.085 \pm 0.044 \pm 0.025$
	GJ	$0.063 \pm 0.067 \pm 0.028$	$0.085 \pm 0.045 \pm 0.023$
15 – 20	HX	$0.046 \pm 0.135 \pm 0.085$	$0.009 \pm 0.087 \pm 0.061$
	CS	$0.051 \pm 0.136 \pm 0.101$	$0.007 \pm 0.087 \pm 0.065$
	GJ	$0.056 \pm 0.136 \pm 0.077$	$0.005 \pm 0.087 \pm 0.061$
20 – 30	HX	$0.474 \pm 0.286 \pm 0.245$	$0.083 \pm 0.152 \pm 0.145$
	CS	$0.484 \pm 0.287 \pm 0.323$	$0.082 \pm 0.153 \pm 0.225$
	GJ	$0.495 \pm 0.288 \pm 0.248$	$0.081 \pm 0.152 \pm 0.176$

## C Polarization results for the $\Upsilon(3S)$ state

Values of the polarization parameters  $\lambda$  and  $\tilde{\lambda}$  for the  $\Upsilon(3S)$  meson are presented in Tables 20 and 21 for the HX frame, in Tables 22 and 23 for the CS frame and in Tables 24 and 25 for the GJ frame for  $\sqrt{s} = 7$  and 8 TeV, respectively. The polarization parameters  $\lambda$  measured in the wide rapidity bin  $2.2 < y^r < 4.5$  are presented in Tables 26 and 27, while the parameters  $\tilde{\lambda}$  are listed in Table 28.

Table 20: Values of  $\lambda_\theta$ ,  $\lambda_{\theta\phi}$ ,  $\lambda_\phi$  and  $\tilde{\lambda}$  measured in the HX frame for the  $\Upsilon(3S)$  produced at  $\sqrt{s} = 7$  TeV. The first uncertainty is statistical and the second systematic.

$p_T^r$ [GeV/c]	$\lambda$	$2.2 < y < 3.0$	$3.0 < y < 3.5$	$3.5 < y < 4.5$
0 – 2	$\lambda_\theta$	$0.479 \pm 0.259 \pm 0.104$	$-0.052 \pm 0.125 \pm 0.074$	$-0.277 \pm 0.154 \pm 0.101$
	$\lambda_{\theta\phi}$	$-0.026 \pm 0.064 \pm 0.015$	$0.068 \pm 0.043 \pm 0.012$	$-0.047 \pm 0.057 \pm 0.020$
	$\lambda_\phi$	$-0.024 \pm 0.034 \pm 0.007$	$-0.050 \pm 0.035 \pm 0.008$	$0.006 \pm 0.035 \pm 0.008$
	$\tilde{\lambda}$	$0.396 \pm 0.276 \pm 0.108$	$-0.193 \pm 0.151 \pm 0.074$	$-0.261 \pm 0.188 \pm 0.106$
2 – 4	$\lambda_\theta$	$0.051 \pm 0.165 \pm 0.065$	$0.021 \pm 0.095 \pm 0.058$	$-0.451 \pm 0.089 \pm 0.058$
	$\lambda_{\theta\phi}$	$-0.098 \pm 0.048 \pm 0.017$	$0.056 \pm 0.040 \pm 0.015$	$0.129 \pm 0.054 \pm 0.026$
	$\lambda_\phi$	$0.029 \pm 0.023 \pm 0.005$	$0.062 \pm 0.027 \pm 0.007$	$0.043 \pm 0.028 \pm 0.010$
	$\tilde{\lambda}$	$0.141 \pm 0.192 \pm 0.075$	$0.218 \pm 0.148 \pm 0.079$	$-0.338 \pm 0.134 \pm 0.083$
4 – 6	$\lambda_\theta$	$0.111 \pm 0.150 \pm 0.059$	$-0.039 \pm 0.085 \pm 0.045$	$-0.030 \pm 0.089 \pm 0.061$
	$\lambda_{\theta\phi}$	$-0.072 \pm 0.060 \pm 0.024$	$0.062 \pm 0.048 \pm 0.018$	$0.088 \pm 0.068 \pm 0.038$
	$\lambda_\phi$	$0.061 \pm 0.027 \pm 0.009$	$0.029 \pm 0.032 \pm 0.010$	$0.022 \pm 0.040 \pm 0.019$
	$\tilde{\lambda}$	$0.314 \pm 0.204 \pm 0.084$	$0.048 \pm 0.146 \pm 0.070$	$0.038 \pm 0.167 \pm 0.115$
6 – 8	$\lambda_\theta$	$-0.244 \pm 0.133 \pm 0.050$	$0.011 \pm 0.090 \pm 0.036$	$-0.035 \pm 0.090 \pm 0.049$
	$\lambda_{\theta\phi}$	$0.029 \pm 0.068 \pm 0.034$	$0.111 \pm 0.053 \pm 0.019$	$0.238 \pm 0.079 \pm 0.045$
	$\lambda_\phi$	$0.100 \pm 0.037 \pm 0.017$	$0.031 \pm 0.045 \pm 0.019$	$-0.041 \pm 0.060 \pm 0.036$
	$\tilde{\lambda}$	$0.063 \pm 0.209 \pm 0.089$	$0.107 \pm 0.167 \pm 0.070$	$-0.151 \pm 0.175 \pm 0.094$
8 – 10	$\lambda_\theta$	$-0.087 \pm 0.144 \pm 0.070$	$0.126 \pm 0.124 \pm 0.070$	$0.015 \pm 0.122 \pm 0.087$
	$\lambda_{\theta\phi}$	$-0.068 \pm 0.074 \pm 0.039$	$0.184 \pm 0.053 \pm 0.014$	$0.209 \pm 0.077 \pm 0.040$
	$\lambda_\phi$	$0.124 \pm 0.050 \pm 0.026$	$-0.071 \pm 0.063 \pm 0.028$	$-0.050 \pm 0.084 \pm 0.060$
	$\tilde{\lambda}$	$0.326 \pm 0.242 \pm 0.116$	$-0.080 \pm 0.163 \pm 0.046$	$-0.129 \pm 0.198 \pm 0.099$
10 – 15	$\lambda_\theta$	$0.192 \pm 0.134 \pm 0.109$	$0.322 \pm 0.121 \pm 0.103$	$0.053 \pm 0.118 \pm 0.121$
	$\lambda_{\theta\phi}$	$0.126 \pm 0.056 \pm 0.026$	$0.091 \pm 0.046 \pm 0.017$	$0.106 \pm 0.055 \pm 0.019$
	$\lambda_\phi$	$0.081 \pm 0.045 \pm 0.028$	$-0.147 \pm 0.062 \pm 0.039$	$-0.026 \pm 0.076 \pm 0.068$
	$\tilde{\lambda}$	$0.474 \pm 0.181 \pm 0.077$	$-0.103 \pm 0.138 \pm 0.043$	$-0.025 \pm 0.185 \pm 0.099$
15 – 20	$\lambda_\theta$	$0.181 \pm 0.203 \pm 0.198$	$0.156 \pm 0.161 \pm 0.125$	$0.521 \pm 0.292 \pm 0.253$
	$\lambda_{\theta\phi}$	$0.084 \pm 0.093 \pm 0.053$	$0.121 \pm 0.093 \pm 0.060$	$0.265 \pm 0.147 \pm 0.080$
	$\lambda_\phi$	$0.137 \pm 0.067 \pm 0.047$	$0.086 \pm 0.082 \pm 0.052$	$0.178 \pm 0.122 \pm 0.087$
	$\tilde{\lambda}$	$0.685 \pm 0.335 \pm 0.204$	$0.453 \pm 0.333 \pm 0.171$	$1.282 \pm 0.644 \pm 0.294$

Table 21: Values of  $\lambda_\theta$ ,  $\lambda_{\theta\phi}$ ,  $\lambda_\phi$  and  $\tilde{\lambda}$  measured in the HX frame for the  $\Upsilon(3S)$  produced at  $\sqrt{s} = 8$  TeV. The first uncertainty is statistical and the second systematic.

$p_T^\Upsilon$ [GeV/c]	$\lambda$	$2.2 < y < 3.0$	$3.0 < y < 3.5$	$3.5 < y < 4.5$
0 – 2	$\lambda_\theta$	$0.212 \pm 0.165 \pm 0.083$	$-0.073 \pm 0.089 \pm 0.078$	$-0.494 \pm 0.101 \pm 0.080$
	$\lambda_{\theta\phi}$	$-0.060 \pm 0.042 \pm 0.011$	$0.015 \pm 0.031 \pm 0.009$	$0.021 \pm 0.039 \pm 0.015$
	$\lambda_\phi$	$-0.004 \pm 0.022 \pm 0.005$	$-0.029 \pm 0.025 \pm 0.006$	$-0.019 \pm 0.024 \pm 0.006$
	$\tilde{\lambda}$	$0.198 \pm 0.180 \pm 0.086$	$-0.155 \pm 0.112 \pm 0.080$	$-0.540 \pm 0.119 \pm 0.081$
2 – 4	$\lambda_\theta$	$0.233 \pm 0.113 \pm 0.045$	$-0.008 \pm 0.063 \pm 0.057$	$-0.147 \pm 0.068 \pm 0.072$
	$\lambda_{\theta\phi}$	$-0.108 \pm 0.033 \pm 0.011$	$0.016 \pm 0.028 \pm 0.013$	$0.014 \pm 0.038 \pm 0.024$
	$\lambda_\phi$	$0.040 \pm 0.016 \pm 0.005$	$0.008 \pm 0.019 \pm 0.006$	$0.027 \pm 0.020 \pm 0.009$
	$\tilde{\lambda}$	$0.367 \pm 0.135 \pm 0.055$	$0.015 \pm 0.091 \pm 0.071$	$-0.068 \pm 0.101 \pm 0.092$
4 – 6	$\lambda_\theta$	$0.106 \pm 0.102 \pm 0.042$	$0.096 \pm 0.061 \pm 0.045$	$-0.183 \pm 0.062 \pm 0.057$
	$\lambda_{\theta\phi}$	$-0.078 \pm 0.041 \pm 0.017$	$0.059 \pm 0.033 \pm 0.020$	$0.267 \pm 0.050 \pm 0.034$
	$\lambda_\phi$	$0.075 \pm 0.019 \pm 0.008$	$0.037 \pm 0.022 \pm 0.011$	$-0.047 \pm 0.028 \pm 0.017$
	$\tilde{\lambda}$	$0.357 \pm 0.141 \pm 0.064$	$0.215 \pm 0.105 \pm 0.077$	$-0.309 \pm 0.104 \pm 0.091$
6 – 8	$\lambda_\theta$	$-0.150 \pm 0.095 \pm 0.042$	$-0.019 \pm 0.062 \pm 0.033$	$-0.088 \pm 0.062 \pm 0.044$
	$\lambda_{\theta\phi}$	$0.024 \pm 0.048 \pm 0.023$	$0.273 \pm 0.038 \pm 0.017$	$0.406 \pm 0.065 \pm 0.042$
	$\lambda_\phi$	$0.080 \pm 0.026 \pm 0.012$	$-0.068 \pm 0.032 \pm 0.016$	$-0.146 \pm 0.047 \pm 0.029$
	$\tilde{\lambda}$	$0.097 \pm 0.145 \pm 0.067$	$-0.210 \pm 0.098 \pm 0.058$	$-0.459 \pm 0.116 \pm 0.080$
8 – 10	$\lambda_\theta$	$-0.100 \pm 0.103 \pm 0.057$	$0.109 \pm 0.078 \pm 0.052$	$0.064 \pm 0.081 \pm 0.063$
	$\lambda_{\theta\phi}$	$0.096 \pm 0.052 \pm 0.030$	$0.193 \pm 0.035 \pm 0.014$	$0.175 \pm 0.050 \pm 0.029$
	$\lambda_\phi$	$0.092 \pm 0.036 \pm 0.019$	$-0.017 \pm 0.041 \pm 0.023$	$-0.049 \pm 0.055 \pm 0.035$
	$\tilde{\lambda}$	$0.194 \pm 0.159 \pm 0.088$	$0.056 \pm 0.116 \pm 0.042$	$-0.079 \pm 0.132 \pm 0.079$
10 – 15	$\lambda_\theta$	$0.222 \pm 0.093 \pm 0.067$	$0.254 \pm 0.075 \pm 0.067$	$0.186 \pm 0.086 \pm 0.072$
	$\lambda_{\theta\phi}$	$0.054 \pm 0.038 \pm 0.021$	$0.129 \pm 0.029 \pm 0.012$	$0.142 \pm 0.037 \pm 0.015$
	$\lambda_\phi$	$-0.017 \pm 0.033 \pm 0.022$	$-0.057 \pm 0.037 \pm 0.025$	$-0.091 \pm 0.051 \pm 0.033$
	$\tilde{\lambda}$	$0.168 \pm 0.108 \pm 0.056$	$0.080 \pm 0.099 \pm 0.046$	$-0.079 \pm 0.112 \pm 0.056$
15 – 20	$\lambda_\theta$	$0.512 \pm 0.153 \pm 0.143$	$0.238 \pm 0.120 \pm 0.128$	$0.313 \pm 0.176 \pm 0.160$
	$\lambda_{\theta\phi}$	$-0.064 \pm 0.073 \pm 0.049$	$0.032 \pm 0.067 \pm 0.056$	$0.176 \pm 0.096 \pm 0.071$
	$\lambda_\phi$	$-0.123 \pm 0.054 \pm 0.045$	$-0.061 \pm 0.060 \pm 0.058$	$-0.203 \pm 0.097 \pm 0.093$
	$\tilde{\lambda}$	$0.126 \pm 0.168 \pm 0.093$	$0.052 \pm 0.184 \pm 0.135$	$-0.246 \pm 0.223 \pm 0.178$

Table 22: Values of  $\lambda_\theta$ ,  $\lambda_{\theta\phi}$ ,  $\lambda_\phi$  and  $\tilde{\lambda}$  measured in the CS frame for the  $\Upsilon(3S)$  produced at  $\sqrt{s} = 7$  TeV. The first uncertainty is statistical and the second systematic.

$p_T^\Upsilon$ [GeV/c]	$\lambda$	$2.2 < y < 3.0$	$3.0 < y < 3.5$	$3.5 < y < 4.5$
0 – 2	$\lambda_\theta$	$0.457 \pm 0.257 \pm 0.104$	$-0.065 \pm 0.125 \pm 0.072$	$-0.189 \pm 0.167 \pm 0.098$
	$\lambda_{\theta\phi}$	$0.089 \pm 0.065 \pm 0.014$	$0.081 \pm 0.042 \pm 0.011$	$-0.047 \pm 0.053 \pm 0.016$
	$\lambda_\phi$	$-0.020 \pm 0.033 \pm 0.008$	$-0.042 \pm 0.035 \pm 0.009$	$-0.008 \pm 0.034 \pm 0.009$
	$\tilde{\lambda}$	$0.388 \pm 0.277 \pm 0.102$	$-0.185 \pm 0.152 \pm 0.071$	$-0.210 \pm 0.192 \pm 0.102$
2 – 4	$\lambda_\theta$	$0.115 \pm 0.173 \pm 0.065$	$0.023 \pm 0.102 \pm 0.060$	$-0.344 \pm 0.111 \pm 0.063$
	$\lambda_{\theta\phi}$	$0.029 \pm 0.047 \pm 0.012$	$0.064 \pm 0.035 \pm 0.007$	$0.010 \pm 0.041 \pm 0.013$
	$\lambda_\phi$	$0.015 \pm 0.023 \pm 0.005$	$0.072 \pm 0.026 \pm 0.006$	$0.045 \pm 0.025 \pm 0.007$
	$\tilde{\lambda}$	$0.161 \pm 0.195 \pm 0.070$	$0.257 \pm 0.151 \pm 0.079$	$-0.218 \pm 0.140 \pm 0.080$
4 – 6	$\lambda_\theta$	$0.240 \pm 0.172 \pm 0.052$	$-0.043 \pm 0.103 \pm 0.047$	$0.047 \pm 0.130 \pm 0.070$
	$\lambda_{\theta\phi}$	$0.106 \pm 0.052 \pm 0.012$	$0.033 \pm 0.039 \pm 0.008$	$0.065 \pm 0.050 \pm 0.013$
	$\lambda_\phi$	$0.052 \pm 0.023 \pm 0.006$	$0.043 \pm 0.027 \pm 0.007$	$0.039 \pm 0.028 \pm 0.010$
	$\tilde{\lambda}$	$0.419 \pm 0.213 \pm 0.064$	$0.091 \pm 0.149 \pm 0.064$	$0.170 \pm 0.174 \pm 0.099$
6 – 8	$\lambda_\theta$	$-0.080 \pm 0.161 \pm 0.047$	$-0.092 \pm 0.096 \pm 0.041$	$-0.224 \pm 0.118 \pm 0.049$
	$\lambda_{\theta\phi}$	$-0.036 \pm 0.063 \pm 0.017$	$0.041 \pm 0.051 \pm 0.014$	$0.109 \pm 0.061 \pm 0.018$
	$\lambda_\phi$	$0.074 \pm 0.027 \pm 0.007$	$0.074 \pm 0.032 \pm 0.013$	$0.055 \pm 0.033 \pm 0.011$
	$\tilde{\lambda}$	$0.153 \pm 0.216 \pm 0.066$	$0.141 \pm 0.169 \pm 0.078$	$-0.063 \pm 0.179 \pm 0.074$
8 – 10	$\lambda_\theta$	$0.201 \pm 0.176 \pm 0.071$	$-0.219 \pm 0.081 \pm 0.031$	$-0.238 \pm 0.115 \pm 0.046$
	$\lambda_{\theta\phi}$	$0.010 \pm 0.086 \pm 0.023$	$0.097 \pm 0.068 \pm 0.016$	$0.076 \pm 0.084 \pm 0.025$
	$\lambda_\phi$	$0.056 \pm 0.035 \pm 0.012$	$0.053 \pm 0.040 \pm 0.011$	$0.049 \pm 0.045 \pm 0.013$
	$\tilde{\lambda}$	$0.393 \pm 0.248 \pm 0.087$	$-0.063 \pm 0.164 \pm 0.053$	$-0.096 \pm 0.200 \pm 0.068$
10 – 15	$\lambda_\theta$	$-0.080 \pm 0.091 \pm 0.035$	$-0.184 \pm 0.060 \pm 0.028$	$-0.137 \pm 0.090 \pm 0.044$
	$\lambda_{\theta\phi}$	$0.025 \pm 0.073 \pm 0.021$	$0.204 \pm 0.063 \pm 0.021$	$0.027 \pm 0.079 \pm 0.033$
	$\lambda_\phi$	$0.159 \pm 0.032 \pm 0.014$	$0.023 \pm 0.042 \pm 0.016$	$0.038 \pm 0.050 \pm 0.022$
	$\tilde{\lambda}$	$0.471 \pm 0.180 \pm 0.076$	$-0.118 \pm 0.138 \pm 0.047$	$-0.024 \pm 0.187 \pm 0.073$
15 – 20	$\lambda_\theta$	$0.010 \pm 0.117 \pm 0.090$	$-0.074 \pm 0.106 \pm 0.094$	$-0.153 \pm 0.146 \pm 0.141$
	$\lambda_{\theta\phi}$	$-0.023 \pm 0.115 \pm 0.067$	$-0.014 \pm 0.095 \pm 0.041$	$0.008 \pm 0.139 \pm 0.067$
	$\lambda_\phi$	$0.184 \pm 0.072 \pm 0.052$	$0.151 \pm 0.083 \pm 0.053$	$0.337 \pm 0.103 \pm 0.066$
	$\tilde{\lambda}$	$0.689 \pm 0.336 \pm 0.207$	$0.447 \pm 0.333 \pm 0.178$	$1.295 \pm 0.652 \pm 0.324$

Table 23: Values of  $\lambda_\theta$ ,  $\lambda_{\theta\phi}$ ,  $\lambda_\phi$  and  $\tilde{\lambda}$  measured in the CS frame for the  $\Upsilon(3S)$  produced at  $\sqrt{s} = 8$  TeV. The first uncertainty is statistical and the second systematic.

$p_T^\Upsilon$ [GeV/c]	$\lambda$	$2.2 < y < 3.0$	$3.0 < y < 3.5$	$3.5 < y < 4.5$
0 – 2	$\lambda_\theta$	$0.231 \pm 0.166 \pm 0.072$	$-0.072 \pm 0.090 \pm 0.076$	$-0.437 \pm 0.108 \pm 0.081$
	$\lambda_{\theta\phi}$	$0.033 \pm 0.043 \pm 0.013$	$0.022 \pm 0.030 \pm 0.008$	$-0.002 \pm 0.036 \pm 0.010$
	$\lambda_\phi$	$-0.007 \pm 0.022 \pm 0.005$	$-0.028 \pm 0.025 \pm 0.007$	$-0.024 \pm 0.024 \pm 0.007$
	$\tilde{\lambda}$	$0.209 \pm 0.181 \pm 0.077$	$-0.151 \pm 0.112 \pm 0.079$	$-0.499 \pm 0.122 \pm 0.083$
2 – 4	$\lambda_\theta$	$0.282 \pm 0.119 \pm 0.052$	$0.023 \pm 0.070 \pm 0.058$	$0.000 \pm 0.086 \pm 0.075$
	$\lambda_{\theta\phi}$	$0.070 \pm 0.032 \pm 0.010$	$0.036 \pm 0.024 \pm 0.007$	$0.003 \pm 0.030 \pm 0.009$
	$\lambda_\phi$	$0.030 \pm 0.016 \pm 0.004$	$0.009 \pm 0.018 \pm 0.005$	$0.013 \pm 0.018 \pm 0.005$
	$\tilde{\lambda}$	$0.382 \pm 0.138 \pm 0.061$	$0.051 \pm 0.093 \pm 0.069$	$0.039 \pm 0.105 \pm 0.086$
4 – 6	$\lambda_\theta$	$0.184 \pm 0.116 \pm 0.044$	$0.060 \pm 0.071 \pm 0.052$	$-0.238 \pm 0.084 \pm 0.064$
	$\lambda_{\theta\phi}$	$0.094 \pm 0.035 \pm 0.011$	$0.082 \pm 0.027 \pm 0.008$	$0.131 \pm 0.032 \pm 0.011$
	$\lambda_\phi$	$0.061 \pm 0.016 \pm 0.005$	$0.061 \pm 0.018 \pm 0.007$	$0.030 \pm 0.018 \pm 0.007$
	$\tilde{\lambda}$	$0.391 \pm 0.145 \pm 0.056$	$0.259 \pm 0.107 \pm 0.075$	$-0.154 \pm 0.108 \pm 0.083$
6 – 8	$\lambda_\theta$	$-0.044 \pm 0.114 \pm 0.041$	$-0.330 \pm 0.059 \pm 0.033$	$-0.404 \pm 0.080 \pm 0.044$
	$\lambda_{\theta\phi}$	$0.040 \pm 0.043 \pm 0.011$	$0.119 \pm 0.033 \pm 0.009$	$0.155 \pm 0.039 \pm 0.015$
	$\lambda_\phi$	$0.068 \pm 0.018 \pm 0.006$	$0.056 \pm 0.021 \pm 0.008$	$0.037 \pm 0.022 \pm 0.010$
	$\tilde{\lambda}$	$0.172 \pm 0.150 \pm 0.056$	$-0.170 \pm 0.099 \pm 0.055$	$-0.302 \pm 0.114 \pm 0.068$
8 – 10	$\lambda_\theta$	$-0.093 \pm 0.108 \pm 0.043$	$-0.213 \pm 0.054 \pm 0.023$	$-0.177 \pm 0.078 \pm 0.036$
	$\lambda_{\theta\phi}$	$0.031 \pm 0.057 \pm 0.017$	$0.078 \pm 0.044 \pm 0.012$	$0.085 \pm 0.054 \pm 0.022$
	$\lambda_\phi$	$0.104 \pm 0.023 \pm 0.010$	$0.092 \pm 0.027 \pm 0.009$	$0.046 \pm 0.030 \pm 0.015$
	$\tilde{\lambda}$	$0.246 \pm 0.163 \pm 0.067$	$0.068 \pm 0.117 \pm 0.044$	$-0.041 \pm 0.134 \pm 0.074$
10 – 15	$\lambda_\theta$	$-0.038 \pm 0.063 \pm 0.027$	$-0.168 \pm 0.039 \pm 0.021$	$-0.213 \pm 0.053 \pm 0.028$
	$\lambda_{\theta\phi}$	$0.110 \pm 0.050 \pm 0.017$	$0.115 \pm 0.040 \pm 0.016$	$0.122 \pm 0.051 \pm 0.024$
	$\lambda_\phi$	$0.068 \pm 0.022 \pm 0.012$	$0.078 \pm 0.027 \pm 0.013$	$0.040 \pm 0.032 \pm 0.016$
	$\tilde{\lambda}$	$0.177 \pm 0.108 \pm 0.049$	$0.073 \pm 0.099 \pm 0.043$	$-0.097 \pm 0.113 \pm 0.051$
15 – 20	$\lambda_\theta$	$-0.083 \pm 0.075 \pm 0.049$	$-0.109 \pm 0.072 \pm 0.070$	$-0.368 \pm 0.082 \pm 0.081$
	$\lambda_{\theta\phi}$	$0.242 \pm 0.074 \pm 0.040$	$0.116 \pm 0.068 \pm 0.035$	$0.107 \pm 0.088 \pm 0.050$
	$\lambda_\phi$	$0.064 \pm 0.048 \pm 0.037$	$0.049 \pm 0.058 \pm 0.048$	$0.044 \pm 0.079 \pm 0.077$
	$\tilde{\lambda}$	$0.117 \pm 0.168 \pm 0.114$	$0.041 \pm 0.183 \pm 0.112$	$-0.246 \pm 0.224 \pm 0.182$

Table 24: Values of  $\lambda_\theta$ ,  $\lambda_{\theta\phi}$ ,  $\lambda_\phi$  and  $\tilde{\lambda}$  measured in the GJ frame for the  $\Upsilon(3S)$  produced at  $\sqrt{s} = 7$  TeV. The first uncertainty is statistical and the second systematic.

$p_T^\Upsilon$ [GeV/c]	$\lambda$	$2.2 < y < 3.0$	$3.0 < y < 3.5$	$3.5 < y < 4.5$
0 – 2	$\lambda_\theta$	$0.317 \pm 0.233 \pm 0.116$	$-0.092 \pm 0.120 \pm 0.070$	$-0.126 \pm 0.170 \pm 0.095$
	$\lambda_{\theta\phi}$	$0.175 \pm 0.074 \pm 0.030$	$0.091 \pm 0.044 \pm 0.016$	$-0.024 \pm 0.053 \pm 0.017$
	$\lambda_\phi$	$0.003 \pm 0.034 \pm 0.008$	$-0.031 \pm 0.035 \pm 0.007$	$-0.015 \pm 0.034 \pm 0.007$
	$\tilde{\lambda}$	$0.326 \pm 0.270 \pm 0.132$	$-0.178 \pm 0.152 \pm 0.070$	$-0.168 \pm 0.194 \pm 0.102$
2 – 4	$\lambda_\theta$	$-0.088 \pm 0.132 \pm 0.074$	$-0.016 \pm 0.093 \pm 0.053$	$-0.227 \pm 0.117 \pm 0.053$
	$\lambda_{\theta\phi}$	$0.091 \pm 0.066 \pm 0.041$	$0.073 \pm 0.039 \pm 0.018$	$-0.025 \pm 0.038 \pm 0.018$
	$\lambda_\phi$	$0.056 \pm 0.028 \pm 0.012$	$0.092 \pm 0.027 \pm 0.008$	$0.038 \pm 0.025 \pm 0.008$
	$\tilde{\lambda}$	$0.085 \pm 0.190 \pm 0.111$	$0.288 \pm 0.152 \pm 0.083$	$-0.119 \pm 0.143 \pm 0.071$
4 – 6	$\lambda_\theta$	$-0.099 \pm 0.104 \pm 0.046$	$-0.052 \pm 0.091 \pm 0.043$	$0.006 \pm 0.126 \pm 0.059$
	$\lambda_{\theta\phi}$	$0.160 \pm 0.071 \pm 0.042$	$0.017 \pm 0.045 \pm 0.019$	$0.118 \pm 0.048 \pm 0.029$
	$\lambda_\phi$	$0.142 \pm 0.034 \pm 0.019$	$0.057 \pm 0.029 \pm 0.010$	$0.077 \pm 0.028 \pm 0.016$
	$\tilde{\lambda}$	$0.382 \pm 0.212 \pm 0.116$	$0.127 \pm 0.151 \pm 0.069$	$0.258 \pm 0.178 \pm 0.105$
6 – 8	$\lambda_\theta$	$-0.110 \pm 0.103 \pm 0.042$	$-0.071 \pm 0.095 \pm 0.037$	$-0.250 \pm 0.122 \pm 0.052$
	$\lambda_{\theta\phi}$	$-0.053 \pm 0.083 \pm 0.053$	$-0.039 \pm 0.049 \pm 0.017$	$-0.026 \pm 0.052 \pm 0.021$
	$\lambda_\phi$	$0.087 \pm 0.051 \pm 0.032$	$0.076 \pm 0.038 \pm 0.017$	$0.081 \pm 0.035 \pm 0.017$
	$\tilde{\lambda}$	$0.165 \pm 0.217 \pm 0.121$	$0.171 \pm 0.171 \pm 0.072$	$-0.008 \pm 0.182 \pm 0.083$
8 – 10	$\lambda_\theta$	$-0.076 \pm 0.115 \pm 0.066$	$-0.171 \pm 0.108 \pm 0.054$	$-0.210 \pm 0.152 \pm 0.068$
	$\lambda_{\theta\phi}$	$0.083 \pm 0.077 \pm 0.050$	$-0.111 \pm 0.048 \pm 0.015$	$-0.092 \pm 0.059 \pm 0.019$
	$\lambda_\phi$	$0.142 \pm 0.061 \pm 0.044$	$0.042 \pm 0.049 \pm 0.020$	$0.043 \pm 0.048 \pm 0.018$
	$\tilde{\lambda}$	$0.409 \pm 0.249 \pm 0.140$	$-0.047 \pm 0.165 \pm 0.050$	$-0.085 \pm 0.202 \pm 0.085$
10 – 15	$\lambda_\theta$	$0.105 \pm 0.119 \pm 0.111$	$-0.315 \pm 0.092 \pm 0.054$	$-0.047 \pm 0.145 \pm 0.084$
	$\lambda_{\theta\phi}$	$-0.128 \pm 0.051 \pm 0.027$	$-0.123 \pm 0.037 \pm 0.011$	$-0.078 \pm 0.055 \pm 0.019$
	$\lambda_\phi$	$0.105 \pm 0.055 \pm 0.050$	$0.064 \pm 0.039 \pm 0.017$	$0.006 \pm 0.047 \pm 0.021$
	$\tilde{\lambda}$	$0.468 \pm 0.178 \pm 0.091$	$-0.130 \pm 0.137 \pm 0.049$	$-0.029 \pm 0.189 \pm 0.075$
15 – 20	$\lambda_\theta$	$0.261 \pm 0.198 \pm 0.277$	$0.188 \pm 0.203 \pm 0.190$	$0.470 \pm 0.331 \pm 0.247$
	$\lambda_{\theta\phi}$	$-0.076 \pm 0.088 \pm 0.065$	$-0.104 \pm 0.084 \pm 0.044$	$-0.249 \pm 0.137 \pm 0.051$
	$\lambda_\phi$	$0.117 \pm 0.086 \pm 0.105$	$0.073 \pm 0.070 \pm 0.041$	$0.193 \pm 0.101 \pm 0.057$
	$\tilde{\lambda}$	$0.693 \pm 0.334 \pm 0.238$	$0.437 \pm 0.332 \pm 0.225$	$1.300 \pm 0.649 \pm 0.346$



Table 25: Values of  $\lambda_\theta$ ,  $\lambda_{\theta\phi}$ ,  $\lambda_\phi$  and  $\tilde{\lambda}$  measured in the GJ frame for the  $\Upsilon(3S)$  produced at  $\sqrt{s} = 8$  TeV. The first uncertainty is statistical and the second systematic.

$p_T^\Upsilon$ [GeV/c]	$\lambda$	$2.2 < y < 3.0$	$3.0 < y < 3.5$	$3.5 < y < 4.5$
0 – 2	$\lambda_\theta$	$0.147 \pm 0.152 \pm 0.072$	$-0.081 \pm 0.087 \pm 0.072$	$-0.385 \pm 0.111 \pm 0.074$
	$\lambda_{\theta\phi}$	$0.110 \pm 0.049 \pm 0.019$	$0.030 \pm 0.031 \pm 0.013$	$-0.009 \pm 0.036 \pm 0.014$
	$\lambda_\phi$	$0.009 \pm 0.023 \pm 0.005$	$-0.024 \pm 0.025 \pm 0.006$	$-0.027 \pm 0.024 \pm 0.006$
	$\tilde{\lambda}$	$0.177 \pm 0.177 \pm 0.079$	$-0.148 \pm 0.112 \pm 0.076$	$-0.453 \pm 0.123 \pm 0.078$
2 – 4	$\lambda_\theta$	$0.008 \pm 0.089 \pm 0.043$	$-0.002 \pm 0.065 \pm 0.051$	$0.054 \pm 0.088 \pm 0.065$
	$\lambda_{\theta\phi}$	$0.156 \pm 0.044 \pm 0.022$	$0.064 \pm 0.026 \pm 0.017$	$0.070 \pm 0.029 \pm 0.022$
	$\lambda_\phi$	$0.084 \pm 0.019 \pm 0.007$	$0.025 \pm 0.018 \pm 0.007$	$0.019 \pm 0.018 \pm 0.008$
	$\tilde{\lambda}$	$0.283 \pm 0.134 \pm 0.067$	$0.075 \pm 0.093 \pm 0.073$	$0.113 \pm 0.108 \pm 0.085$
4 – 6	$\lambda_\theta$	$-0.166 \pm 0.071 \pm 0.049$	$-0.038 \pm 0.060 \pm 0.037$	$-0.247 \pm 0.081 \pm 0.045$
	$\lambda_{\theta\phi}$	$0.114 \pm 0.048 \pm 0.043$	$0.079 \pm 0.030 \pm 0.019$	$0.058 \pm 0.031 \pm 0.024$
	$\lambda_\phi$	$0.138 \pm 0.023 \pm 0.017$	$0.099 \pm 0.020 \pm 0.011$	$0.068 \pm 0.018 \pm 0.013$
	$\tilde{\lambda}$	$0.288 \pm 0.142 \pm 0.118$	$0.289 \pm 0.108 \pm 0.076$	$-0.044 \pm 0.110 \pm 0.082$
6 – 8	$\lambda_\theta$	$-0.223 \pm 0.066 \pm 0.031$	$-0.306 \pm 0.056 \pm 0.024$	$-0.375 \pm 0.080 \pm 0.032$
	$\lambda_{\theta\phi}$	$-0.011 \pm 0.055 \pm 0.043$	$-0.106 \pm 0.032 \pm 0.016$	$-0.074 \pm 0.036 \pm 0.020$
	$\lambda_\phi$	$0.119 \pm 0.033 \pm 0.024$	$0.062 \pm 0.025 \pm 0.014$	$0.060 \pm 0.023 \pm 0.016$
	$\tilde{\lambda}$	$0.153 \pm 0.150 \pm 0.110$	$-0.129 \pm 0.100 \pm 0.055$	$-0.207 \pm 0.116 \pm 0.064$
8 – 10	$\lambda_\theta$	$-0.157 \pm 0.077 \pm 0.046$	$-0.134 \pm 0.074 \pm 0.039$	$-0.183 \pm 0.098 \pm 0.049$
	$\lambda_{\theta\phi}$	$-0.078 \pm 0.056 \pm 0.048$	$-0.132 \pm 0.032 \pm 0.011$	$-0.060 \pm 0.039 \pm 0.016$
	$\lambda_\phi$	$0.128 \pm 0.043 \pm 0.041$	$0.069 \pm 0.031 \pm 0.014$	$0.054 \pm 0.031 \pm 0.021$
	$\tilde{\lambda}$	$0.259 \pm 0.163 \pm 0.122$	$0.079 \pm 0.117 \pm 0.044$	$-0.024 \pm 0.136 \pm 0.074$
10 – 15	$\lambda_\theta$	$-0.114 \pm 0.069 \pm 0.072$	$-0.126 \pm 0.067 \pm 0.051$	$-0.218 \pm 0.086 \pm 0.049$
	$\lambda_{\theta\phi}$	$-0.058 \pm 0.031 \pm 0.019$	$-0.133 \pm 0.025 \pm 0.010$	$-0.130 \pm 0.033 \pm 0.011$
	$\lambda_\phi$	$0.092 \pm 0.035 \pm 0.036$	$0.063 \pm 0.027 \pm 0.015$	$0.035 \pm 0.029 \pm 0.015$
	$\tilde{\lambda}$	$0.178 \pm 0.107 \pm 0.068$	$0.068 \pm 0.099 \pm 0.047$	$-0.117 \pm 0.113 \pm 0.054$
15 – 20	$\lambda_\theta$	$-0.213 \pm 0.099 \pm 0.126$	$-0.115 \pm 0.118 \pm 0.121$	$-0.066 \pm 0.181 \pm 0.164$
	$\lambda_{\theta\phi}$	$-0.159 \pm 0.047 \pm 0.029$	$-0.121 \pm 0.051 \pm 0.025$	$-0.239 \pm 0.077 \pm 0.046$
	$\lambda_\phi$	$0.102 \pm 0.050 \pm 0.054$	$0.047 \pm 0.046 \pm 0.028$	$-0.068 \pm 0.063 \pm 0.036$
	$\tilde{\lambda}$	$0.105 \pm 0.167 \pm 0.115$	$0.028 \pm 0.182 \pm 0.126$	$-0.252 \pm 0.223 \pm 0.148$

Table 26: Values of  $\lambda_\theta$ ,  $\lambda_{\theta\phi}$  and  $\lambda_\phi$  measured in the HX, CS and GJ frames for the  $\Upsilon(3S)$  produced at  $\sqrt{s} = 7$  TeV in the rapidity range  $2.2 < y^\Upsilon < 4.5$ . The first uncertainty is statistical and the second systematic.

$p_T^\Upsilon$ [GeV/c]		$\lambda_\theta$	$\lambda_{\theta\phi}$	$\lambda_\phi$
0 – 2	HX	$-0.054 \pm 0.087 \pm 0.069$	$0.012 \pm 0.030 \pm 0.009$	$-0.026 \pm 0.020 \pm 0.006$
	CS	$-0.039 \pm 0.089 \pm 0.069$	$0.038 \pm 0.029 \pm 0.007$	$-0.026 \pm 0.020 \pm 0.004$
	GJ	$-0.054 \pm 0.086 \pm 0.068$	$0.065 \pm 0.030 \pm 0.012$	$-0.018 \pm 0.020 \pm 0.004$
2 – 4	HX	$-0.141 \pm 0.057 \pm 0.046$	$0.022 \pm 0.026 \pm 0.013$	$0.043 \pm 0.015 \pm 0.005$
	CS	$-0.097 \pm 0.064 \pm 0.052$	$0.023 \pm 0.022 \pm 0.006$	$0.040 \pm 0.014 \pm 0.004$
	GJ	$-0.123 \pm 0.059 \pm 0.042$	$0.034 \pm 0.024 \pm 0.014$	$0.055 \pm 0.015 \pm 0.006$
4 – 6	HX	$-0.004 \pm 0.054 \pm 0.037$	$0.027 \pm 0.032 \pm 0.016$	$0.040 \pm 0.018 \pm 0.010$
	CS	$0.028 \pm 0.069 \pm 0.043$	$0.053 \pm 0.025 \pm 0.007$	$0.044 \pm 0.015 \pm 0.007$
	GJ	$-0.075 \pm 0.057 \pm 0.031$	$0.068 \pm 0.028 \pm 0.016$	$0.080 \pm 0.017 \pm 0.011$
6 – 8	HX	$-0.056 \pm 0.053 \pm 0.027$	$0.098 \pm 0.035 \pm 0.017$	$0.049 \pm 0.025 \pm 0.015$
	CS	$-0.101 \pm 0.064 \pm 0.028$	$0.032 \pm 0.031 \pm 0.009$	$0.074 \pm 0.017 \pm 0.009$
	GJ	$-0.115 \pm 0.059 \pm 0.025$	$-0.038 \pm 0.031 \pm 0.015$	$0.083 \pm 0.021 \pm 0.014$
8 – 10	HX	$-0.008 \pm 0.067 \pm 0.039$	$0.120 \pm 0.035 \pm 0.015$	$0.001 \pm 0.035 \pm 0.022$
	CS	$-0.148 \pm 0.061 \pm 0.023$	$0.048 \pm 0.042 \pm 0.012$	$0.051 \pm 0.022 \pm 0.013$
	GJ	$-0.148 \pm 0.069 \pm 0.032$	$-0.074 \pm 0.032 \pm 0.010$	$0.052 \pm 0.028 \pm 0.016$
10 – 15	HX	$0.176 \pm 0.067 \pm 0.064$	$0.126 \pm 0.028 \pm 0.012$	$-0.010 \pm 0.033 \pm 0.026$
	CS	$-0.147 \pm 0.042 \pm 0.019$	$0.073 \pm 0.038 \pm 0.012$	$0.091 \pm 0.022 \pm 0.013$
	GJ	$-0.066 \pm 0.064 \pm 0.037$	$-0.128 \pm 0.026 \pm 0.010$	$0.064 \pm 0.025 \pm 0.013$
15 – 20	HX	$0.227 \pm 0.112 \pm 0.108$	$0.138 \pm 0.058 \pm 0.034$	$0.125 \pm 0.048 \pm 0.040$
	CS	$-0.062 \pm 0.068 \pm 0.068$	$-0.018 \pm 0.062 \pm 0.031$	$0.204 \pm 0.048 \pm 0.041$
	GJ	$0.281 \pm 0.128 \pm 0.108$	$-0.122 \pm 0.055 \pm 0.033$	$0.111 \pm 0.046 \pm 0.028$
20 – 30	HX	$0.570 \pm 0.221 \pm 0.232$	$0.149 \pm 0.113 \pm 0.102$	$0.017 \pm 0.074 \pm 0.069$
	CS	$-0.226 \pm 0.099 \pm 0.134$	$0.083 \pm 0.082 \pm 0.048$	$0.239 \pm 0.083 \pm 0.094$
	GJ	$0.313 \pm 0.212 \pm 0.231$	$-0.274 \pm 0.096 \pm 0.089$	$0.093 \pm 0.069 \pm 0.060$

Table 27: Values of  $\lambda_\theta$ ,  $\lambda_{\theta\phi}$  and  $\lambda_\phi$  measured in the HX, CS and GJ frames for the  $\Upsilon(3S)$  produced at  $\sqrt{s} = 8$  TeV in the rapidity range  $2.2 < y^\Upsilon < 4.5$ . The first uncertainty is statistical and the second systematic.

$p_T^\Upsilon$ [GeV/c]		$\lambda_\theta$	$\lambda_{\theta\phi}$	$\lambda_\phi$
0 – 2	HX	$-0.141 \pm 0.059 \pm 0.063$	$-0.010 \pm 0.021 \pm 0.009$	$-0.016 \pm 0.014 \pm 0.003$
	CS	$-0.119 \pm 0.061 \pm 0.067$	$0.007 \pm 0.020 \pm 0.006$	$-0.019 \pm 0.014 \pm 0.003$
	GJ	$-0.122 \pm 0.059 \pm 0.063$	$0.027 \pm 0.021 \pm 0.011$	$-0.015 \pm 0.014 \pm 0.003$
2 – 4	HX	$-0.014 \pm 0.041 \pm 0.048$	$-0.022 \pm 0.018 \pm 0.013$	$0.026 \pm 0.010 \pm 0.005$
	CS	$0.044 \pm 0.046 \pm 0.053$	$0.025 \pm 0.015 \pm 0.006$	$0.016 \pm 0.010 \pm 0.004$
	GJ	$-0.017 \pm 0.042 \pm 0.045$	$0.076 \pm 0.017 \pm 0.015$	$0.038 \pm 0.010 \pm 0.006$
4 – 6	HX	$0.008 \pm 0.037 \pm 0.037$	$0.057 \pm 0.022 \pm 0.017$	$0.036 \pm 0.013 \pm 0.010$
	CS	$-0.009 \pm 0.046 \pm 0.045$	$0.079 \pm 0.017 \pm 0.007$	$0.051 \pm 0.010 \pm 0.007$
	GJ	$-0.139 \pm 0.038 \pm 0.030$	$0.065 \pm 0.019 \pm 0.016$	$0.093 \pm 0.011 \pm 0.010$
6 – 8	HX	$-0.076 \pm 0.036 \pm 0.027$	$0.205 \pm 0.025 \pm 0.014$	$-0.019 \pm 0.018 \pm 0.014$
	CS	$-0.270 \pm 0.042 \pm 0.027$	$0.091 \pm 0.020 \pm 0.007$	$0.059 \pm 0.011 \pm 0.009$
	GJ	$-0.291 \pm 0.037 \pm 0.020$	$-0.083 \pm 0.021 \pm 0.012$	$0.072 \pm 0.014 \pm 0.014$
8 – 10	HX	$0.033 \pm 0.045 \pm 0.029$	$0.154 \pm 0.024 \pm 0.011$	$0.017 \pm 0.024 \pm 0.014$
	CS	$-0.172 \pm 0.039 \pm 0.017$	$0.059 \pm 0.027 \pm 0.010$	$0.086 \pm 0.015 \pm 0.010$
	GJ	$-0.146 \pm 0.046 \pm 0.029$	$-0.104 \pm 0.021 \pm 0.009$	$0.077 \pm 0.018 \pm 0.014$
10 – 15	HX	$0.198 \pm 0.045 \pm 0.039$	$0.114 \pm 0.018 \pm 0.012$	$-0.049 \pm 0.022 \pm 0.016$
	CS	$-0.150 \pm 0.027 \pm 0.014$	$0.101 \pm 0.025 \pm 0.011$	$0.063 \pm 0.015 \pm 0.013$
	GJ	$-0.129 \pm 0.041 \pm 0.026$	$-0.112 \pm 0.016 \pm 0.010$	$0.055 \pm 0.016 \pm 0.013$
15 – 20	HX	$0.307 \pm 0.080 \pm 0.075$	$0.042 \pm 0.042 \pm 0.029$	$-0.111 \pm 0.037 \pm 0.030$
	CS	$-0.169 \pm 0.043 \pm 0.038$	$0.140 \pm 0.042 \pm 0.026$	$0.048 \pm 0.034 \pm 0.030$
	GJ	$-0.123 \pm 0.070 \pm 0.077$	$-0.156 \pm 0.032 \pm 0.018$	$0.030 \pm 0.029 \pm 0.022$
20 – 30	HX	$0.060 \pm 0.114 \pm 0.168$	$0.087 \pm 0.066 \pm 0.060$	$0.004 \pm 0.046 \pm 0.040$
	CS	$-0.086 \pm 0.077 \pm 0.133$	$-0.021 \pm 0.059 \pm 0.040$	$0.046 \pm 0.064 \pm 0.113$
	GJ	$0.069 \pm 0.128 \pm 0.198$	$-0.037 \pm 0.060 \pm 0.060$	$-0.011 \pm 0.047 \pm 0.044$

Table 28: Values of  $\tilde{\lambda}$  measured in the HX, CS and GJ frames for the  $\Upsilon(3S)$  produced at  $\sqrt{s} = 7$  and 8 TeV in the rapidity range  $2.2 < y^\Upsilon < 4.5$ . The first uncertainty is statistical and the second systematic.

$p_T^\Upsilon$ [GeV/c]	$\tilde{\lambda}$	$\sqrt{s} = 7$ TeV	$\sqrt{s} = 8$ TeV
0 – 2	HX	$-0.129 \pm 0.102 \pm 0.070$	$-0.187 \pm 0.071 \pm 0.066$
	CS	$-0.113 \pm 0.103 \pm 0.069$	$-0.174 \pm 0.071 \pm 0.070$
	GJ	$-0.105 \pm 0.102 \pm 0.072$	$-0.165 \pm 0.071 \pm 0.067$
2 – 4	HX	$-0.012 \pm 0.080 \pm 0.063$	$0.065 \pm 0.056 \pm 0.064$
	CS	$0.024 \pm 0.082 \pm 0.063$	$0.095 \pm 0.057 \pm 0.064$
	GJ	$0.043 \pm 0.082 \pm 0.061$	$0.100 \pm 0.057 \pm 0.064$
4 – 6	HX	$0.121 \pm 0.089 \pm 0.068$	$0.120 \pm 0.061 \pm 0.070$
	CS	$0.167 \pm 0.091 \pm 0.066$	$0.153 \pm 0.062 \pm 0.068$
	GJ	$0.181 \pm 0.091 \pm 0.067$	$0.155 \pm 0.062 \pm 0.068$
6 – 8	HX	$0.097 \pm 0.097 \pm 0.063$	$-0.129 \pm 0.061 \pm 0.059$
	CS	$0.130 \pm 0.099 \pm 0.056$	$-0.099 \pm 0.062 \pm 0.055$
	GJ	$0.145 \pm 0.099 \pm 0.059$	$-0.081 \pm 0.062 \pm 0.056$
8 – 10	HX	$-0.004 \pm 0.102 \pm 0.055$	$0.086 \pm 0.071 \pm 0.048$
	CS	$0.007 \pm 0.103 \pm 0.056$	$0.093 \pm 0.071 \pm 0.049$
	GJ	$0.009 \pm 0.103 \pm 0.052$	$0.093 \pm 0.071 \pm 0.049$
10 – 15	HX	$0.143 \pm 0.091 \pm 0.042$	$0.047 \pm 0.057 \pm 0.042$
	CS	$0.140 \pm 0.091 \pm 0.043$	$0.043 \pm 0.057 \pm 0.043$
	GJ	$0.136 \pm 0.091 \pm 0.037$	$0.039 \pm 0.057 \pm 0.042$
15 – 20	HX	$0.689 \pm 0.218 \pm 0.134$	$-0.023 \pm 0.104 \pm 0.069$
	CS	$0.692 \pm 0.218 \pm 0.142$	$-0.027 \pm 0.104 \pm 0.076$
	GJ	$0.692 \pm 0.218 \pm 0.108$	$-0.033 \pm 0.104 \pm 0.058$
20 – 30	HX	$0.631 \pm 0.360 \pm 0.327$	$0.073 \pm 0.187 \pm 0.215$
	CS	$0.646 \pm 0.365 \pm 0.313$	$0.056 \pm 0.187 \pm 0.276$
	GJ	$0.654 \pm 0.366 \pm 0.335$	$0.035 \pm 0.186 \pm 0.201$

## References

- [1] E. Braaten and J. Russ, *J/ψ and Υ polarization in hadronic production processes*, Annu. Rev. Nucl. Part. Sci. **64** (2014) 221, [arXiv:1401.7352](#).
- [2] P. Faccioli *et al.*, *Quarkonium production in the LHC era: A polarized perspective*, Phys. Lett. **B736** (2014) 98, [arXiv:1403.3970](#).
- [3] W. E. Caswell and G. P. Lepage, *Effective Lagrangians for bound state problems in QED, QCD, and other field theories*, Phys. Lett. **B167** (1986) 437.
- [4] G. T. Bodwin, E. Braaten, and G. P. Lepage, *Rigorous QCD analysis of inclusive annihilation and production of heavy quarkonium*, Phys. Rev. **D51** (1995) 1125, Erratum *ibid.* **55** (1997) 5853, [arXiv:hep-ph/9407339](#).
- [5] E. Braaten and S. Fleming, *Color octet fragmentation and the ψ' surplus at the Tevatron*, Phys. Rev. Lett. **74** (1995) 3327, [arXiv:hep-ph/9411365](#).
- [6] V. G. Kartvelishvili, A. K. Likhoded, and S. R. Slabospitsky, *D meson and ψ meson production in hadronic interactions*, Sov. J. Nucl. Phys. **28** (1978) 678, [*Yad. Fiz.* **28** (1978) 1315].
- [7] R. Baier and R. Rückl, *Hadronic production of J/ψ and Υ: Transverse momentum distributions*, Phys. Lett. **B102** (1981) 364.
- [8] E. L. Berger and D. Jones, *Inelastic photoproduction of J/ψ and Υ by gluons*, Phys. Rev. **D23** (1981) 1521.
- [9] J. M. Campbell, F. Maltoni, and F. Tramontano, *QCD corrections to J/ψ and Υ production at hadron colliders*, Phys. Rev. Lett. **98** (2007) 252002, [arXiv:hep-ph/0703113](#).
- [10] B. Gong and J.-X. Wang, *Next-to-leading-order QCD corrections to J/ψ polarization at Tevatron and Large Hadron Collider energies*, Phys. Rev. Lett. **100** (2008) 232001, [arXiv:0802.3727](#).
- [11] P. Artoisenet *et al.*, *Υ production at Fermilab Tevatron and LHC energies*, Phys. Rev. Lett. **101** (2008) 152001, [arXiv:0806.3282](#).
- [12] J.-P. Lansberg, *On the mechanisms of heavy-quarkonium hadroproduction*, Eur. Phys. J. **C61** (2009) 693, [arXiv:0811.4005](#).
- [13] H. Han *et al.*, *Υ(nS) and χ<sub>b</sub>(nP) production at hadron colliders in nonrelativistic QCD*, Phys. Rev. **D94** (2016) 014028, [arXiv:1410.8537](#).
- [14] B. Gong, L.-P. Wan, J.-X. Wang, and H.-F. Zhang, *Complete next-to-leading-order study on the yield and polarization of Υ(1S, 2S, 3S) at the Tevatron and LHC*, Phys. Rev. Lett. **112** (2014) 032001, [arXiv:1305.0748](#).
- [15] N. Brambilla *et al.*, *Heavy quarkonium: Progress, puzzles, and opportunities*, Eur. Phys. J. **C71** (2011) 1534, [arXiv:1010.5827](#).

- [16] CDF collaboration, D. Acosta *et al.*,  $\Upsilon$  production and polarization in  $p\bar{p}$  collisions at  $\sqrt{s} = 1.8$  TeV, Phys. Rev. Lett. **88** (2002) 161802.
- [17] LHCb collaboration, R. Aaij *et al.*, Measurement of  $\Upsilon$  production in pp collisions at  $\sqrt{s} = 7$  TeV, Eur. Phys. J. **C72** (2012) 2025, arXiv:1202.6579.
- [18] LHCb collaboration, R. Aaij *et al.*, Production of  $J/\psi$  and  $\Upsilon$  mesons in pp collisions at  $\sqrt{s} = 8$  TeV, JHEP **06** (2013) 064, arXiv:1304.6977.
- [19] LHCb collaboration, R. Aaij *et al.*, Measurement of  $\Upsilon$  production in pp collisions at  $\sqrt{s} = 2.76$  TeV, Eur. Phys. J. **C74** (2014) 2835, arXiv:1402.2539.
- [20] LHCb collaboration, R. Aaij *et al.*, Forward production of  $\Upsilon$  mesons in pp collisions at  $\sqrt{s} = 7$  and 8 TeV, JHEP **11** (2015) 103, arXiv:1509.02372.
- [21] CMS collaboration, V. Khachatryan *et al.*, Upsilon production cross section in pp collisions at  $\sqrt{s} = 7$  TeV, Phys. Rev. **D83** (2011) 112004, arXiv:1012.5545.
- [22] ATLAS collaboration, G. Aad *et al.*, Measurement of upsilon production in 7 TeV pp collisions at ATLAS, Phys. Rev. **D87** (2013) 052004, arXiv:1211.7255.
- [23] LHCb collaboration, R. Aaij *et al.*, Measurement of  $J/\psi$  polarization in pp collisions at  $\sqrt{s} = 7$  TeV, Eur. Phys. J. **C73** (2013) 2631, arXiv:1307.6379.
- [24] LHCb collaboration, R. Aaij *et al.*, Measurement of  $\psi(2S)$  polarisation in pp collisions at  $\sqrt{s} = 7$  TeV, Eur. Phys. J. **C74** (2014) 2872, arXiv:1403.1339.
- [25] D0 collaboration, V. M. Abazov *et al.*, Observation of a narrow mass state decaying into  $\Upsilon(1S) + \gamma$  in  $p\bar{p}$  collisions at  $\sqrt{s} = 1.96$  TeV, Phys. Rev. **D86** (2012) 031103, arXiv:1203.6034.
- [26] ATLAS collaboration, G. Aad *et al.*, Observation of a new  $\chi_b$  state in radiative transitions to  $\Upsilon(1S)$  and  $\Upsilon(2S)$  at ATLAS, Phys. Rev. Lett. **108** (2012) 152001, arXiv:1112.5154.
- [27] LHCb collaboration, R. Aaij *et al.*, Measurement of the fraction of  $\Upsilon(1S)$  originating from  $\chi_b(1P)$  decays in pp collisions at  $\sqrt{s} = 7$  TeV, JHEP **11** (2012) 031, arXiv:1209.0282.
- [28] LHCb collaboration, R. Aaij *et al.*, Study of  $\chi_b$  meson production in pp collisions at  $\sqrt{s} = 7$  and 8 TeV and observation of the decay  $\chi_b \rightarrow \Upsilon(3S)\gamma$ , Eur. Phys. J. **C74** (2014) 3092, arXiv:1407.7734.
- [29] LHCb collaboration, R. Aaij *et al.*, Measurement of the  $\chi_b(3P)$  mass and of the relative rate of  $\chi_{b1}(1P)$  and  $\chi_{b2}(1P)$  production, JHEP **10** (2014) 088, arXiv:1409.1408.
- [30] Y. Feng, B. Gong, L.-P. Wan, and J.-X. Wang, An updated study of  $\Upsilon$  production and polarization at the Tevatron and LHC, Chin. Phys. **C39** (2015) 123102, arXiv:1503.08439.
- [31] CDF collaboration, T. Aaltonen *et al.*, Measurements of the angular distributions of muons from  $\Upsilon$  decays in  $p\bar{p}$  collisions at  $\sqrt{s} = 1.96$  TeV, Phys. Rev. Lett. **108** (2012) 151802, arXiv:1112.1591.

- [32] D0 collaboration, V. M. Abazov *et al.*, *Measurement of the polarization of the  $\Upsilon(1S)$  and  $\Upsilon(2S)$  states in  $p\bar{p}$  collisions at  $\sqrt{s} = 1.96$  TeV*, Phys. Rev. Lett. **101** (2008) 182004, arXiv:0804.2799.
- [33] CMS collaboration, S. Chatrchyan *et al.*, *Measurement of the  $\Upsilon(1S)$ ,  $\Upsilon(2S)$  and  $\Upsilon(3S)$  polarizations in pp collisions at  $\sqrt{s} = 7$  TeV*, Phys. Rev. Lett. **110** (2013) 081802, arXiv:1209.2922.
- [34] R. J. Oakes, *Muon pair production in strong interactions*, Nuovo Cim. **A44** (1966) 440.
- [35] C. S. Lam and W.-K. Tung, *Systematic approach to inclusive lepton pair production in hadronic collisions*, Phys. Rev. **D18** (1978) 2447.
- [36] P. Faccioli, C. Lourenço, J. Seixas, and H. K. Wöhri, *Towards the experimental clarification of quarkonium polarization*, Eur. Phys. J. **C69** (2010) 657, arXiv:1006.2738.
- [37] M. Beneke, M. Krämer, and M. Vanttinen, *Inelastic photoproduction of polarized  $J/\psi$* , Phys. Rev. **D57** (1998) 4258, arXiv:hep-ph/9709376.
- [38] M. Jacob and G. C. Wick, *On the general theory of collisions for particles with spin*, Ann. Phys. **7** (1959) 404.
- [39] LHCb collaboration, A. A. Alves Jr. *et al.*, *The LHCb detector at the LHC*, JINST **3** (2008) S08005.
- [40] J. C. Collins and D. E. Soper, *Angular distribution of dileptons in high-energy hadron collisions*, Phys. Rev. **D16** (1977) 2219.
- [41] K. Gottfried and J. D. Jackson, *On the connection between production mechanism and decay of resonances at high energies*, Nuovo Cim. **33** (1964) 309.
- [42] H. H. Barschall and W. Haeberli, eds., *Polarization phenomena in nuclear reactions: Proceedings of 3<sup>rd</sup> international symposium on polarization phenomena in nuclear reactions*, University of Wisconsin Press, Madison, 1971.
- [43] S. Falciano *et al.*, *Angular distributions of muon pairs produced by 194 GeV/c negative pions*, Z. Phys. **C31** (1986) 513.
- [44] P. Faccioli, C. Lourenço, and J. Seixas, *Rotation-invariant relations in vector meson decays into fermion pairs*, Phys. Rev. Lett. **105** (2010) 061601, arXiv:1005.2601.
- [45] P. Faccioli, C. Lourenço, and J. Seixas, *New approach to quarkonium polarization studies*, Phys. Rev. **D81** (2010) 111502, arXiv:1005.2855.
- [46] O. V. Teryaev, *Kinematic azimuthal asymmetries and Lam-Tung relation*, in *Proceedings of XI Advanced Research Workshop on High Energy Spin Physics DUBNA-SPIN-05, Dubna, September 27–October 1, 2005* (A. V. Efremov, ed.), Dubna, 2006.
- [47] F. Faccioli, C. Lourenço, J. Seixas, and H. K. Wöhri, *Rotation-invariant observables in parity-violating decays of vector particles to fermion pairs*, Phys. Rev. **D82** (2010) 96002, arXiv:1010.1552.

- [48] P. Faccioli, C. Lourenço, J. Seixas, and H. K. Wöhri, *Model-independent constraints on the shape parameters of dilepton angular distributions*, Phys. Rev. **D83** (2011) 056008, arXiv:1102.3946.
- [49] LHCb collaboration, R. Aaij *et al.*, *LHCb detector performance*, Int. J. Mod. Phys. **A30** (2015) 1530022, arXiv:1412.6352.
- [50] A. A. Alves Jr. *et al.*, *Performance of the LHCb muon system*, JINST **8** (2013) P02022, arXiv:1211.1346.
- [51] R. Aaij *et al.*, *The LHCb trigger and its performance in 2011*, JINST **8** (2013) P04022, arXiv:1211.3055.
- [52] T. Sjöstrand, S. Mrenna, and P. Skands, *PYTHIA 6.4 physics and manual*, JHEP **05** (2006) 026, arXiv:hep-ph/0603175.
- [53] I. Belyaev *et al.*, *Handling of the generation of primary events in GAUSS, the LHCb simulation framework*, J. Phys. Conf. Ser. **331** (2011) 032047.
- [54] D. J. Lange, *The EVTGEN particle decay simulation package*, Nucl. Instrum. Meth. **A462** (2001) 152.
- [55] P. Golonka and Z. Was, *PHOTOS Monte Carlo: A precision tool for QED corrections in Z and W decays*, Eur. Phys. J. **C45** (2006) 97, arXiv:hep-ph/0506026.
- [56] Geant4 collaboration, J. Allison *et al.*, *GEANT4 developments and applications*, IEEE Trans. Nucl. Sci. **53** (2006) 270; Geant4 collaboration, S. Agostinelli *et al.*, *GEANT4: A simulation toolkit*, Nucl. Instrum. Meth. **A506** (2003) 250.
- [57] M. Clemencic *et al.*, *The LHCb simulation application, GAUSS: Design, evolution and experience*, J. Phys. Conf. Ser. **331** (2011) 032023.
- [58] M. Bargiotti and V. Vagnoni, *Heavy Quarkonia sector in PYTHIA 6.324: Tuning, validation and perspectives at LHC(b)*, Tech. Rep. CERN-LHCb-2007-042, CERN, Geneva, Jun, 2007.
- [59] LHCb collaboration, R. Aaij *et al.*, *Measurement of the track reconstruction efficiency at LHCb*, JINST **10** (2015) P02007, arXiv:1408.1251.
- [60] F. Archilli *et al.*, *Performance of the muon identification at LHCb*, JINST **8** (2013) P10020, arXiv:1306.0249.
- [61] W. D. Hulsbergen, *Decay chain fitting with a Kalman filter*, Nucl. Instrum. Meth. **A552** (2005) 566, arXiv:physics/0503191.
- [62] T. Skwarnicki, *A study of the radiative cascade transitions between the Upsilon-prime and Upsilon resonances*, PhD thesis, Institute of Nuclear Physics, Krakow, 1986, DESY-F31-86-02.
- [63] LHCb collaboration, R. Aaij *et al.*, *Observation of J/ψ-pair production in pp collisions at  $\sqrt{s} = 7$  TeV*, Phys. Lett. **B707** (2012) 52, arXiv:1109.0963.



- [64] Particle Data Group, C. Patrignani *et al.*, *Review of particle physics*, Chin. Phys. **C40** (2016) 100001, and 2017 update.
- [65] Y. Xie, *sFit: A method for background subtraction in maximum likelihood fit*, arXiv:0905.0724.
- [66] M. Pivk and F. R. Le Diberder, *sPlot: A statistical tool to unfold data distributions*, Nucl. Instrum. Meth. **A555** (2005) 356, arXiv:physics/0402083.
- [67] LHCb collaboration, R. Aaij *et al.*, *Measurement of CP violation and the  $B_s^0$  meson decay width difference with  $B_s^0 \rightarrow J/\psi K^+ K^-$  and  $B_s^0 \rightarrow J/\psi \pi^+ \pi^-$  decays*, Phys. Rev. **D87** (2013) 112010, arXiv:1304.2600.
- [68] W. T. Eadie *et al.*, *Statistical methods in experimental physics*, North Holland, Amsterdam, 1971.
- [69] O. V. Teryaev, *Positivity constraints for quarkonia polarization*, Nucl. Phys. Proc. Suppl. **214** (2011) 118.
- [70] O. V. Teryaev, *Angular distributions of dileptons in hadronic and heavy ions collisions*, in *Proceedings of XIV Advanced research workshop on High Energy Spin Physics DUBNA-SPIN-11, JINR, Dubna, September 20-24, 2011* (A. V. Efremov and S. V. Goloskokov, eds.), Dubna, 2012.
- [71] C. S. Lam and W.-K. Tung, *A parton model relation without quantum-chromodynamic modifications in lepton pair productions*, Phys. Rev. **D21** (1980) 2712.
- [72] S. Palestini, *Angular distribution and rotations of frame in vector meson decays into lepton pairs*, Phys. Rev. **D83** (2011) 031503, arXiv:1012.2485.

## LHCb collaboration

R. Aaij<sup>40</sup>, B. Adeva<sup>39</sup>, M. Adinolfi<sup>48</sup>, Z. Ajaltouni<sup>5</sup>, S. Akar<sup>59</sup>, J. Albrecht<sup>10</sup>, F. Alessio<sup>40</sup>, M. Alexander<sup>53</sup>, A. Alfonso Alberio<sup>38</sup>, S. Ali<sup>43</sup>, G. Alkhazov<sup>31</sup>, P. Alvarez Cartelle<sup>55</sup>, A.A. Alves Jr<sup>59</sup>, S. Amato<sup>2</sup>, S. Amerio<sup>23</sup>, Y. Amhis<sup>7</sup>, L. An<sup>3</sup>, L. Anderlini<sup>18</sup>, G. Andreassi<sup>41</sup>, M. Andreotti<sup>17,g</sup>, J.E. Andrews<sup>60</sup>, R.B. Appleby<sup>56</sup>, F. Archilli<sup>43</sup>, P. d'Argent<sup>12</sup>, J. Arnau Romeu<sup>6</sup>, A. Artamonov<sup>37</sup>, M. Artuso<sup>61</sup>, E. Aslanides<sup>6</sup>, G. Auriemma<sup>26</sup>, M. Baalouch<sup>5</sup>, I. Babuschkin<sup>56</sup>, S. Bachmann<sup>12</sup>, J.J. Back<sup>50</sup>, A. Badalov<sup>38,m</sup>, C. Baesso<sup>62</sup>, S. Baker<sup>55</sup>, V. Balagura<sup>7,b</sup>, W. Baldini<sup>17</sup>, A. Baranov<sup>35</sup>, R.J. Barlow<sup>56</sup>, C. Barschel<sup>40</sup>, S. Barsuk<sup>7</sup>, W. Barter<sup>56</sup>, F. Baryshnikov<sup>32</sup>, V. Batozskaya<sup>29</sup>, V. Battista<sup>41</sup>, A. Bay<sup>41</sup>, L. Beaucourt<sup>4</sup>, J. Beddow<sup>53</sup>, F. Bedeschi<sup>24</sup>, I. Bediaga<sup>1</sup>, A. Beiter<sup>61</sup>, L.J. Bel<sup>43</sup>, N. Bely<sup>63</sup>, V. Bellec<sup>41</sup>, N. Belloli<sup>21,i</sup>, K. Belous<sup>37</sup>, I. Belyaev<sup>32</sup>, E. Ben-Haim<sup>8</sup>, G. Bencivenni<sup>19</sup>, S. Benson<sup>43</sup>, S. Beranek<sup>9</sup>, A. Berezhnoy<sup>33</sup>, R. Bernet<sup>42</sup>, D. Berninghoff<sup>12</sup>, E. Bertholet<sup>8</sup>, A. Bertolin<sup>23</sup>, C. Betancourt<sup>42</sup>, F. Betti<sup>15</sup>, M.-O. Bettler<sup>40</sup>, M. van Beuzekom<sup>43</sup>, I.a. Bezshyiko<sup>42</sup>, S. Bifani<sup>47</sup>, P. Billoir<sup>8</sup>, A. Birnkraut<sup>10</sup>, A. Bizzeti<sup>18,u</sup>, M. Bjørn<sup>57</sup>, T. Blake<sup>50</sup>, F. Blanc<sup>41</sup>, J. Blouw<sup>11,†</sup>, S. Blusk<sup>61</sup>, V. Bocci<sup>26</sup>, T. Boettcher<sup>58</sup>, A. Bondar<sup>36,w</sup>, N. Bondar<sup>31</sup>, W. Bonivento<sup>16</sup>, I. Bordyuzhin<sup>32</sup>, A. Borgheresi<sup>21,i</sup>, S. Borghi<sup>56</sup>, M. Borisyak<sup>35</sup>, M. Borsato<sup>39</sup>, F. Bossu<sup>7</sup>, M. Boubdir<sup>9</sup>, T.J.V. Bowcock<sup>54</sup>, E. Bowen<sup>42</sup>, C. Bozzi<sup>17,40</sup>, S. Braun<sup>12</sup>, T. Britton<sup>61</sup>, J. Brodzicka<sup>27</sup>, D. Brundu<sup>16</sup>, E. Buchanan<sup>48</sup>, C. Burr<sup>56</sup>, A. Bursche<sup>16,f</sup>, J. Buytaert<sup>40</sup>, W. Byczynski<sup>40</sup>, S. Cadeddu<sup>16</sup>, H. Cai<sup>64</sup>, R. Calabrese<sup>17,g</sup>, R. Calladine<sup>47</sup>, M. Calvi<sup>21,i</sup>, M. Calvo Gomez<sup>38,m</sup>, A. Camboni<sup>38,m</sup>, P. Campana<sup>19</sup>, D.H. Campora Perez<sup>40</sup>, L. Capriotti<sup>56</sup>, A. Carbone<sup>15,e</sup>, G. Carboni<sup>25,j</sup>, R. Cardinale<sup>20,h</sup>, A. Cardini<sup>16</sup>, P. Carniti<sup>21,i</sup>, L. Carson<sup>52</sup>, K. Carvalho Akiba<sup>2</sup>, G. Casse<sup>54</sup>, L. Cassina<sup>21</sup>, L. Castillo Garcia<sup>41</sup>, M. Cattaneo<sup>40</sup>, G. Cavallero<sup>20,40,h</sup>, R. Cenci<sup>24,t</sup>, D. Chamont<sup>7</sup>, M.G. Chapman<sup>48</sup>, M. Charles<sup>8</sup>, Ph. Charpentier<sup>40</sup>, G. Chatzikonstantinidis<sup>47</sup>, M. Chefdeville<sup>4</sup>, S. Chen<sup>56</sup>, S.F. Cheung<sup>57</sup>, S.-G. Chitic<sup>40</sup>, V. Chobanova<sup>39</sup>, M. Chrzaszcz<sup>42,27</sup>, A. Chubykin<sup>31</sup>, P. Ciambone<sup>19</sup>, X. Cid Vidal<sup>39</sup>, G. Ciezarek<sup>43</sup>, P.E.L. Clarke<sup>52</sup>, M. Clemencic<sup>40</sup>, H.V. Cliff<sup>49</sup>, J. Closier<sup>40</sup>, J. Cogan<sup>6</sup>, E. Cogneras<sup>5</sup>, V. Cogoni<sup>16,f</sup>, L. Cojocariu<sup>30</sup>, P. Collins<sup>40</sup>, T. Colombo<sup>40</sup>, A. Comerma-Montells<sup>12</sup>, A. Contu<sup>40</sup>, A. Cook<sup>48</sup>, G. Coombs<sup>40</sup>, S. Coquereau<sup>38</sup>, G. Corti<sup>40</sup>, M. Corvo<sup>17,g</sup>, C.M. Costa Sobral<sup>50</sup>, B. Couturier<sup>40</sup>, G.A. Cowan<sup>52</sup>, D.C. Craik<sup>58</sup>, A. Crocombe<sup>50</sup>, M. Cruz Torres<sup>1</sup>, R. Currie<sup>52</sup>, C. D'Ambrosio<sup>40</sup>, F. Da Cunha Marinho<sup>2</sup>, E. Dall'Occo<sup>43</sup>, J. Dalseno<sup>48</sup>, A. Davis<sup>3</sup>, O. De Aguiar Francisco<sup>54</sup>, S. De Capua<sup>56</sup>, M. De Cian<sup>12</sup>, J.M. De Miranda<sup>1</sup>, L. De Paula<sup>2</sup>, M. De Serio<sup>14,d</sup>, P. De Simone<sup>19</sup>, C.T. Dean<sup>53</sup>, D. Decamp<sup>4</sup>, L. Del Buono<sup>8</sup>, H.-P. Dembinski<sup>11</sup>, M. Demmer<sup>10</sup>, A. Dendek<sup>28</sup>, D. Derkach<sup>35</sup>, O. Deschamps<sup>5</sup>, F. Dettori<sup>54</sup>, B. Dey<sup>65</sup>, A. Di Canto<sup>40</sup>, P. Di Nezza<sup>19</sup>, H. Dijkstra<sup>40</sup>, F. Dordei<sup>40</sup>, M. Dorigo<sup>40</sup>, A. Dosil Suárez<sup>39</sup>, L. Douglas<sup>53</sup>, A. Dovbnya<sup>45</sup>, K. Dreimanis<sup>54</sup>, L. Dufour<sup>43</sup>, G. Dujany<sup>8</sup>, P. Durante<sup>40</sup>, R. Dzhelyadin<sup>37</sup>, M. Dziewiecki<sup>12</sup>, A. Dziurda<sup>40</sup>, A. Dzyuba<sup>31</sup>, S. Easo<sup>51</sup>, M. Ebert<sup>52</sup>, U. Egede<sup>55</sup>, V. Egorychev<sup>32</sup>, S. Eidelman<sup>36,w</sup>, S. Eisenhardt<sup>52</sup>, U. Eitschberger<sup>10</sup>, R. Ekelhof<sup>10</sup>, L. Eklund<sup>53</sup>, S. Ely<sup>61</sup>, S. Esen<sup>12</sup>, H.M. Evans<sup>49</sup>, T. Evans<sup>57</sup>, A. Falabella<sup>15</sup>, N. Farley<sup>47</sup>, S. Farry<sup>54</sup>, D. Fazzini<sup>21,i</sup>, L. Federici<sup>25</sup>, D. Ferguson<sup>52</sup>, G. Fernandez<sup>38</sup>, P. Fernandez Declara<sup>40</sup>, A. Fernandez Prieto<sup>39</sup>, F. Ferrari<sup>15</sup>, F. Ferreira Rodrigues<sup>2</sup>, M. Ferro-Luzzi<sup>40</sup>, S. Filippov<sup>34</sup>, R.A. Fini<sup>14</sup>, M. Fiorini<sup>17,g</sup>, M. Firlej<sup>28</sup>, C. Fitzpatrick<sup>41</sup>, T. Fiutowski<sup>28</sup>, F. Fleuret<sup>7,b</sup>, K. Fohl<sup>40</sup>, M. Fontana<sup>16,40</sup>, F. Fontanelli<sup>20,h</sup>, D.C. Forshaw<sup>61</sup>, R. Forty<sup>40</sup>, V. Franco Lima<sup>54</sup>, M. Frank<sup>40</sup>, C. Frei<sup>40</sup>, J. Fu<sup>22,q</sup>, W. Funk<sup>40</sup>, E. Furfaro<sup>25,j</sup>, C. Färber<sup>40</sup>, E. Gabriel<sup>52</sup>, A. Gallas Torreira<sup>39</sup>, D. Galli<sup>15,e</sup>, S. Gallorini<sup>23</sup>, S. Gambetta<sup>52</sup>, M. Gandelman<sup>2</sup>, P. Gandini<sup>57</sup>, Y. Gao<sup>3</sup>, L.M. Garcia Martin<sup>70</sup>, J. García Pardiñas<sup>39</sup>, J. Garra Tico<sup>49</sup>, L. Garrido<sup>38</sup>, P.J. Garsed<sup>49</sup>, D. Gascon<sup>38</sup>, C. Gaspar<sup>40</sup>, L. Gavardi<sup>10</sup>, G. Gazzoni<sup>5</sup>, D. Gerick<sup>12</sup>, E. Gersabeck<sup>12</sup>, M. Gersabeck<sup>56</sup>, T. Gershon<sup>50</sup>, Ph. Ghez<sup>4</sup>, S. Gianì<sup>41</sup>, V. Gibson<sup>49</sup>, O.G. Girard<sup>41</sup>, L. Giubega<sup>30</sup>, K. Gizdov<sup>52</sup>, V.V. Gligorov<sup>8</sup>, D. Golubkov<sup>32</sup>, A. Golutvin<sup>55,40</sup>, A. Gomes<sup>1,a</sup>, I.V. Gorelov<sup>33</sup>, C. Gotti<sup>21,i</sup>, E. Govorkova<sup>43</sup>,

J.P. Grabowski<sup>12</sup>, R. Graciani Diaz<sup>38</sup>, L.A. Granado Cardoso<sup>40</sup>, E. Graugés<sup>38</sup>, E. Graverini<sup>42</sup>,  
 G. Graziani<sup>18</sup>, A. Grecu<sup>30</sup>, R. Greim<sup>9</sup>, P. Griffith<sup>16</sup>, L. Grillo<sup>21,40,i</sup>, L. Gruber<sup>40</sup>,  
 B.R. Gruberg Cazon<sup>57</sup>, O. Grünberg<sup>67</sup>, E. Gushchin<sup>34</sup>, Yu. Guz<sup>37</sup>, T. Gys<sup>40</sup>, C. Göbel<sup>62</sup>,  
 T. Hadavizadeh<sup>57</sup>, C. Hadjivasiliou<sup>5</sup>, G. Haefeli<sup>41</sup>, C. Haen<sup>40</sup>, S.C. Haines<sup>49</sup>, B. Hamilton<sup>60</sup>,  
 X. Han<sup>12</sup>, T.H. Hancock<sup>57</sup>, S. Hansmann-Menzemer<sup>12</sup>, N. Harnew<sup>57</sup>, S.T. Harnew<sup>48</sup>, C. Hasse<sup>40</sup>,  
 M. Hatch<sup>40</sup>, J. He<sup>63</sup>, M. Hecker<sup>55</sup>, K. Heinicke<sup>10</sup>, A. Heister<sup>9</sup>, K. Hennessy<sup>54</sup>, P. Henrard<sup>5</sup>,  
 L. Henry<sup>70</sup>, E. van Herwijnen<sup>40</sup>, M. Heß<sup>67</sup>, A. Hicheur<sup>2</sup>, D. Hill<sup>57</sup>, C. Hombach<sup>56</sup>,  
 P.H. Hopchev<sup>41</sup>, Z.C. Huard<sup>59</sup>, W. Hulsbergen<sup>43</sup>, T. Humair<sup>55</sup>, M. Hushchyn<sup>35</sup>, D. Hutchcroft<sup>54</sup>,  
 P. Ibis<sup>10</sup>, M. Idzik<sup>28</sup>, P. Ilten<sup>58</sup>, R. Jacobsson<sup>40</sup>, J. Jalocha<sup>57</sup>, E. Jans<sup>43</sup>, A. Jawahery<sup>60</sup>,  
 F. Jiang<sup>3</sup>, M. John<sup>57</sup>, D. Johnson<sup>40</sup>, C.R. Jones<sup>49</sup>, C. Joram<sup>40</sup>, B. Jost<sup>40</sup>, N. Jurik<sup>57</sup>,  
 S. Kandybei<sup>45</sup>, M. Karacson<sup>40</sup>, J.M. Kariuki<sup>48</sup>, S. Karodia<sup>53</sup>, N. Kazeev<sup>35</sup>, M. Kecke<sup>12</sup>,  
 M. Kelsey<sup>61</sup>, M. Kenzie<sup>49</sup>, T. Ketel<sup>44</sup>, E. Khairullin<sup>35</sup>, B. Khanji<sup>12</sup>, C. Khurewathanakul<sup>41</sup>,  
 T. Kirn<sup>9</sup>, S. Klaver<sup>56</sup>, K. Klimaszewski<sup>29</sup>, T. Klimkovich<sup>11</sup>, S. Kolliiev<sup>46</sup>, M. Kolpin<sup>12</sup>,  
 I. Komarov<sup>41</sup>, R. Kopečna<sup>12</sup>, P. Koppenburg<sup>43</sup>, A. Kosmyntseva<sup>32</sup>, S. Kotriakhova<sup>31</sup>,  
 M. Kozeiha<sup>5</sup>, L. Kravchuk<sup>34</sup>, M. Kreps<sup>50</sup>, P. Krokovny<sup>36,w</sup>, F. Kruse<sup>10</sup>, W. Krzemien<sup>29</sup>,  
 W. Kucewicz<sup>27,l</sup>, M. Kucharczyk<sup>27</sup>, V. Kudryavtsev<sup>36,w</sup>, A.K. Kuonen<sup>41</sup>, K. Kurek<sup>29</sup>,  
 T. Kvaratskheliya<sup>32,40</sup>, D. Lacarrere<sup>40</sup>, G. Lafferty<sup>56</sup>, A. Lai<sup>16</sup>, G. Lanfranchi<sup>19</sup>,  
 C. Langenbruch<sup>9</sup>, T. Latham<sup>50</sup>, C. Lazzeroni<sup>47</sup>, R. Le Gac<sup>6</sup>, A. Leflat<sup>33,40</sup>, J. Lefrançois<sup>7</sup>,  
 R. Lefèvre<sup>5</sup>, F. Lemaitre<sup>40</sup>, E. Lemos Cid<sup>39</sup>, O. Leroy<sup>6</sup>, T. Lesiak<sup>27</sup>, B. Leverington<sup>12</sup>,  
 P.-R. Li<sup>63</sup>, T. Li<sup>3</sup>, Y. Li<sup>7</sup>, Z. Li<sup>61</sup>, T. Likhomanenko<sup>68</sup>, R. Lindner<sup>40</sup>, F. Lionetto<sup>42</sup>,  
 V. Lisovskyi<sup>7</sup>, X. Liu<sup>3</sup>, D. Loh<sup>50</sup>, A. Loi<sup>16</sup>, I. Longstaff<sup>53</sup>, J.H. Lopes<sup>2</sup>, D. Lucchesi<sup>23,o</sup>,  
 A. Luchinsky<sup>37</sup>, M. Lucio Martinez<sup>39</sup>, H. Luo<sup>52</sup>, A. Lupato<sup>23</sup>, E. Luppi<sup>17,g</sup>, O. Lupton<sup>40</sup>,  
 A. Lusiani<sup>24</sup>, X. Lyu<sup>63</sup>, F. Machefert<sup>7</sup>, F. Maciuc<sup>30</sup>, V. Macko<sup>41</sup>, P. Mackowiak<sup>10</sup>,  
 S. Maddrell-Mander<sup>48</sup>, O. Maev<sup>31,40</sup>, K. Maguire<sup>56</sup>, D. Maisuzenko<sup>31</sup>, M.W. Majewski<sup>28</sup>,  
 S. Malde<sup>57</sup>, A. Malinin<sup>68</sup>, T. Maltsev<sup>36,w</sup>, G. Manca<sup>16,f</sup>, G. Mancinelli<sup>6</sup>, D. Marangotto<sup>22,q</sup>,  
 J. Maratas<sup>5,v</sup>, J.F. Marchand<sup>4</sup>, U. Marconi<sup>15</sup>, C. Marin Benito<sup>38</sup>, M. Marinangeli<sup>41</sup>,  
 P. Marino<sup>41</sup>, J. Marks<sup>12</sup>, G. Martellotti<sup>26</sup>, M. Martin<sup>6</sup>, M. Martinelli<sup>41</sup>, D. Martinez Santos<sup>39</sup>,  
 F. Martinez Vidal<sup>70</sup>, D. Martins Tostes<sup>2</sup>, L.M. Massacrier<sup>7</sup>, A. Massafferri<sup>1</sup>, R. Matev<sup>40</sup>,  
 A. Mathad<sup>50</sup>, Z. Mathe<sup>40</sup>, C. Matteuzzi<sup>21</sup>, A. Mauri<sup>42</sup>, E. Maurice<sup>7,b</sup>, B. Maurin<sup>41</sup>,  
 A. Mazurov<sup>47</sup>, M. McCann<sup>55,40</sup>, A. McNab<sup>56</sup>, R. McNulty<sup>13</sup>, J.V. Mead<sup>54</sup>, B. Meadows<sup>59</sup>,  
 C. Meaux<sup>6</sup>, F. Meier<sup>10</sup>, N. Meinert<sup>67</sup>, D. Melnychuk<sup>29</sup>, M. Merk<sup>43</sup>, A. Merli<sup>22,40,q</sup>,  
 E. Michielin<sup>23</sup>, D.A. Milanese<sup>66</sup>, E. Millard<sup>50</sup>, M.-N. Minard<sup>4</sup>, L. Minzoni<sup>17</sup>, D.S. Mitzel<sup>12</sup>,  
 A. Mogini<sup>8</sup>, J. Molina Rodriguez<sup>1</sup>, T. Mombächer<sup>10</sup>, I.A. Monroy<sup>66</sup>, S. Monteil<sup>5</sup>,  
 M. Morandin<sup>23</sup>, M.J. Morello<sup>24,t</sup>, O. Morgunova<sup>68</sup>, J. Moron<sup>28</sup>, A.B. Morris<sup>52</sup>, R. Mountain<sup>61</sup>,  
 F. Muheim<sup>52</sup>, M. Mulder<sup>43</sup>, D. Müller<sup>56</sup>, J. Müller<sup>10</sup>, K. Müller<sup>42</sup>, V. Müller<sup>10</sup>, P. Naik<sup>48</sup>,  
 T. Nakada<sup>41</sup>, R. Nandakumar<sup>51</sup>, A. Nandi<sup>57</sup>, I. Nasteva<sup>2</sup>, M. Needham<sup>52</sup>, N. Neri<sup>22,40</sup>,  
 S. Neubert<sup>12</sup>, N. Neufeld<sup>40</sup>, M. Neuner<sup>12</sup>, T.D. Nguyen<sup>41</sup>, C. Nguyen-Mau<sup>41,n</sup>, S. Nieswand<sup>9</sup>,  
 R. Niet<sup>10</sup>, N. Nikitin<sup>33</sup>, T. Nikodem<sup>12</sup>, A. Nogay<sup>68</sup>, D.P. O’Hanlon<sup>50</sup>, A. Oblakowska-Mucha<sup>28</sup>,  
 V. Obraztsov<sup>37</sup>, S. Ogilvy<sup>19</sup>, R. Oldeman<sup>16,f</sup>, C.J.G. Onderwater<sup>71</sup>, A. Ossowska<sup>27</sup>,  
 J.M. Otalora Goicochea<sup>2</sup>, P. Owen<sup>42</sup>, A. Oyanguren<sup>70</sup>, P.R. Pais<sup>41</sup>, A. Palano<sup>14,d</sup>,  
 M. Palutan<sup>19,40</sup>, A. Papanestis<sup>51</sup>, M. Pappagallo<sup>14,d</sup>, L.L. Pappalardo<sup>17,g</sup>, W. Parker<sup>60</sup>,  
 C. Parkes<sup>56</sup>, G. Passaleva<sup>18</sup>, A. Pastore<sup>14,d</sup>, M. Patel<sup>55</sup>, C. Patrignani<sup>15,e</sup>, A. Pearce<sup>40</sup>,  
 A. Pellegrino<sup>43</sup>, G. Penso<sup>26</sup>, M. Pepe Altarelli<sup>40</sup>, S. Perazzini<sup>40</sup>, P. Perret<sup>5</sup>, L. Pescatore<sup>41</sup>,  
 K. Petridis<sup>48</sup>, A. Petrolini<sup>20,h</sup>, A. Petrov<sup>68</sup>, M. Petruzzo<sup>22,q</sup>, E. Picatoste Olloqui<sup>38</sup>,  
 B. Pietrzyk<sup>4</sup>, M. Pikies<sup>27</sup>, D. Pinci<sup>26</sup>, F. Pisani<sup>40</sup>, A. Pistone<sup>20,h</sup>, A. Piucci<sup>12</sup>, V. Placinta<sup>30</sup>,  
 S. Playfer<sup>52</sup>, M. Plo Casasus<sup>39</sup>, F. Polci<sup>8</sup>, M. Poli Lener<sup>19</sup>, A. Poluektov<sup>50</sup>, I. Polyakov<sup>61</sup>,  
 E. Polcarpo<sup>2</sup>, G.J. Pomery<sup>48</sup>, S. Ponce<sup>40</sup>, A. Popov<sup>37</sup>, D. Popov<sup>11,40</sup>, S. Poslavskii<sup>37</sup>,  
 C. Potterat<sup>2</sup>, E. Price<sup>48</sup>, J. Prisciandaro<sup>39</sup>, C. Prouve<sup>48</sup>, V. Pugatch<sup>46</sup>, A. Puig Navarro<sup>42</sup>,  
 H. Pullen<sup>57</sup>, G. Punzi<sup>24,p</sup>, W. Qian<sup>50</sup>, R. Quagliani<sup>7,48</sup>, B. Quintana<sup>5</sup>, B. Rachwal<sup>28</sup>,  
 J.H. Rademacker<sup>48</sup>, M. Rama<sup>24</sup>, M. Ramos Pernas<sup>39</sup>, M.S. Rangel<sup>2</sup>, I. Raniuk<sup>45,†</sup>,

F. Ratnikov<sup>35</sup>, G. Raven<sup>44</sup>, M. Ravonel Salzgeber<sup>40</sup>, M. Reboud<sup>4</sup>, F. Redi<sup>55</sup>, S. Reichert<sup>10</sup>, A.C. dos Reis<sup>1</sup>, C. Remon Alepuz<sup>70</sup>, V. Renaudin<sup>7</sup>, S. Ricciardi<sup>51</sup>, S. Richards<sup>48</sup>, M. Rihl<sup>40</sup>, K. Rinnert<sup>54</sup>, V. Rives Molina<sup>38</sup>, P. Robbe<sup>7</sup>, A. Robert<sup>8</sup>, A.B. Rodrigues<sup>1</sup>, E. Rodrigues<sup>59</sup>, J.A. Rodriguez Lopez<sup>66</sup>, P. Rodriguez Perez<sup>56,†</sup>, A. Rogozhnikov<sup>35</sup>, S. Roiser<sup>40</sup>, A. Rollings<sup>57</sup>, V. Romanovskiy<sup>37</sup>, A. Romero Vidal<sup>39</sup>, J.W. Ronayne<sup>13</sup>, M. Rotondo<sup>19</sup>, M.S. Rudolph<sup>61</sup>, T. Ruf<sup>40</sup>, P. Ruiz Valls<sup>70</sup>, J. Ruiz Vidal<sup>70</sup>, J.J. Saborido Silva<sup>39</sup>, E. Sadykhov<sup>32</sup>, N. Sagidova<sup>31</sup>, B. Saitta<sup>16,f</sup>, V. Salustino Guimaraes<sup>1</sup>, C. Sanchez Mayordomo<sup>70</sup>, B. Sanmartin Sedes<sup>39</sup>, R. Santacesaria<sup>26</sup>, C. Santamarina Rios<sup>39</sup>, M. Santimaria<sup>19</sup>, E. Santovetti<sup>25,j</sup>, G. Sarpis<sup>56</sup>, A. Sarti<sup>26</sup>, C. Satriano<sup>26,s</sup>, A. Satta<sup>25</sup>, D.M. Saunders<sup>48</sup>, D. Savrina<sup>32,33</sup>, S. Schael<sup>9</sup>, M. Schellenberg<sup>10</sup>, M. Schiller<sup>53</sup>, H. Schindler<sup>40</sup>, M. Schlupp<sup>10</sup>, M. Schmelling<sup>11</sup>, T. Schmelzer<sup>10</sup>, B. Schmidt<sup>40</sup>, O. Schneider<sup>41</sup>, A. Schopper<sup>40</sup>, H.F. Schreiner<sup>59</sup>, K. Schubert<sup>10</sup>, M. Schubiger<sup>41</sup>, M.-H. Schune<sup>7</sup>, R. Schwemmer<sup>40</sup>, B. Sciascia<sup>19</sup>, A. Sciubba<sup>26,k</sup>, A. Semennikov<sup>32</sup>, E.S. Sepulveda<sup>8</sup>, A. Sergi<sup>47</sup>, N. Serra<sup>42</sup>, J. Serrano<sup>6</sup>, L. Sestini<sup>23</sup>, P. Seyfert<sup>40</sup>, M. Shapkin<sup>37</sup>, I. Shapoval<sup>45</sup>, Y. Shcheglov<sup>31</sup>, T. Shears<sup>54</sup>, L. Shekhtman<sup>36,w</sup>, V. Shevchenko<sup>68</sup>, B.G. Siddi<sup>17,40</sup>, R. Silva Coutinho<sup>42</sup>, L. Silva de Oliveira<sup>2</sup>, G. Simi<sup>23,o</sup>, S. Simone<sup>14,d</sup>, M. Sirendi<sup>49</sup>, N. Skidmore<sup>48</sup>, T. Skwarnicki<sup>61</sup>, E. Smith<sup>55</sup>, I.T. Smith<sup>52</sup>, J. Smith<sup>49</sup>, M. Smith<sup>55</sup>, I. Soares Lavra<sup>1</sup>, M.D. Sokoloff<sup>59</sup>, F.J.P. Soler<sup>53</sup>, B. Souza De Paula<sup>2</sup>, B. Spaan<sup>10</sup>, P. Spradlin<sup>53</sup>, S. Sridharan<sup>40</sup>, F. Stagni<sup>40</sup>, M. Stahl<sup>12</sup>, S. Stahl<sup>40</sup>, P. Stefko<sup>41</sup>, S. Stefkova<sup>55</sup>, O. Steinkamp<sup>42</sup>, S. Stemmler<sup>12</sup>, O. Stenyakin<sup>37</sup>, M. Stepanova<sup>31</sup>, H. Stevens<sup>10</sup>, S. Stone<sup>61</sup>, B. Storaci<sup>42</sup>, S. Stracka<sup>24,p</sup>, M.E. Stramaglia<sup>41</sup>, M. Straticiu<sup>30</sup>, U. Straumann<sup>42</sup>, J. Sun<sup>3</sup>, L. Sun<sup>64</sup>, W. Sutcliffe<sup>55</sup>, K. Swientek<sup>28</sup>, V. Syropoulos<sup>44</sup>, M. Szczekowski<sup>29</sup>, T. Szumlak<sup>28</sup>, M. Szymanski<sup>63</sup>, S. T'Jampens<sup>4</sup>, A. Tayduganov<sup>6</sup>, T. Tekampe<sup>10</sup>, G. Tellarini<sup>17,g</sup>, F. Teubert<sup>40</sup>, E. Thomas<sup>40</sup>, J. van Tilburg<sup>43</sup>, M.J. Tilley<sup>55</sup>, V. Tisserand<sup>4</sup>, M. Tobin<sup>41</sup>, S. Tolck<sup>49</sup>, L. Tomassetti<sup>17,g</sup>, D. Tonelli<sup>24</sup>, F. Toriello<sup>61</sup>, R. Tourinho Jadallah Aoude<sup>1</sup>, E. Tournefier<sup>4</sup>, M. Traill<sup>53</sup>, M.T. Tran<sup>41</sup>, M. Tresch<sup>42</sup>, A. Trisovic<sup>40</sup>, A. Tsaregorodtsev<sup>6</sup>, P. Tsopelas<sup>43</sup>, A. Tully<sup>49</sup>, N. Tuning<sup>43,40</sup>, A. Ukleja<sup>29</sup>, A. Usachov<sup>7</sup>, A. Ustyuzhanin<sup>35</sup>, U. Uwer<sup>12</sup>, C. Vacca<sup>16,f</sup>, A. Vagner<sup>69</sup>, V. Vagnoni<sup>15,40</sup>, A. Valassi<sup>40</sup>, S. Valat<sup>40</sup>, G. Valenti<sup>15</sup>, R. Vazquez Gomez<sup>19</sup>, P. Vazquez Regueiro<sup>39</sup>, S. Vecchi<sup>17</sup>, M. van Veghel<sup>43</sup>, J.J. Velthuis<sup>48</sup>, M. Veltri<sup>18,r</sup>, G. Veneziano<sup>57</sup>, A. Venkateswaran<sup>61</sup>, T.A. Verlage<sup>9</sup>, M. Vernet<sup>5</sup>, M. Vesterinen<sup>57</sup>, J.V. Viana Barbosa<sup>40</sup>, B. Viaud<sup>7</sup>, D. Vieira<sup>63</sup>, M. Vieites Diaz<sup>39</sup>, H. Viemann<sup>67</sup>, X. Vilasis-Cardona<sup>38,m</sup>, M. Vitti<sup>49</sup>, V. Volkov<sup>33</sup>, A. Vollhardt<sup>42</sup>, B. Voneki<sup>40</sup>, A. Vorobyev<sup>31</sup>, V. Vorobyev<sup>36,w</sup>, C. Vob<sup>9</sup>, J.A. de Vries<sup>43</sup>, C. Vázquez Sierra<sup>39</sup>, R. Waldi<sup>67</sup>, C. Wallace<sup>50</sup>, R. Wallace<sup>13</sup>, J. Walsh<sup>24</sup>, J. Wang<sup>61</sup>, D.R. Ward<sup>49</sup>, H.M. Wark<sup>54</sup>, N.K. Watson<sup>47</sup>, D. Websdale<sup>55</sup>, A. Weiden<sup>42</sup>, M. Whitehead<sup>40</sup>, J. Wicht<sup>50</sup>, G. Wilkinson<sup>57,40</sup>, M. Wilkinson<sup>61</sup>, M. Williams<sup>56</sup>, M.P. Williams<sup>47</sup>, M. Williams<sup>58</sup>, T. Williams<sup>47</sup>, F.F. Wilson<sup>51</sup>, J. Wimberley<sup>60</sup>, M. Winn<sup>7</sup>, J. Wishahi<sup>10</sup>, W. Wislicki<sup>29</sup>, M. Witek<sup>27</sup>, G. Wormser<sup>7</sup>, S.A. Wotton<sup>49</sup>, K. Wraight<sup>53</sup>, K. Wyllie<sup>40</sup>, Y. Xie<sup>65</sup>, Z. Xu<sup>4</sup>, Z. Yang<sup>3</sup>, Z. Yang<sup>60</sup>, Y. Yao<sup>61</sup>, H. Yin<sup>65</sup>, J. Yu<sup>65</sup>, X. Yuan<sup>61</sup>, O. Yushchenko<sup>37</sup>, K.A. Zarebski<sup>47</sup>, M. Zavertyaev<sup>11,c</sup>, L. Zhang<sup>3</sup>, Y. Zhang<sup>7</sup>, A. Zhelezov<sup>12</sup>, Y. Zheng<sup>63</sup>, X. Zhu<sup>3</sup>, V. Zhukov<sup>33</sup>, J.B. Zonneveld<sup>52</sup>, S. Zucchelli<sup>15</sup>.

<sup>1</sup>Centro Brasileiro de Pesquisas Físicas (CBPF), Rio de Janeiro, Brazil

<sup>2</sup>Universidade Federal do Rio de Janeiro (UFRJ), Rio de Janeiro, Brazil

<sup>3</sup>Center for High Energy Physics, Tsinghua University, Beijing, China

<sup>4</sup>LAPP, Université Savoie Mont-Blanc, CNRS/IN2P3, Annecy-Le-Vieux, France

<sup>5</sup>Clermont Université, Université Blaise Pascal, CNRS/IN2P3, LPC, Clermont-Ferrand, France

<sup>6</sup>Aix Marseille Univ, CNRS/IN2P3, CPPM, Marseille, France

<sup>7</sup>LAL, Université Paris-Sud, CNRS/IN2P3, Orsay, France

<sup>8</sup>LPNHE, Université Pierre et Marie Curie, Université Paris Diderot, CNRS/IN2P3, Paris, France

<sup>9</sup>I. Physikalisches Institut, RWTH Aachen University, Aachen, Germany

<sup>10</sup>Fakultät Physik, Technische Universität Dortmund, Dortmund, Germany

<sup>11</sup>Max-Planck-Institut für Kernphysik (MPIK), Heidelberg, Germany

<sup>12</sup>Physikalisches Institut, Ruprecht-Karls-Universität Heidelberg, Heidelberg, Germany

- <sup>13</sup>*School of Physics, University College Dublin, Dublin, Ireland*
- <sup>14</sup>*Sezione INFN di Bari, Bari, Italy*
- <sup>15</sup>*Sezione INFN di Bologna, Bologna, Italy*
- <sup>16</sup>*Sezione INFN di Cagliari, Cagliari, Italy*
- <sup>17</sup>*Universita e INFN, Ferrara, Ferrara, Italy*
- <sup>18</sup>*Sezione INFN di Firenze, Firenze, Italy*
- <sup>19</sup>*Laboratori Nazionali dell'INFN di Frascati, Frascati, Italy*
- <sup>20</sup>*Sezione INFN di Genova, Genova, Italy*
- <sup>21</sup>*Universita e INFN, Milano-Bicocca, Milano, Italy*
- <sup>22</sup>*Sezione di Milano, Milano, Italy*
- <sup>23</sup>*Sezione INFN di Padova, Padova, Italy*
- <sup>24</sup>*Sezione INFN di Pisa, Pisa, Italy*
- <sup>25</sup>*Sezione INFN di Roma Tor Vergata, Roma, Italy*
- <sup>26</sup>*Sezione INFN di Roma La Sapienza, Roma, Italy*
- <sup>27</sup>*Henryk Niewodniczanski Institute of Nuclear Physics Polish Academy of Sciences, Kraków, Poland*
- <sup>28</sup>*AGH - University of Science and Technology, Faculty of Physics and Applied Computer Science, Kraków, Poland*
- <sup>29</sup>*National Center for Nuclear Research (NCBJ), Warsaw, Poland*
- <sup>30</sup>*Horia Hulubei National Institute of Physics and Nuclear Engineering, Bucharest-Magurele, Romania*
- <sup>31</sup>*Petersburg Nuclear Physics Institute (PNPI), Gatchina, Russia*
- <sup>32</sup>*Institute of Theoretical and Experimental Physics (ITEP), Moscow, Russia*
- <sup>33</sup>*Institute of Nuclear Physics, Moscow State University (SINP MSU), Moscow, Russia*
- <sup>34</sup>*Institute for Nuclear Research of the Russian Academy of Sciences (INR RAN), Moscow, Russia*
- <sup>35</sup>*Yandex School of Data Analysis, Moscow, Russia*
- <sup>36</sup>*Budker Institute of Nuclear Physics (SB RAS), Novosibirsk, Russia*
- <sup>37</sup>*Institute for High Energy Physics (IHEP), Protvino, Russia*
- <sup>38</sup>*ICCUB, Universitat de Barcelona, Barcelona, Spain*
- <sup>39</sup>*Universidad de Santiago de Compostela, Santiago de Compostela, Spain*
- <sup>40</sup>*European Organization for Nuclear Research (CERN), Geneva, Switzerland*
- <sup>41</sup>*Institute of Physics, Ecole Polytechnique Fédérale de Lausanne (EPFL), Lausanne, Switzerland*
- <sup>42</sup>*Physik-Institut, Universität Zürich, Zürich, Switzerland*
- <sup>43</sup>*Nikhef National Institute for Subatomic Physics, Amsterdam, The Netherlands*
- <sup>44</sup>*Nikhef National Institute for Subatomic Physics and VU University Amsterdam, Amsterdam, The Netherlands*
- <sup>45</sup>*NSC Kharkiv Institute of Physics and Technology (NSC KIPT), Kharkiv, Ukraine*
- <sup>46</sup>*Institute for Nuclear Research of the National Academy of Sciences (KINR), Kyiv, Ukraine*
- <sup>47</sup>*University of Birmingham, Birmingham, United Kingdom*
- <sup>48</sup>*H.H. Wills Physics Laboratory, University of Bristol, Bristol, United Kingdom*
- <sup>49</sup>*Cavendish Laboratory, University of Cambridge, Cambridge, United Kingdom*
- <sup>50</sup>*Department of Physics, University of Warwick, Coventry, United Kingdom*
- <sup>51</sup>*STFC Rutherford Appleton Laboratory, Didcot, United Kingdom*
- <sup>52</sup>*School of Physics and Astronomy, University of Edinburgh, Edinburgh, United Kingdom*
- <sup>53</sup>*School of Physics and Astronomy, University of Glasgow, Glasgow, United Kingdom*
- <sup>54</sup>*Oliver Lodge Laboratory, University of Liverpool, Liverpool, United Kingdom*
- <sup>55</sup>*Imperial College London, London, United Kingdom*
- <sup>56</sup>*School of Physics and Astronomy, University of Manchester, Manchester, United Kingdom*
- <sup>57</sup>*Department of Physics, University of Oxford, Oxford, United Kingdom*
- <sup>58</sup>*Massachusetts Institute of Technology, Cambridge, MA, United States*
- <sup>59</sup>*University of Cincinnati, Cincinnati, OH, United States*
- <sup>60</sup>*University of Maryland, College Park, MD, United States*
- <sup>61</sup>*Syracuse University, Syracuse, NY, United States*
- <sup>62</sup>*Pontifícia Universidade Católica do Rio de Janeiro (PUC-Rio), Rio de Janeiro, Brazil, associated to <sup>2</sup>*
- <sup>63</sup>*University of Chinese Academy of Sciences, Beijing, China, associated to <sup>3</sup>*
- <sup>64</sup>*School of Physics and Technology, Wuhan University, Wuhan, China, associated to <sup>3</sup>*
- <sup>65</sup>*Institute of Particle Physics, Central China Normal University, Wuhan, Hubei, China, associated to <sup>3</sup>*
- <sup>66</sup>*Departamento de Física, Universidad Nacional de Colombia, Bogota, Colombia, associated to <sup>8</sup>*

- <sup>67</sup> *Institut für Physik, Universität Rostock, Rostock, Germany, associated to* <sup>12</sup>  
<sup>68</sup> *National Research Centre Kurchatov Institute, Moscow, Russia, associated to* <sup>32</sup>  
<sup>69</sup> *National Research Tomsk Polytechnic University, Tomsk, Russia, associated to* <sup>32</sup>  
<sup>70</sup> *Instituto de Fisica Corpuscular, Centro Mixto Universidad de Valencia - CSIC, Valencia, Spain, associated to* <sup>38</sup>  
<sup>71</sup> *Van Swinderen Institute, University of Groningen, Groningen, The Netherlands, associated to* <sup>43</sup>

- <sup>a</sup> *Universidade Federal do Triângulo Mineiro (UFTM), Uberaba-MG, Brazil*  
<sup>b</sup> *Laboratoire Leprince-Ringuet, Palaiseau, France*  
<sup>c</sup> *P.N. Lebedev Physical Institute, Russian Academy of Science (LPI RAS), Moscow, Russia*  
<sup>d</sup> *Università di Bari, Bari, Italy*  
<sup>e</sup> *Università di Bologna, Bologna, Italy*  
<sup>f</sup> *Università di Cagliari, Cagliari, Italy*  
<sup>g</sup> *Università di Ferrara, Ferrara, Italy*  
<sup>h</sup> *Università di Genova, Genova, Italy*  
<sup>i</sup> *Università di Milano Bicocca, Milano, Italy*  
<sup>j</sup> *Università di Roma Tor Vergata, Roma, Italy*  
<sup>k</sup> *Università di Roma La Sapienza, Roma, Italy*  
<sup>l</sup> *AGH - University of Science and Technology, Faculty of Computer Science, Electronics and Telecommunications, Kraków, Poland*  
<sup>m</sup> *LIFAELS, La Salle, Universitat Ramon Llull, Barcelona, Spain*  
<sup>n</sup> *Hanoi University of Science, Hanoi, Viet Nam*  
<sup>o</sup> *Università di Padova, Padova, Italy*  
<sup>p</sup> *Università di Pisa, Pisa, Italy*  
<sup>q</sup> *Università degli Studi di Milano, Milano, Italy*  
<sup>r</sup> *Università di Urbino, Urbino, Italy*  
<sup>s</sup> *Università della Basilicata, Potenza, Italy*  
<sup>t</sup> *Scuola Normale Superiore, Pisa, Italy*  
<sup>u</sup> *Università di Modena e Reggio Emilia, Modena, Italy*  
<sup>v</sup> *Iligan Institute of Technology (IIT), Iligan, Philippines*  
<sup>w</sup> *Novosibirsk State University, Novosibirsk, Russia*  
<sup>†</sup> *Deceased*